

Ultimate Bearing Strength of Post-tensioned Local Anchorage Zones in Lightweight Concrete

By

Daniel P. Axson

Thesis submitted to the faculty of the Virginia Polytechnic Institute and State University in
partial fulfillment of the requirements for the degree of

Master of Science

In

Civil Engineering

APPROVED:

Dr. Carin L. Roberts-Wollmann, Chairperson

Dr. Thomas E. Cousins, Committee Member

Dr. Finley A. Charney, Committee Member

May 21, 2008

Blacksburg, VA

Keywords: Lightweight Concrete, Post-tensioning, Tensile Strength, Modulus of Elasticity

Ultimate Bearing Strength of Post-tensioned Local Anchorage Zones in Lightweight Concrete

Daniel P. Axson

ABSTRACT

Currently, NCHRP Report 356 has published an equation to estimate the ultimate strength of the local zone in normal weight concrete. The local zone is the area of concrete directly ahead of the bearing plate. The equation can be broken into two distinct parts: unconfined bearing strength of concrete enhanced by the A/A_b ratio and the enhancement of strength due to the presence of confining. Research has shown that the strength enhancement of the A/A_b ratio and confining reinforcing is less in lightweight concrete than in normal weight concrete.

To determine the strength of the local zone in lightweight concrete 30 reinforced prisms, 2 unreinforced prisms, and concrete cylinders were tested. The dimensions of the prisms were 8 in. x 8 in. x 16 in. and the cylinders were 4 in. x 8 in. cylinders. The simulated reinforcing in the prisms extended only through the top 8 in. of the prism and consisted of either ties or spirals with different spacing or pitch, respectively. To determine the effect of the A/A_b ratio for each spacing or pitch arrangement of the reinforcing, one of two different size bearing plates were used.

From the testing performed in this research and other research, it is apparent that the NCHRP equation is unconservative when estimating the ultimate strength of the local zone in lightweight concrete. By modifying both parts of the NCHRP equation it is possible to conservatively predict the ultimate strength of the local zone in lightweight concrete.

Also investigated in this thesis are equations to predict the splitting cylinder strength and modulus of elasticity of lightweight concrete. For a sand-lightweight concrete, as defined by ACI 318-05 Building code and Commentary, the splitting tensile strength can be accurately predicted by multiplying the square root of the compressive strength by 5.7.

Acknowledgements

I would like to thank my advisor and friend, Dr. Roberts-Wollmann, for all of the help and guidance through the last three years. I would like to thank my other committee members, Dr. Cousins and Dr. Charney for their time and effort involved in the pursuit of my master's degree.

I would like to thank my family for all of the help and support throughout my entire life, without which I would have never made it this far.

I would also like to thank Vickie Mouras for all of her help and guidance throughout my undergrad career. Vickie always had a great perspective on things and who was more than just a teacher inside the classroom, but outside the classroom as well.

I would like to thank Brett Farmer and Dennis Huffman, without whose help and friendship my lab work would have taken much longer to accomplish. I would also like to thank all of the students from the lab who helped me with my lab work.

I would also like to thank all of my friends, past and present, for all of the good times we've had and all of the good times we've yet to have. I would especially like to thank all of my friends, family, and Virginia Tech community for the support in the aftermath of the events of April 16, 2007. I will continue to pray for peace for all of those affected.

Table of Contents

Table of Figures	vii
Table of Tables	x
Nomenclature	xi
Chapter 1.0 Introduction	1
1.1 Objectives and Scope of Research	5
1.2 Thesis Organization	7
Chapter 2.0 Literature Review	8
2.1 Unconfined Bearing Strength.....	8
2.1.1 Early Models	9
2.1.2 Hawkins (1968).....	10
2.1.3 Niyogi (1973, 1974).....	11
2.1.4 Bonetti (2005)	13
2.1.5 ACI 318 and AASHTO Design Codes.....	17
2.1.6 Roberts-Wollmann, Banta, Bonetti, and Charney (2006).....	18
2.2 Confined Concrete Bearing Strength	21
2.2.1 Richart, Brandtzaeg, and Brown (1928, 1929).....	21
2.2.2 Zieliński and Rowe (1960).....	22
2.2.3 Niyogi (1975).....	22
2.2.4 Bassett and Uzumeri (1986).....	23
2.2.5 Martinez, Nilson, and Slate (1984)	23
2.2.6 Heilmann (1983)	25
2.2.7 NCHRP Report 356 (1994).....	25
2.2.8 Bonetti (2005)	29

2.3 Splitting Tensile Strength of Lightweight Concrete	32
2.4 Modulus of Elasticity of Lightweight Concrete.....	34
2.5 Summary	35
Chapter 3.0 Testing Program.....	36
3.1 Concrete Prism Properties.....	36
3.2 Testing Procedures for Concrete Prisms	40
3.3 Concrete Cylinders.....	42
3.3.1 Compressive Strength Tests	42
3.3.2 Splitting Cylinder Strength Tests	42
3.3.3 Modulus of Elasticity Tests.....	42
3.3.4 A/A _b tests.....	43
3.4 Concrete Properties	45
Chapter 4.0 Results and Data Analysis	49
4.1 Unreinforced Bearing Strength	49
4.1.1 Results and Observations	49
4.1.2 Analysis of Unreinforced Bearing Strength Data	54
4.2 Reinforced Bearing Strength.....	57
4.2.1 Results and Observations	57
4.2.2 Analysis of Reinforced Bearing Strength Data	61
4.2.2.1 Analysis of Test Results.....	62
4.2.2.2 Analysis of Heilmann Data	69
4.2.2.3 Analysis of Slab Anchor Testing	73
4.2.3 Analysis of First Cracking Data.....	80
4.3 Splitting Tensile Strength of Lightweight Concrete	82

4.4 Modulus of Elasticity of Lightweight Concrete.....	84
Chapter 5.0 Conclusions and Recommendations.....	86
5.1 Conclusions.....	86
5.2 Recommendations.....	88
References	89

Table of Figures

Figure 1-1: Definition of the Local and General Zones	2
Figure 1-2: AASHTO cyclic test.....	3
Figure 1-3: Stress Distribution in the Anchorage Zone Region (Bonetti 2005)	4
Figure 2-1: A/A_b Ratio	9
Figure 2-2: Hawkins' Failure Model.....	11
Figure 2-3: Niyogi's 2D Bearing Stress Model	12
Figure 2-4: Niyogi's Comparison of Aspect Ratio (Niyogi 1973).....	12
Figure 2-5: Comparison of Bonetti Data from normal weight concrete, High-Strength normal weight concrete, and lightweight concrete cylinder and prism tests.....	13
Figure 2-6: Modified Mohr Failure Criterion	14
Figure 2-7: Plan view of One-way Bearing vs. Two-way Bearing (Bonetti 2005)	14
Figure 2-8: Description of Variables (Bonetti 2005)	16
Figure 2-9: Application of frustum to find A_2 in stepped or sloped Supports (After Figure R10.17 from ACI 318-05).....	18
Figure 2-10: Lightweight Data (Roberts-Wollmann et al. 2006).....	20
Figure 2-11: Normal Weight Data (Hawkins 1968b; Niyogi 1973; Roberts-Wollmann et al. 2006).....	20
Figure 2-12: Richart, Brandtzaeg, and Brown Test Setup	21
Figure 2-13: Spiral Reinforcing	27
Figure 2-14: Tied Reinforcing.....	27
Figure 2-15: Well Confined Core with Spiral Reinforcing.....	28
Figure 2-16: Well Confined Core with Tied Reinforcing.....	29
Figure 2-17: Bowing Action in Ties from Lateral Pressure.....	29
Figure 2-18: F_{sp} Data.....	33
Figure 3-1: Example of Specimen (Profile view)	37
Figure 3-2: Example of Specimens (Plan View).....	37
Figure 3-3: Reinforcing cages in the formwork	38
Figure 3-4: Homasote Board attached to formwork to contain epoxy layer.....	38
Figure 3-5: Naming Convention	39
Figure 3-6: Test setup of Concrete Prisms	40
Figure 3-7: Split Cylinder Device	42

Figure 3-8: External Strain Gage for a 4 in. x 8 in. cylinder.....	43
Figure 3-9: Cylinder Test Setup.....	44
Figure 3-10: Compressive Strength Gain Chart.....	46
Figure 3-11: Tensile Strength Gain Chart.....	47
Figure 3-12: Modulus of Elasticity Data.....	48
Figure 4-1: Plan View of Failed of Concrete Cylinders	50
Figure 4-2: Profile View of Concrete Cylinder.....	51
Figure 4-3: Plan and Profile View of Punching.....	51
Figure 4-4: Close up of Cone of Concrete formed beneath Bearing Plate.....	52
Figure 4-5: Picture of the Top of Unreinforced Prisms	52
Figure 4-6: Cone of Concrete.....	53
Figure 4-7: Graphical Representation of the Experimental Data vs. of Bearing Strength Equations.....	54
Figure 4-8: Comparison of Experimental Data and Previous Data vs. Bearing Strength Prediction Equations.....	56
Figure 4-9: Failed Prisms with Tied Reinforcing	58
Figure 4-10: Failed Prisms with Spiral Reinforced.....	58
Figure 4-11: Bearing Pad Expansion under 4 inch and 2.5 inch bearing pad.....	59
Figure 4-12: Top Surface after failure: 4 in. bearing pad.....	59
Figure 4-13: Top Surface after failure: 2.5 in. bearing pad.....	60
Figure 4-14: Detail of Concrete Beneath the Bearing Plate.....	60
Figure 4-15: NCHRP Equation with no modification (Equation 2-15)	63
Figure 4-16: Ultimate load vs. Lateral Confining Pressure	64
Figure 4-17: Experimental and NCHRP Ultimate Load vs. Lateral Confining Pressure for 4 in. Bearing Pads ($k = 4.1$ and $\lambda = 1.0$).....	65
Figure 4-18: Experimental and Modified NCHRP Ultimate Load vs. Lateral Confining Pressure ($k = 2.5$ and $\lambda = 0.9$), 4 in. bearing pad.....	65
Figure 4-19: Experimental vs. Predicted load for $k = 2.5$ and $\lambda = 0.90$ (Current Research)	66
Figure 4-20: Experimental vs. Predicted load for $k = 2.5$ and $\lambda = 0.90$, Area Modification (Current Research)	67
Figure 4-21: Comparison of Experimental Data versus Equation 2-20 (Current research).....	68
Figure 4-22: Comparison of Experimental Data versus Equation 2-23 (Current research).....	68
Figure 4-23: Heilmann and NCHRP Ultimate Load vs. Lateral Confining Pressure ($k = 4.1$ and $\lambda = 1.0$)	69

Figure 4-24: Heilmann and Modified NCHRP Ultimate Load vs. Lateral Confining Pressure ($k = 1.5$ and $\lambda = 0.75$).....	70
Figure 4-25: Experimental vs. Predicted load for $k = 1.5$, $\lambda = 0.75$, and Area Modification (Heilmann Data).....	70
Figure 4-26: Heilmann and Modified NCHRP Ultimate Load vs. Lateral Confining $k = 2.5$, $\lambda = 0.75$, and Area Modification	71
Figure 4-27: Experimental vs. Predicted load for $k = 2.5$, $\lambda = 0.75$, and Area Modification (Heilmann Data).....	71
Figure 4-28: Comparison of Experimental Data vs. Equation 2-20 (Heilmann Data).....	72
Figure 4-29: Comparison of Experimental Data vs. Equation 2-23 (Heilmann Data).....	73
Figure 4-30: DSI Test Specimen Detail	75
Figure 4-31: VSL Test Specimen Detail	76
Figure 4-32: Experimental versus Predicted NCHRP Load for $k = 4.1$ and $\lambda = 1.0$	77
Figure 4-33: Experimental versus Predicted NCHRP Load for $k = 2.5$ and $\lambda = 0.85$	77
Figure 4-34: Profile View of DSI Anchor.....	78
Figure 4-35: Plan View of DSI Anchor	78
Figure 4-36: Ultimate Load vs. Min. First Cracking load: separated by reinforcing type and bearing pad size.....	81
Figure 4-37: F_{sp} for Sand-Lightweight Concrete	82
Figure 4-38: Percentage f_{ct} of f'_c versus f'_c of Sand-Lightweight Data.....	83
Figure 4-39: Current Research vs. Modulus of Elasticity Estimates	84
Figure 4-40: Dymond (2007) Data vs. Modulus of Elasticity Estimates	85

Table of Tables

Table 1-1: Concrete classification (Martinez et al. 1984).....	1
Table 2-1: Values of F_{sp}	32
Table 3-1: Details of Prism Specimens.....	39
Table 3-2: Design Lightweight Concrete Mix Proportions.....	45
Table 3-3: Compressive Strength Gain Data.....	46
Table 3-4: Tensile Strength Gain Data.....	46
Table 3-5: Concrete Properties from Dymond 2007.....	47
Table 3-6: Experimental Modulus of Elasticity Data.....	47
Table 4-1: Unreinforced Bearing Strength Data.....	50
Table 4-2: Comparison of Experimental Data vs. Bearing Strength Equations.....	54
Table 4-3: First Cracking and Ultimate Load Data.....	57
Table 4-4: Comparison of the Experimental Loads vs. the NCHRP predicted load.....	62
Table 4-5: Summary of data in Table 4-4.....	63
Table 4-6: Comparison of Experimental/Analytical Mean and Standard Deviation for Area Modification (Current Research) ($k = 2.5$ and $\lambda = 0.90$).....	67
Table 4-7: Comparison of Experimental/Analytical Mean and Standard Deviation for Equation 2-20 (Current Research).....	68
Table 4-8: Comparison of Experimental/Analytical Mean and Standard Deviation for Equation 2-23 (Current Research).....	69
Table 4-9: Comparison of Experimental/Analytical Mean and Standard Deviation for Area Modification (Heilmann Data).....	72
Table 4-10: Comparison of Experimental/Analytical Mean and Standard Deviation Bonetti's Reinforced Bearing Strength Equations.....	73
Table 4-11: Ultimate Loads from Slab Anchor Testing, kips.....	74
Table 4-12: First Cracking Stress / Ultimate Bearing Stress Summary.....	80
Table 4-13: First Cracking Stress / Ultimate Bearing Stress Summary with low values removed.....	80
Table 4-14: Modulus of Elasticity versus Equation Estimates.....	84

Nomenclature

A	=	Gross area of the concrete specimen
A_b	=	Area of the Bearing Plate
A_{core}	=	Area of the Confined Core
A_{duct}	=	Area of the Duct
A_{eff}	=	Effective Core Area
A_s	=	Area of the lateral steel reinforcing
A_y	=	Area under assumed uniform state of stress
A_1	=	Bearing Area, (Area of the Bearing Plate)
A_2	=	Supporting Area, (Defined in Equation 2-9)
D	=	Side length or diameter of the lateral reinforcing
E_c	=	Modulus of Elasticity of Concrete
F_{sp}	=	Ratio of f_{ct} to the square root of f'_c , (Equation 2-25)
F_{ult}	=	Ultimate Load of the Local Zone, (Equation 1-1)
P	=	Ultimate bearing strength
$2a$	=	Side length of concrete specimen (Niyogi 1973; Niyogi 1975; Niyogi 1974)
$2a'$	=	Side length of bearing pad (Niyogi 1973; Niyogi 1975; Niyogi 1974)
d_c	=	Tie side length or spiral diameter of the lateral reinforcing
f_b	=	Bearing Pressure
f'_c	=	Unconfined Compressive Strength of the Concrete
f_{cc}	=	Confined Compressive Strength of the Concrete
f_{co}	=	Unconfined Compressive Strength of the Concrete
f_{ct}	=	Splitting cylinder strength
f_{lat}	=	Lateral Confining Pressure provided by lateral reinforcing
f_{uc}	=	Unconfined Compressive Strength of the Concrete
f_y	=	Yield strength of reinforcing steel
h	=	<ul style="list-style-type: none"> • Width of concrete specimen (Bonetti) • Height of specimen (Niyogi)
k	=	Factor function of the mechanical reinforcing ratio, (Equation 2-21)
n	=	Ultimate bearing stress over f'_c , (Niyogi 1973; Niyogi 1975; Niyogi 1974)
m	=	Ratio of f'_c to f_{lat} , (Equation 2-4), (Bonetti 2005)
m_r	=	Ratio of f'_c to $(f_{lat} + f_{ct})$, (Equation 2-23), (Bonetti 2005)
q	=	Ultimate bearing stress
s	=	Tie spacing or spiral pitch of the lateral reinforcing
w_c	=	Unit Weight of the Concrete
y	=	Distance from bearing surface to the point of maximum tensile stress
α	=	<ul style="list-style-type: none"> • A/A_y, (Bonetti 2005)

- Angle between horizontal and cone (Hawkins Model, Figure 2-2)
- β = Normalized maximum tensile stress, $f_{t\ max} / (P/A)$, (Bonetti 2005)
- λ = Plain bearing strength modification factor
- σ_1 = Maximum principle stress, $f_{t\ max}$ (tension)
- σ_3 = Maximum principle stress, $f_{c\ max}$ (compression)
- ϕ = ACI 318-05 phi factor
- ω = Mechanical reinforcing ratio

Chapter 1.0 Introduction

Post-tensioned concrete has been around for many years and is an essential technology for building with concrete. In the recent years, the use of lightweight concrete in structures has increased and future post-tensioned designs will likely utilize lightweight concrete. Lightweight concrete mixes can be designed to have strengths that are comparable to those of normal weight concrete, as seen in Table 1-1. With the advent of higher strength lightweight concrete, there is a desire to use the material to reduce the dead load of concrete structures and increase span lengths. Presently, there has been little research into the behavior of lightweight concrete subjected to high bearing stresses similar to those anticipated in the anchorage zone of post-tensioned concrete.

There have been many investigations into the stress strain behavior of both plain and confined lightweight concrete. Lightweight concrete tends to have much lower modulus of elasticity than normal weight concrete (Gjørsv and Zhang 1991). Lightweight concrete exhibits a more brittle behavior than a normal weight concrete, characterized by a steep descending branch of the stress strain curve.

Table 1-1: Concrete classification (Martinez et al. 1984)

Type of Concrete	Approximate Unit Weight, pcf	Approximate Strength, psi
Normal Strength, Normal Weight	145	< 5000
Medium Strength, Normal Weight	145	5000 – 8000
High Strength, Normal Weight	145	8000 – 12000
Normal Strength, Lightweight	115	< 4000
Medium Strength, Lightweight	115	4000 – 6000
High Strength, Lightweight	115	6000 – 9000

The anchorage zone is the critical area of concrete ahead of the anchorage device and is broken into two zones, the local zone and general zone (See Figure 1-1). A difficulty of designing a post-tensioned system is preventing the concrete from failing under the high bearing stress that is introduced into the concrete at the strand anchorage. The National Cooperative Highway Research Program (NCHRP) sponsored a program to investigate the parameters that affect the strength of anchorage zones in post-tensioned concrete (Breen et al. 1994). The local zone is the critical zone just ahead of the anchorage device that is subjected to the highest bearing

stresses and therefore requires extensive confining reinforcing. The NCHRP investigation resulted in an equation to estimate the strength of the local zone of the concrete and a testing procedure to verify the strength of the local zone.

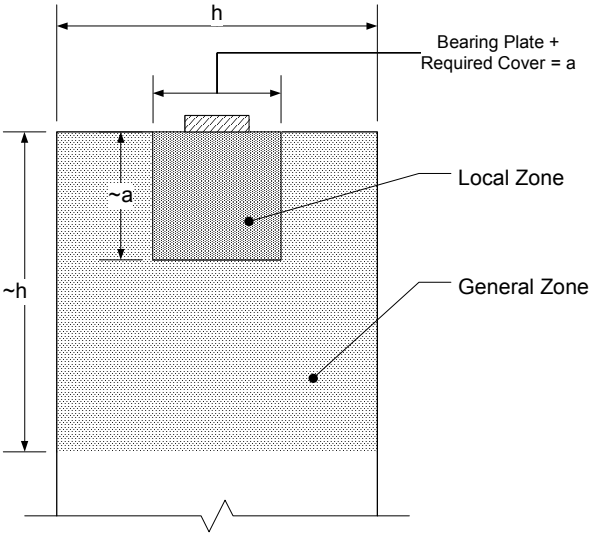


Figure 1-1: Definition of the Local and General Zones

The testing program for the anchorage zone requires that a representative section of the anchorage zone concrete section be tested by one of three testing protocols. The three programs are the cyclic, sustained, and monotonic. Generally the cyclic program is the desired program because it takes the least amount of time to complete and passing criteria is the less harsh than the other two programs.

The cyclic loading subjects the concrete section to 10 loading and unloading cycles. The loading cycles are from 10% of the guaranteed ultimate tensile strength (GUTS) of the strands to 80% of GUTS (See Figure 1-2). After completion of the loading cycles the section is loaded to 110% of GUTS. During the testing, the crack widths on the side faces are monitored from 0% GUTS to 80% GUTS, at the 80% GUTS mark of the last three cycles, and at 90% GUTS. For the anchorage zone to pass the testing program, the crack widths are required not to exceed specified maximum widths and the increase of the crack width over the last three cycles must not exceed 0.001 in. In addition to the crack width requirements, the ultimate load of the specimen is required to exceed 110% of GUTS.

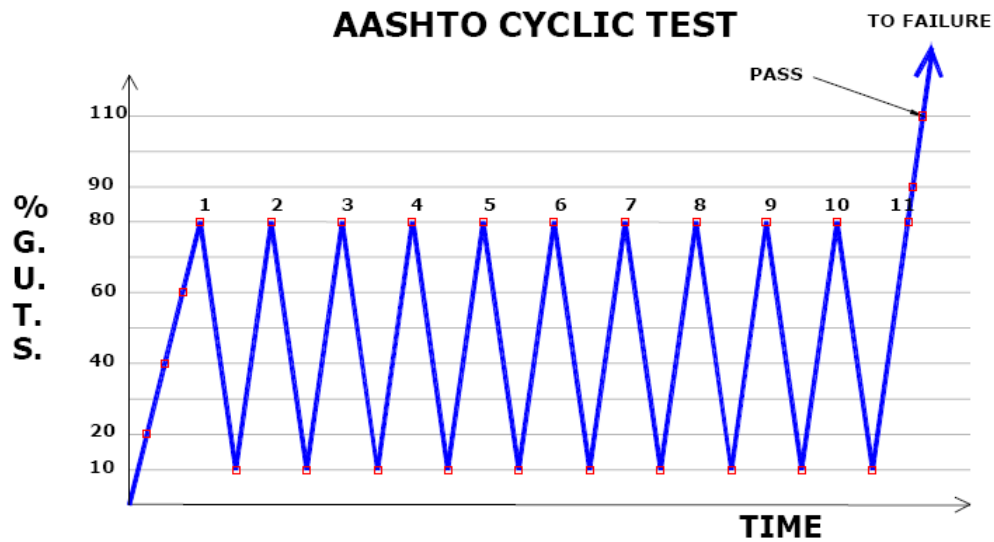


Figure 1-2: AASHTO cyclic test

The NCHRP equation to estimate the strength of the local zone is generally used to design the reinforcing before testing and is not recognized without the testing program. There are two parameters that will increase the ultimate strength of the local zone are they are the A/A_b ratio and the presence of confining reinforcing. The NCHRP equation can be broken down into two parts, the part that accounts for the increased strength due to the A/A_b ratio and the part that accounts for the presence of confining reinforcing. The equation is as follows with the parameters defined in the Nomenclature section on page xi:

$$F_{ult} = 0.80 f'_c \sqrt{\frac{A}{A_b}} (A_b) + 4.1 f_{lat} A_{core} \left(1 - \frac{s}{D}\right)^2$$

*Equation 1-1: NCHRP
Ultimate Bearing Strength
of the Local Zone*

Where:

- F_{ult} = ultimate load of the local zone
- f'_c = unconfined compressive strength of concrete
- A = gross area of concrete specimen
- A_b = area of the bearing plate
- f_{lat} = lateral confining pressure provided by lateral reinforcing
- A_{core} = area of confined core
- s = tie spacing or spiral pitch of the lateral reinforcing
- D = side length or spiral diameter of the lateral reinforcing

Due to Poisson's effect, concrete expands laterally when subjected to a compressive force. The lateral strains that develop in concrete under compression can easily overcome the typically low

tensile strain capacity of the concrete and cause the concrete to fail. Figure 1-3 shows the typical distribution of compressive and tensile stresses developed in the anchorage zone region. The addition of confining reinforcing can reduce the lateral strains in the concrete and the ultimate strength of the local zone can be increased.

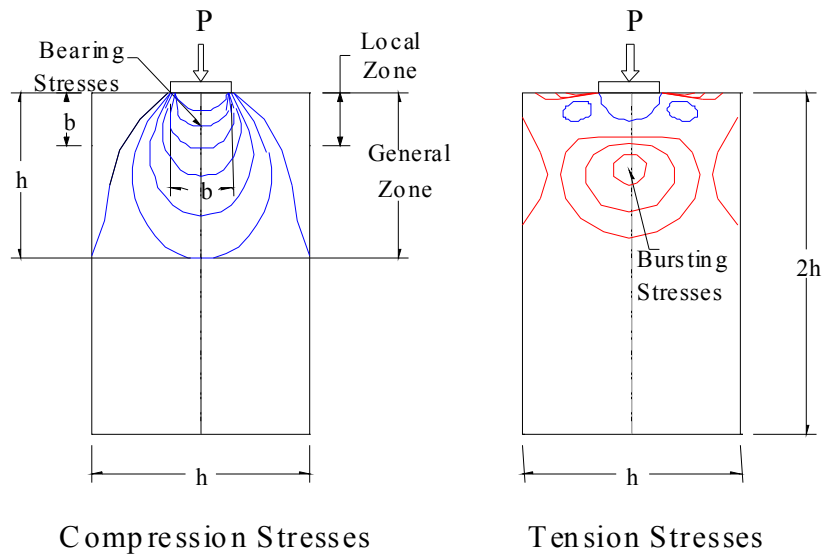


Figure 1-3: Stress Distribution in the Anchorage Zone Region (Bonetti 2005)

As concrete expands under load, confinement of the local zone can restrain the expansion. The effectiveness of confinement for normal weight concrete has been heavily researched, but little research has been done to investigate the effectiveness of confinement in lightweight concrete.

The ratio of the area of the supporting concrete (A) to the bearing area (A_b) is known as the A/A_b ratio. Previous research has shown that as the A/A_b ratio increases the ultimate bearing strength of the concrete section increases (Billig 1948; Komendant 1952). The increased strength is due to the confinement from the area of supporting concrete that surrounds the bearing area and functions similarly to confining reinforcing. Investigations into the effectiveness of the confinement by the surrounding concrete have shown that lightweight concrete will have a smaller increase in ultimate bearing strength as compared to normal weight concrete with the same A/A_b ratio (Roberts-Wollmann et al. 2006).

Research that has investigated the effectiveness of confining reinforcing in lightweight concrete has shown that confining reinforcing is less effective in lightweight concrete than it is in normal weight concrete (Khaloo and Bozorgzadeh 2001; Martinez et al. 1984; Shah et al. 1983). Existing models to determine the ultimate strength of confined lightweight concrete are therefore unconservative (Basset and Uzumeri 1986). Present research has shown that lightweight concrete behaves similarly to high-strength normal weight concrete and is less affected by the presence of confinement. When compared to normal strength concrete, high-strength normal weight concretes and lightweight concretes show smaller lateral strains for similar axial strains. The theory is that lower lateral strains would engage less of the confining reinforcing before the lateral tensile stresses eclipsed the tensile strength of the concrete (Shah et al. 1983).

1.1 Objectives and Scope of Research

Currently, the equation presented in NCHRP Report 356 is widely accepted to calculate the strength of the local zone for post-tensioned members of normal weight concrete. Research has shown that confinement has a smaller affect on lightweight concrete than on normal weight concrete and would, therefore, make the predictions of the NCHRP equation unconservative.

The ultimate goal of this research is to investigate the effectiveness of confining reinforcing in lightweight concrete and to determine if the NCHRP equation for designing local zone reinforcing is adequate for designing local zone reinforcing in lightweight concrete. Thirty-two lightweight concrete specimens were cast with varying amounts and forms of confining reinforcing. Both tied and spiral reinforcing were tested with varying spacing and pitches. The size of the bearing plate was also varied to determine the effect of the A/A_b ratio on the bearing strength of confined lightweight concrete. To further test the effectiveness of the A/A_b ratio on unconfined lightweight concrete, concrete cylinders were tested with varying A/A_b ratios.

The adequacy of the NCHRP equation for designing local zone reinforcing was evaluated and a modification to the equation was developed. The modified equation conservatively predicts the ultimate strength of lightweight concrete accounting for all of the parameters mentioned above. Data found in literature and data from local anchorage zone testing done at Virginia Tech was compared to the developed equation.

The tensile strength and modulus of elasticity were also tracked over the age of the concrete from the time it was cast. The tensile strength was tracked through the splitting cylinder test and the modulus of elasticity was tracked using an external strain gage that attaches to the outside of a cylinder. The values were compared to code equations and equations developed through research that predicts the modulus of elasticity and splitting cylinder strength.

1.2 Thesis Organization

Chapter 1 includes the introduction of the thesis, the scope of the thesis, and the organization of the thesis. Chapter 2 contains a discussion of previous research that covers the subjects of the unconfined bearing strength of concrete, the confined bearing strength of concrete, the tensile strength of lightweight concrete and the modulus of elasticity of lightweight concrete. Chapter 3 contains a detailed layout of the testing program and testing setup. The results of the compressive strength test, splitting cylinder strength, and modulus of elasticity of the lightweight concrete are also provided in Chapter 3. The discussion of the results of the unreinforced and reinforced bearing strength tests and analysis of the effectiveness of the NCHRP equation and splitting cylinder and modulus of elasticity equations are discussed in Chapter 4. The conclusions and recommendations are presented in Chapter 5.

Chapter 2.0 Literature Review

Chapter 2.0 presents an investigation into previous research into the subjects that will be covered in this research. Those subjects are the unconfined bearing strength of concrete, confined bearing strength of concrete, splitting tensile strength of lightweight concrete, and modulus of elasticity of lightweight concrete.

Previous research into the unconfined bearing strength of includes work from Billig, Komendant, Hawkins, Niyogi, and Bonetti, which are all based on normal weight concrete. A review of the ACI 318-05 and the AASHTO 2007 code equations to calculate the unconfined bearing strength of normal weight concrete. One paper on the unconfined bearing strength of lightweight concrete is reviewed.

Previous research into the confined bearing strength of concrete includes research conducted by Richart et al., Niyogi, Bassett and Uzumeri, Martinez et al., Heilmann, NCHRP Report 356, and Bonetti. Currently, the NCHRP Report 356 publishes a widely accepted equation to estimate the bearing strength of a confined local zone in post tensioned concrete.

Two methods of estimating the splitting cylinder strength of concrete will be examined and compared to several sources of data. Several equations developed from previous research to predict the modulus of elasticity will be compared to the data gathered in this research and from Dymond's research.

2.1 Unconfined Bearing Strength

With an increased use of post-tensioned construction through the mid 1900s, researchers recognized the importance of understanding the parameters that affected concrete bearing strength. The most important factor that affects the ultimate bearing strength of concrete, aside from the compressive strength f'_c , is the ratio of the area of the loaded face (A) to the area of the bearing plate (A_b). This ratio is known as the A/A_b ratio. Figure 2-1 illustrates the A/A_b ratio for square, concentric load surface.

2.1.1 Early Models

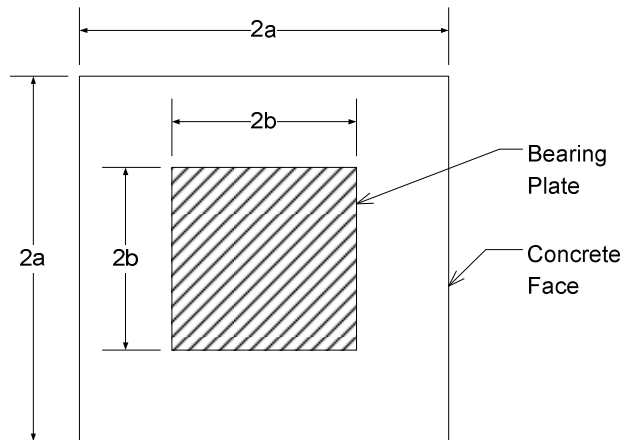
Bearing strength equations were initially based on a Billig's cube root function of the A/A_b ratio with a limiting value being the bearing strength (f'_c) of the concrete (Billig 1948)(Equation 2-1). In 1952, Komendant provided further research that showed that a square root function of the A/A_b ratio was better for design (Komendant 1952). Komendant's equation is identical to Billig's equation except that the square root of the A/A_b ratio is taken instead of the cube root.

$$f_b = (0.6 f'_c) \sqrt[3]{A/A_b} \leq f'_c$$

Equation 2-1: Billig's Bearing Equation

Where:

- f_b = bearing pressure
- f'_c = unconfined compressive strength of concrete
- A = gross area of the concrete specimen
- A_b = area of the bearing plate



Where:

$$A = 4a^2$$
$$A_b = 4b^2$$

Figure 2-1: A/A_b Ratio

2.1.2 Hawkins (1968)

In 1968 and 1969, Hawkins investigated the bearing strength of concrete through both rigid and flexible plates. Hawkins loaded concrete prisms with both concentric and eccentric loads.

The principal failure mechanism of his model was based on the development of tensile stresses generated from the penetration of an inverted cone of concrete directly beneath the bearing plate as seen in Figure 2-2. Hawkins' model is based on the dual failure criterion developed by Cowan. Cowan's failure model predicts that the failure will occur due to sliding on planes that are inclined to the direction of principle stresses (Cowan 1953; Hawkins 1968b).

Hawkins developed Equation 2-2 to estimate the bearing strength of concrete loaded concentrically through rigid plates. Hawkins estimated the K value to be 50 for normal and lightweight concrete with 3/4 inch aggregate (Hawkins 1968b).

$$q/f'_c = 1 + K/f'_c \left(\sqrt{A/A_b} - 1 \right)$$

Equation 2-2: Hawkins' Bearing Equation

Where:

q = ultimate bearing stress

α = See Figure 2-2

f_t = tensile strength of concrete

f'_c = unconfined compressive strength of concrete

$K = B \cot^2(\alpha)$

$$B = \frac{f_t}{\sqrt{f'_c}}$$

A = gross area of concrete specimen

A_b = area of the bearing plate

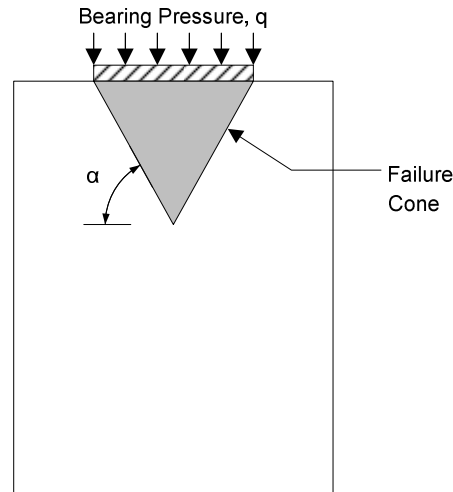


Figure 2-2: Hawkins' Failure Model

2.1.3 Niyogi (1973, 1974)

Niyogi published extensive research that investigated how geometric variations of the bearing plate and concrete prism, support conditions, specimen size, and concrete strength affect the ultimate bearing strength of the concrete. Niyogi made several conclusions that are important to this research.

The conclusions are listed below:

- As the concrete strength increases, the lower the ratio f_b/f'_c for a given A/A_b ratio.
- For similar shapes, the ratio f_b/f'_c decreases with an increase in specimen size.
- Enhanced strength due to the A/A_b ratio was diminished when the aspect ratio $(h/2a) < 1$ and the A/A_b ratio > 8 (See Figure 2-3). This effect is shown in Figure 2-4 for aspect ratios between 0.5 and 3. Diminished strength for low aspect ratios was also recognized by Meyerhof in 1953 (Meyerhof 1953).
- Using a cube root equation, such as the one developed by Billig, overestimates the ultimate bearing strength of the concrete.

Equation 2-3 was developed by Niyogi to calculate the bearing strength of a concrete prism concentrically loaded with a bearing plate, both of which having a square cross section. Niyogi's equation was developed using a 2-D one-way bearing model similar to Guyon's model (Guyon 1953).

$$f_b/f_c = 0.84\left(\sqrt{a/a'}\right) - 0.23$$

Equation 2-3: Niyogi Bearing equation

Where:

- f_b = bearing pressure
- f'_c = unconfined compressive strength of concrete
- a = See Figure 2-3
- a' = See Figure 2-3

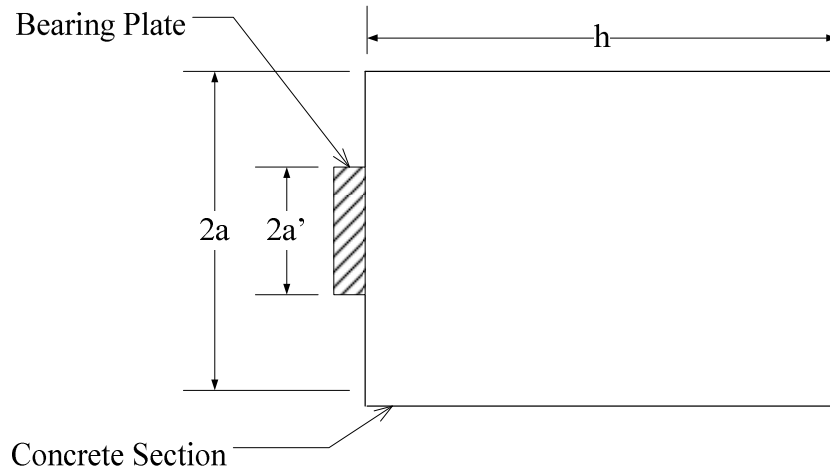


Figure 2-3: Niyogi's 2D Bearing Stress Model

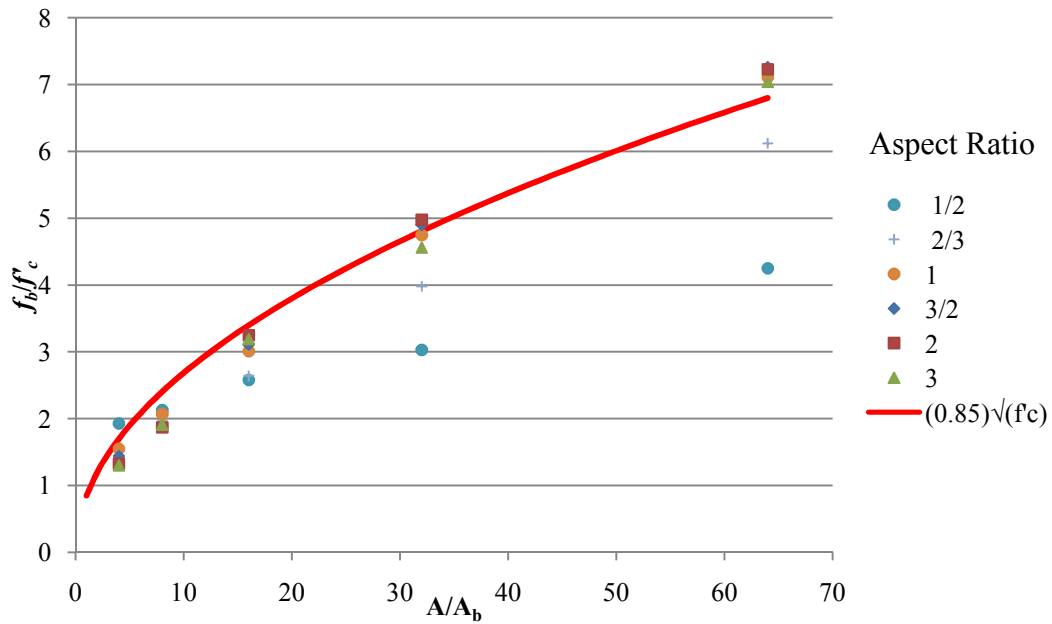


Figure 2-4: Niyogi's Comparison of Aspect Ratio (Niyogi 1973)

2.1.4 Bonetti (2005)

Research performed by Bonetti in 2005 at Virginia Tech investigated how the shape of the bearing plate, size of the bearing plate, concrete strength, and concrete density affects the ultimate strength of the concrete. Two normal weight concrete mixes with strengths to 5,000 psi and 8,000 psi and one lightweight concrete mix of 8,000 psi were used. Square, round, and hexagonal bearing plates were used in the testing program. All specimens were concentrically loaded.

The research showed that the shape of the bearing pad had no effect of the ultimate bearing strength of the concrete when the A/A_b ratio is between 2 and 16, which were the extents of the A/A_b ratios tested. The performance comparison of the three different concrete types showed that at higher A/A_b ratios, lightweight concrete and high-strength normal weight concrete showed less strength gain than normal strength normal weight concrete for the same increase in A/A_b ratio (Figure 2-5).

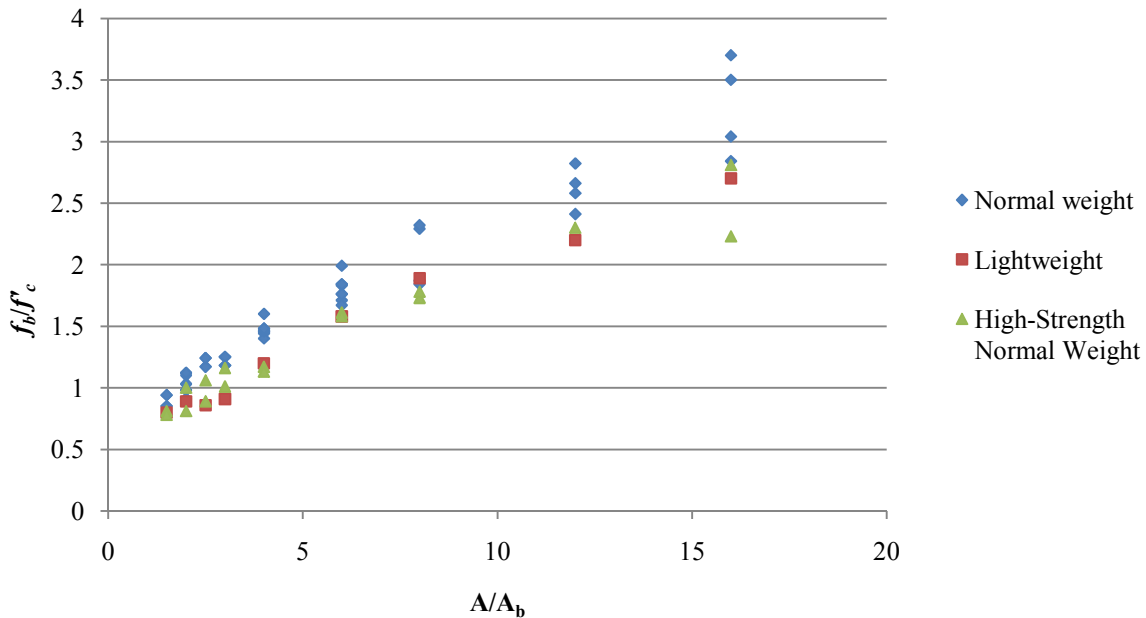


Figure 2-5: Comparison of Bonetti Data from normal weight concrete, High-Strength normal weight concrete, and lightweight concrete cylinder and prism tests

In his thesis, Bonetti developed an equation, based on a modified Mohr's Failure Criterion (See Figure 2-6). The derivations were developed based on a linear elastic finite element model of a

concrete prism with a square cross-section loaded in concentric compression using different A/A_b ratios. Bonetti's model is based on a 3-D state of stress instead of a 2-D state of stress used by Guyon (See Figure 2-7). Bonetti expected a 3-D model to act differently than a 2-D model.

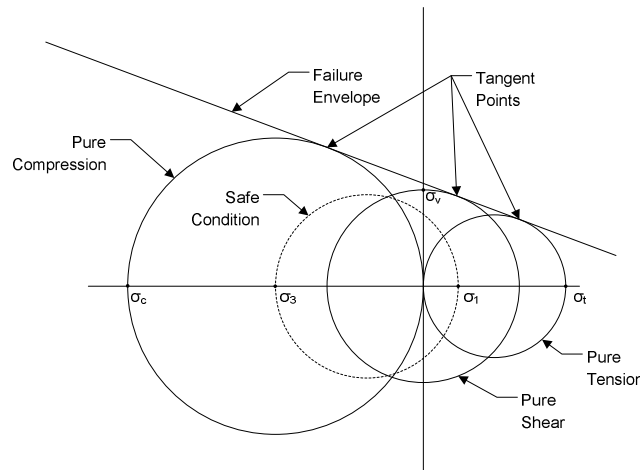


Figure 2-6: Modified Mohr Failure Criterion

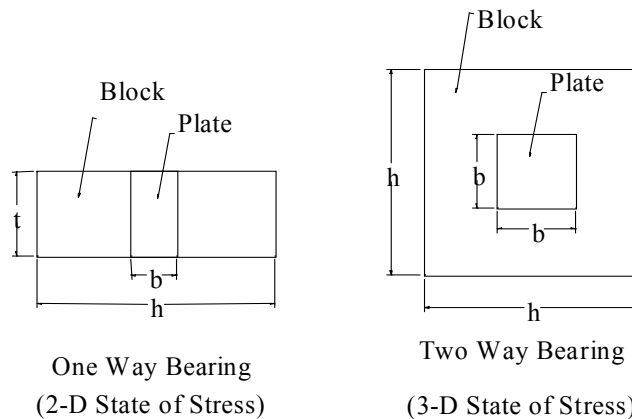


Figure 2-7: Plan view of One-way Bearing vs. Two-way Bearing (Bonetti 2005)

Bonetti made the following assumptions to derive his equation.

- Failure is mainly controlled by the maximum tensile stress and initiates in a plane located at the position of maximum stress, y .
- Behavior of plain concrete in tension is linear up to the point of failure. The ultimate tensile strength of the concrete is assumed to be equal to the split cylinder test strength.

- The principle compressive stress is taken as an average stress at point y , assuming spreading of compressive stresses at a 45-degree angle from the top surface of the block. This average stress acts on an area described by the intersection points of a horizontal plane and the 45-degree angle projection lines.
- The aspect ratio, length/width, of the concrete element is greater than 1.5. This condition ensures that no significant effects on the ultimate bearing strength are going to take place due to the boundary condition at the bottom of the prism (Niyogi 1974).

Bonetti's equation is as follows:

$$P = \frac{Af'_c}{m\beta + \alpha}$$

*Equation 2-4:
Bonetti Bearing
equation*

Where:

P = ultimate bearing strength

A = gross area of the concrete specimen

f'_c = unconfined bearing strength of the concrete

m = ratio of f'_c to f_{lat}

α = See Equation 2-7

β = See Equation 2-5

$$\beta = \frac{0.114}{\left(\frac{b}{h}\right)^{1.03}} \quad \text{for } \frac{b}{h} < 0.5 \quad (a)$$

*Equation 2-5: β
Factor*

$$\beta = 0.466 - 0.469\left(\frac{b}{h}\right) \quad \text{for } \frac{b}{h} \geq 0.5 \quad (b)$$

The β factor is the normalized ratio of f_t max, from the linear elastic solution done by Bonetti, to the average stress, P/A . Using the linear elastic model, Bonetti developed an equation to determine the location below the top face of the maximum tensile stress.

$$\frac{y}{h} = 0.20 \ln\left(\frac{b}{h}\right) + 0.56 \quad \text{for } \frac{b}{h} < 0.5 \quad (a)$$

*Equation 2-6: Location
of maximum Tensile
Stress*

$$\frac{y}{h} = 0.17\left(\frac{b}{h}\right) + 0.34 \quad \text{for } \frac{b}{h} \geq 0.5 \quad (b)$$

The variable y is the location of maximum tensile stress, f_t , in the lateral direction below the loaded face (See Figure 2-8).

$$\alpha = 1.0 \quad \text{for} \quad y \geq \frac{h-b}{2} \quad (a)$$

$$\alpha = \frac{A}{A_y} \quad \text{for} \quad y < \frac{h-b}{2} \quad (b)$$

Equation 2-7: α
Factor

The α -factor is based on the gross area of the section divided by the area supporting load at point y below the top face (See Figure 2-8).

$$A_y = (b + 2y)^2 \quad (a)$$

For square blocks loaded through square plates

$$A_y = \left(\frac{\pi}{4}\right)(b + 2y)^2 \quad (b)$$

For cylindrical prisms loaded through round plates

Equation 2-8: Loaded
Area at Location y

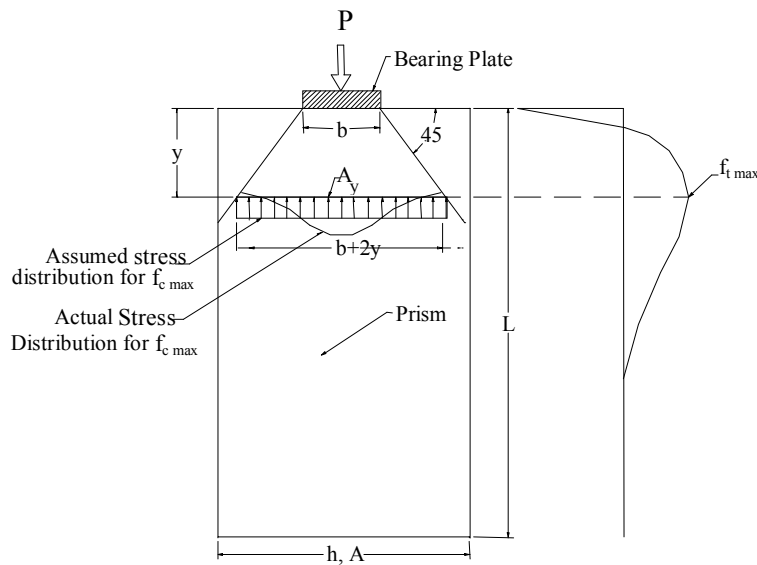


Figure 2-8: Description of Variables (Bonetti 2005)

2.1.5 ACI 318 and AASHTO Design Codes

The American Concrete Institute's Building Code and Commentary (ACI 318-05) as well as the American Association of State Highway and Transportation Officials (AASHTO 2007) address the bearing strength of concrete in very similar ways.

The ACI 318-05 bearing equation is given in Equation 2-9. In ACI 318-05, the square root of the A/A_b ratio is not permitted to be taken greater than 2. For the condition of bearing ϕ is taken to be 0.65 for design purposes.

For shear design ACI 318-05 requires the user to multiply the shear design equations for normal weight concrete by 0.85 for a sand-lightweight concrete and 0.75 for an all-lightweight concrete. A sand-lightweight concrete is considered to be a lightweight concrete where natural sand is used along with lightweight aggregate. An all-lightweight concrete uses lightweight manufactured sand along with a lightweight aggregate to produce a lightweight concrete. Figure 2-9 defines the variables of A_1 and A_2 . Currently ACI does not require the bearing strength equation to be factored for use with lightweight concrete.(ACI 2005)

$$F_{ult} = \phi(0.85f'_cA_1)\sqrt{A_2/A_1} \quad \text{Where} \quad \sqrt{A_2/A_1} \leq 2$$

*Equation 2-9: ACI
Ultimate Bearing
Strength Equation*

Where:

F_{ult} = ultimate bearing strength

f'_c = unconfined bearing strength

A_1 = bearing area (See Figure 2-9)

A_2 = supporting area (See Figure 2-9)

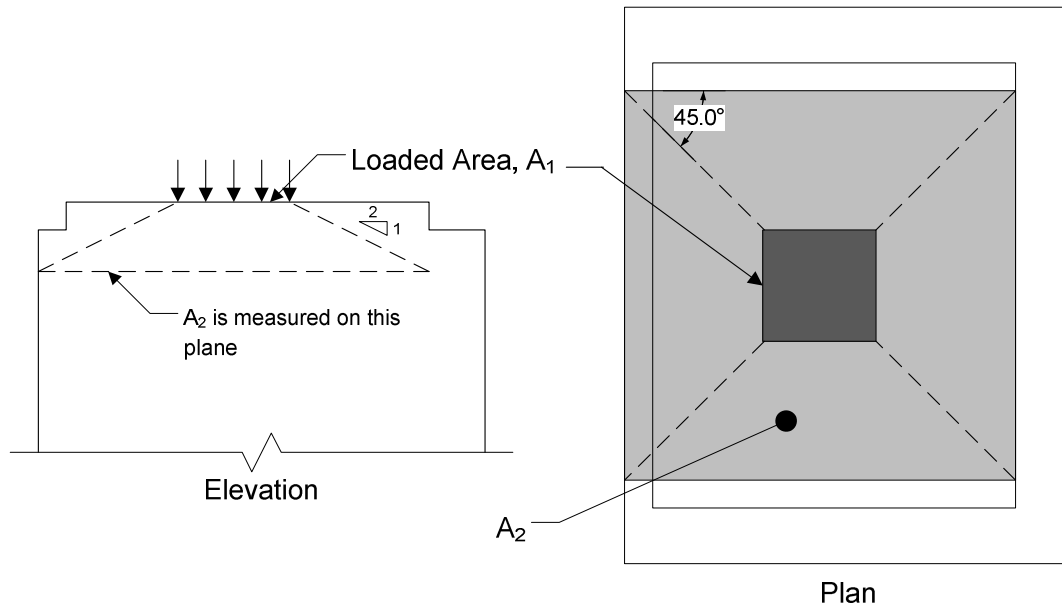


Figure 2-9: Application of frustum to find A_2 in stepped or sloped Supports (After Figure R10.17 from ACI 318-05)

The AASHTO bearing strength equation is very similar to the ACI 318-05 equation but with an additional provision. The factor m defines how the A/A_b ratio will affect the strength and under normal conditions the square root of the A/A_b ratio is limited to 2, but for the condition that the pressure distribution over the loaded area is non-uniform the square root of the A/A_b ratio multiplied by 0.75 is limited to 1.5 (AASHTO 2007).

$$F_{ult} = \phi(0.85f'_c A_1)m \quad \text{where: } m = \sqrt{\frac{A_2}{A_1}} \leq 2$$

$$\text{For non-uniform distributed loads } m = 0.75\sqrt{\frac{A_2}{A_1}} \leq 1.5$$

*Equation 2-10:
AASHTO Ultimate
Bearing Strength
Equation*

AASHTO also has different ϕ -factors than ACI 318-05. For the condition of pure bearing ϕ is equal to 0.70. In anchorage zones in normal weight concrete and lightweight concrete ϕ is equal to 0.80 and 0.65 respectively.

2.1.6 Roberts-Wollmann, Banta, Bonetti, and Charney (2006)

In 2006, an investigation into the ultimate bearing strength of unreinforced lightweight concrete was performed at Virginia Tech. The parameters of the test included the strength of the concrete

and the density. Two batches of concrete with strengths of 5000 psi and 8000 psi respectively, were mixed for both normal weight and lightweight concrete.

The data was compared to both the ACI 318-05 bearing strength criteria and the equation developed by Bonetti in the previous section. It was proposed that the ACI 318-05 bearing strength equation, Equation 2-9, be modified by a λ factor for lightweight concrete (See Equation 2-11).

From the research it was determined that Equation 2-11 is the simpler of the two equations but the equation developed by Bonetti in 2005 (Equation 2-4) is a better representation of the behavior at low A/A_b ratios. For the purpose of design, it was determined that m , the ratio of f'_c to f_{ct} in Bonetti's equation, can be assumed to be 10 for normal weight concrete and 12 for sand lightweight concrete.

$$F_{ult} = \lambda(0.85f'_cA_1)\sqrt{A_2/A_1} \leq 1.75f'_cA_1 \quad \text{where } \lambda = 0.70$$

*Equation 2-11: Modified
ACI Ultimate Bearing
Strength Equation*

Where:

F_{ult} = bearing strength

λ = modification factor, 0.70

f'_c = unconfined compressive strength of the concrete

A_1 = bearing area (See Figure 2-9)

A_2 = supporting area (See Figure 2-9)

Figure 2-10 and Figure 2-11 present bearing strength data for normal weight and lightweight concrete collected from previous research. In each figure, the data is compared with the ACI 318-05 bearing strength equation and the equation developed by Bonetti. In both cases, the equations are multiplied by the ACI ϕ -factor of 0.65 for bearing on concrete. The equation developed by Bonetti better represents the data for low A/A_b ratios than the ACI 318-05 bearing strength equation.

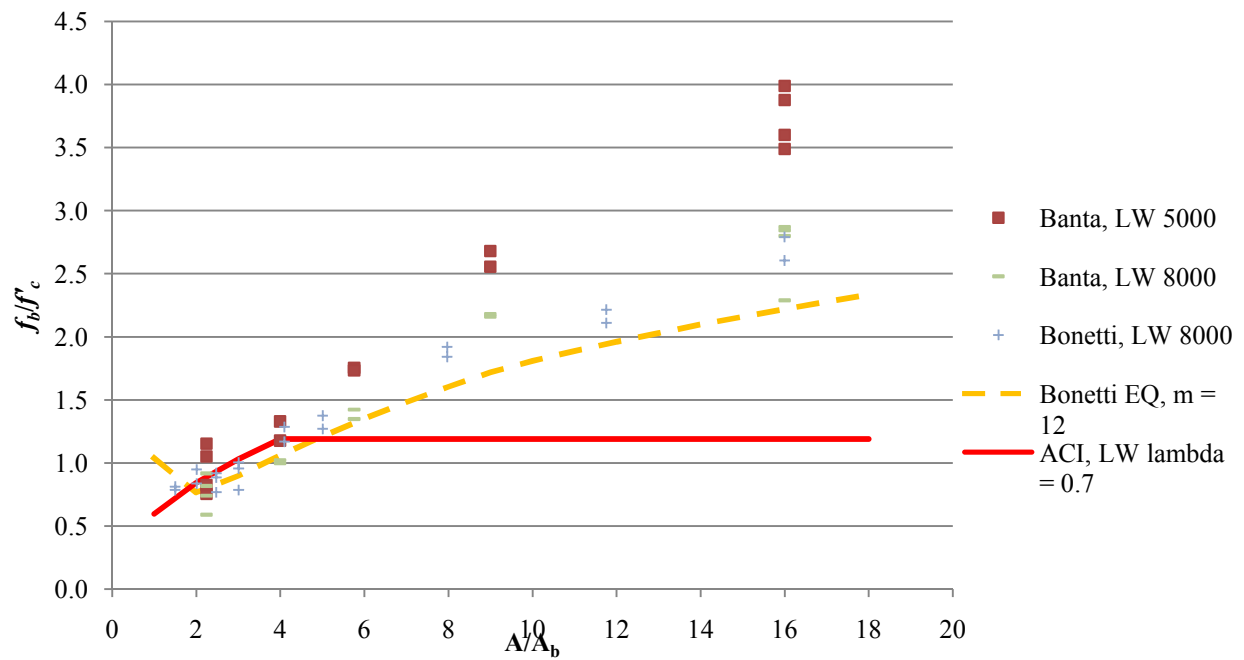


Figure 2-10: Lightweight Data (Roberts-Wollmann et al. 2006)

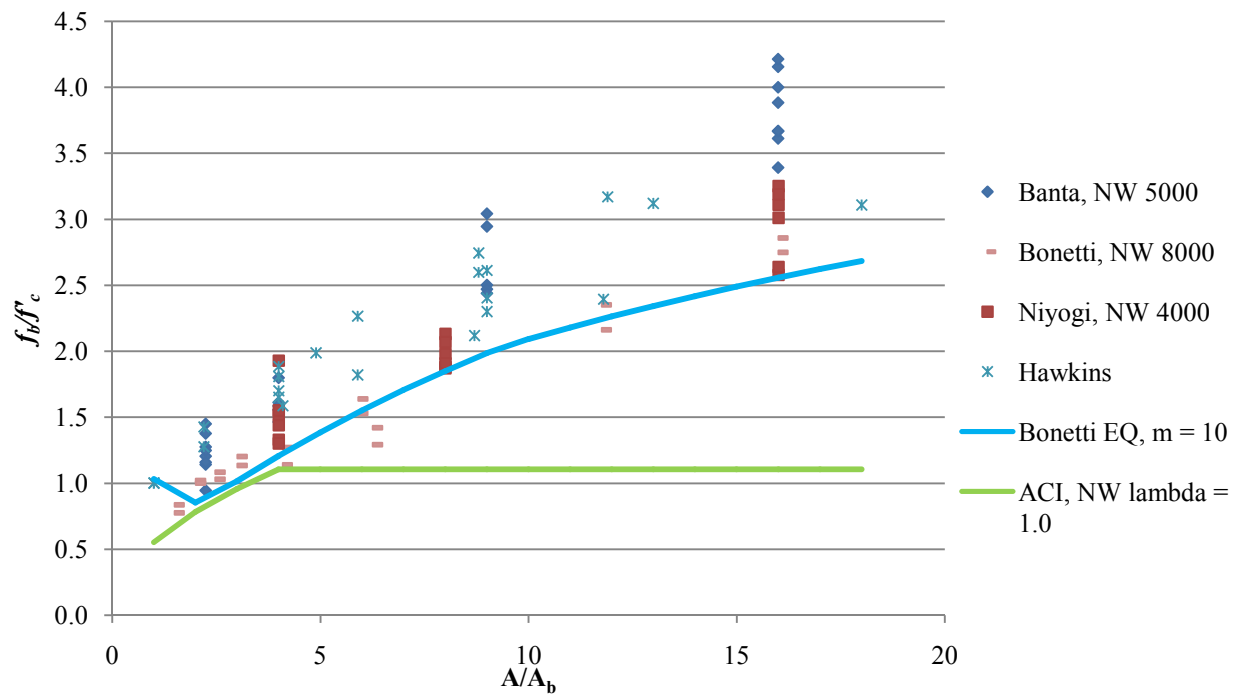


Figure 2-11: Normal Weight Data (Hawkins 1968b; Niyogi 1973; Roberts-Wollmann et al. 2006)

2.2 Confined Concrete Bearing Strength

2.2.1 Richart, Brandtzaeg, and Brown (1928, 1929)

Research published by the University of Illinois, Urbana investigated the strength of concrete under one, two, and three dimensional stress states (Richart et al. 1929; Richart et al. 1928). The goal of the research was to investigate how the material breaks down internally and the affect of lateral compressive stresses on the axial capacity of concrete.

In 1928, in three test series, concrete cylinders were subjected to a two dimensional state of stress, a three dimensional state of stress with stress in one direction much greater than the other two, and a three dimensional state of stress with one stress much less than the other two. The tests were done on concrete cylinders with fluid pressure applied to the curved sides and an axial load applied by a load test machine (Figure 2-12). Richart et al. determined that the unconfined compressive strength of the concrete increased by 4.1 times the lateral confining pressure shown in Equation 2-12 (Richart et al. 1928).

$$f_{cc} = f_{uc} + 4.1f_{lat}$$

*Equation 2-12: Richart, Brandtzaeg,
Brown Bearing Equation*

Where:

f_{cc} = confined compressive strength of the concrete
 f_{uc} = unconfined compressive strength of the concrete
 f_{lat} = lateral confining pressure

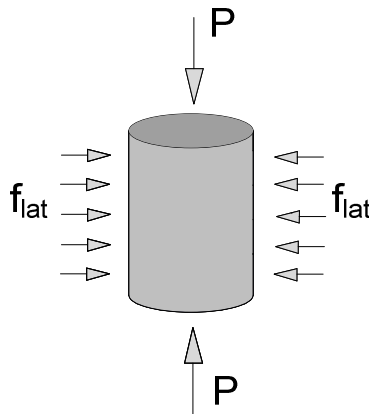


Figure 2-12: Richart, Brandtzaeg, and Brown Test Setup

In a research report published one year later, Richart et al. (1929) used spiral confining steel to confine concrete cylinders and then loaded the cylinders to failure to determine if spiral

reinforcing could provide the same increased strength as a fluid pressure. The pitch and the diameter of the confining steel were varied. From the testing, Richart et al. determined that Equation 2-12 developed from concrete confined by active oil pressure has a very good correlation to concrete confined by spirals (Richart et al. 1929).

2.2.2 Zieliński and Rowe (1960)

In 1960, research conducted by Zieliński and Rowe investigated the stress distributions in the anchorage zones of post-tensioned concrete members. The research investigated the effects of the presence of confining reinforcing, the presence of duct-tubes, the effects of embedded versus external bearing plates, and the effects of the A/A_b ratio.

Zieliński and Rowe concluded the size and shape of a post-tensioning anchor, whether it is external or embedded, does not significantly affect the distribution of stresses. The research showed that the controlling factor that determined the ultimate bearing strength of the concrete is the A/A_b ratio (Zieliński and Rowe 1960). This is a similar conclusion reached by Bonetti in 2005 (Bonetti 2005).

Another conclusion from Zieliński and Rowe was that the amount of reinforcement in the cross section will significantly affect the ultimate bearing strength for contact stresses up to 1.9 times the cube strength of the concrete. However, when the bearing stresses are in the range of 1.9 to 3.4 times the cube strength, no increase in ultimate bearing strength is apparent (Zieliński and Rowe 1960).

2.2.3 Niyogi (1975)

Continuing with research into the ultimate bearing strength of concrete discussed in Section 2.1.3, Niyogi investigated the effects of confinement in combination with A/A_b ratio on the ultimate bearing strength of concrete. The specimens were 8 in. cubes with either spiral or grid reinforcing to serve as confining reinforcing. The parameters of the research were the strength of the concrete, diameter of the spiral reinforcing, depth of the reinforcing, A/A_b ratio, and reinforcing configuration.

Niyogi concluded that an increase in the percentage of lateral steel increases the ultimate bearing strength of concrete for a given A/A_b ratio. As the A/A_b ratio increased, Niyogi observed that the difference between the first cracking load and the ultimate load was smaller.

Niyogi also observed that the depth of the reinforcing from the top face has little effect on the ultimate bearing strength of the concrete and that for an increase in the compressive strength of the concrete, f'_c , with A/A_b being constant; the bearing strength ratio n was decreased, which was also observed in his research on the ultimate bearing strength of unreinforced concrete (Niyogi 1975).

2.2.4 Bassett and Uzumeri (1986)

In 1986, Basset and Uzumeri investigated the effects of confinement on lightweight concrete. The parameters of the testing included different lateral reinforcement configurations and longitudinal reinforcement configurations. Basset and Uzumeri determined that though lightweight concrete is very brittle, according to the steep descending branch of the stress-strain diagram. Basset and Uzumeri concluded that adding a significant amount of confining reinforcing will increase the strength and ductility of the material. Basset and Uzumeri suggested that lightweight concrete in bearing behaves similarly to high-strength normal weight concrete in bearing (Basset and Uzumeri 1986).

2.2.5 Martinez, Nilson, and Slate (1984)

In 1984, in-depth research published by Martinez, Nilson, and Slate investigated the differences between normal weight concretes with compressive strengths ranging from 4,000 psi to 21,000 psi and lightweight concretes with compressive strengths ranging from 4,000 psi to 11,000 psi. The strengths were reached by varying the mix proportions and admixtures. All of the lightweight concrete mixes were sand-lightweight mixes. The research was carried out on 4 in. x 8 in., 4 in. x 16 in., 5 in. x 24 in., and 6 in. x 24 in. cylinders. The parameters of the research included size effects, varying wire diameter and spacing. Spiral reinforcing was the only reinforcing configuration investigated.

Several conclusions were reached by Martinez et al. that are important for the current research. First, confining reinforcing is about 63% less effective in lightweight concrete than in normal

weight concrete. Also, higher-strength concretes for both normal and lightweight concrete exhibited less strength gain for the same amount of confinement than did lower-strength normal weight and lightweight concrete. Data presented by Martinez et al. showed that with an increase in strength there was an increase in the slope of the ascending branch of the stress-strain curve. With a steeper slope, high-strength concretes also had lower lateral strains and therefore did not engage the confining steel as well as a lower-strength concrete.

The following equations were recommended for normal and high strength columns.

$$f_{cc} = 0.85f'_c + 4.0f'_2 \left(1 - \frac{s}{d_c}\right)$$

For,
 $3000\text{psi} \leq f'_c \leq 12000\text{psi}$

*Equation 2-13:
Normal Weight
Bearing Strength*

Where:

- f_{cc} = confined compressive strength of the concrete
- f'_c = unconfined compressive strength of the concrete
- f'_2 = lateral confining pressure provided by confining reinforcing
- s = tie spacing or spiral pitch of the lateral reinforcing
- d_c = tie side length of spiral diameter of the lateral reinforcing

$$f_{cc} = 0.85f'_c + 1.5f'_2 \left(1 - \frac{s}{d_c}\right)$$

For,
 $3000\text{psi} \leq f'_c \leq 9000\text{psi}$

*Equation 2-14:
Lightweight Bearing
Strength*

Where:

- f_{cc} = confined compressive strength of the concrete
- f'_c = unconfined compressive strength of the concrete
- f'_2 = lateral confining pressure provided by confining reinforcing
- s = tie spacing or spiral pitch of the lateral reinforcing
- d_c = tie side length of spiral diameter of the lateral reinforcing

The difference between Equation 2-13 and Equation 2-14 is the reduction of 4.0 to 1.5. This reduction takes into account that spiral reinforcing is less effective in light weight concrete than normal weight concrete. It should be noted that neither of the equations contain factors to include the effects of the A/A_b ratio. In applications of columns, the entire cross section is loaded instead of being loaded through a smaller bearing plate.

Martinez et al. recommended that ACI methods for design of spiral reinforcing are unconservative for use with lightweight concrete and should not be used for the design of spiral reinforcing in lightweight concrete.

2.2.6 Heilmann (1983)

In 1983, Heilmann performed load tests on lightweight concrete specimens similar to the specimens used in this research. The specimens had a cross section of 11.81 in. (30 cm) square and were 23.62 in. (60 cm) tall. The reinforcing consisted of ties at 3.15 in. (8 cm) on center over the whole height of the specimen and spiral reinforcing with a pitch of 2.36 in. (6 cm) in the top half of the specimen. The side length of the ties and the diameter of the spiral were both 10.63 in. (27 cm).

The concrete used by Heilmann was a lightweight concrete with a fresh unit weight of 96.8 pcf and a hard unit weight of 93.0 pcf. The average compressive strength of the concrete was 4454 psi and the average splitting cylinder strength of the concrete was 217 psi.

Heilmann found that providing confining reinforcing can increase the ultimate strength of lightweight concrete. However, the increase in strength of lightweight concrete specimens was less than that of normal weight concrete specimens having the same reinforcing.

2.2.7 NCHRP Report 356 (1994)

NCHRP Report 356 is a wide-ranging investigation of anchorage zone reinforcement for post-tensioned concrete girders. In the investigation to develop an equation to predict the ultimate bearing strength of the local zone, two key parameters were identified that greatly affected the ultimate bearing strength of the local zone. The two parameters are the A/A_b ratio and the confinement by the reinforcing steel. Previous research has shown that the two parameters work together to affect the capacity of the local zone.

Report 356 specifically defines the local zone as a volume of concrete directly behind the loading plate with dimensions that depend on the geometry of the anchorage device being used. Figure 1-1 defines the locations of both the general and local zone.

The equation to predict the ultimate load of the local zone modifies Equation 2-12 by including factors for the A/A_b ratio effect and an efficiency factor to modify the area of confined concrete core. The equation, considered a guideline for designing the reinforcing in a local zone for testing, is as follows:

$$F_{ult} = 0.80f'_c\sqrt{\frac{A}{A_b}}(A_b) + 4.1f_{lat}A_{core}\left(1 - \frac{s}{D}\right)^2$$

*Equation 1-1: NCHRP
Ultimate Bearing Strength
of the Local Zone*

Equation 2-15 and Equation 2-16 calculate f_{lat} for spiral and tied reinforcing respectively and the model used to derive each equation is shown in Figure 2-13 and Figure 2-14 for spirals and ties respectively. The equations make the assumption that the spiral steel is yielding and is backed by research (Roberts 1990).

$$f_{lat} = \frac{2A_s f_y}{(D)(s)}$$

*Equation 2-15: f_{lat}
for Spiral reinforcing*

Where:

- f_{lat} = lateral confining pressure provided by lateral reinforcing
- A_s = area of the lateral steel reinforcing
- f_y = yield strength of reinforcing steel
- D = spiral diameter
- s = spiral pitch

$$f_{lat} = \frac{2A_s f_y}{(L)(s)}$$

*Equation 2-16: f_{lat}
for Tied Reinforcing*

Where:

- f_{lat} = lateral confining pressure provided by lateral reinforcing
- A_s = area of the lateral steel reinforcing
- f_y = yield strength of reinforcing steel
- L = tie side length
- s = tie spacing

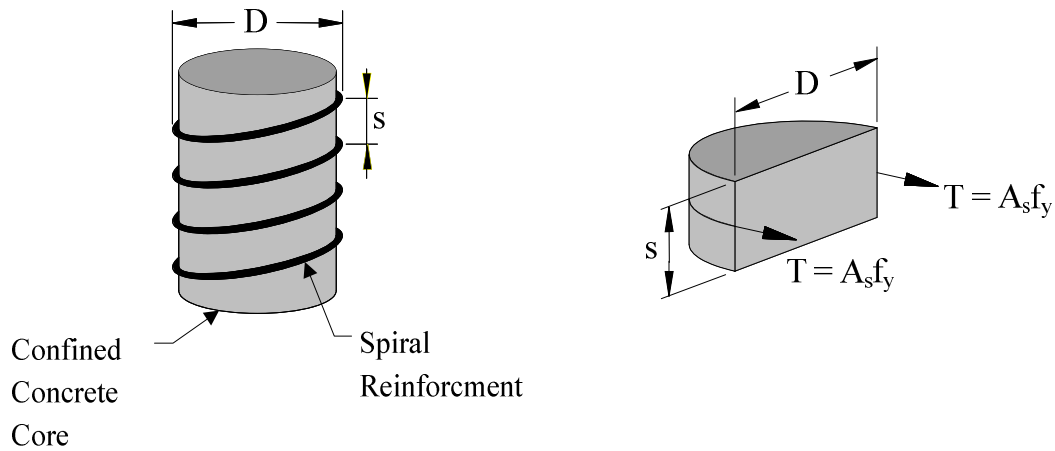


Figure 2-13: Spiral Reinforcing

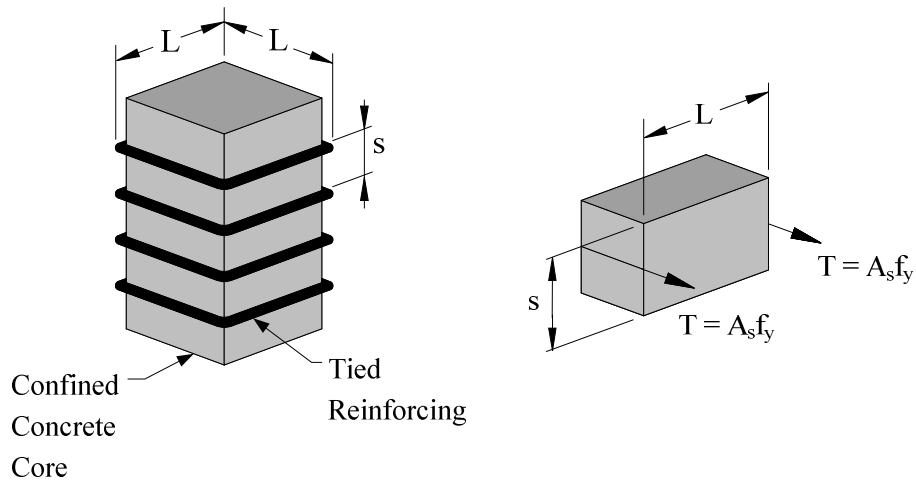


Figure 2-14: Tied Reinforcing

Researchers have shown that as the spacing reaches either the diameter or side length of a spiral or tie respectively, the lateral reinforcing becomes less effective. The reduced effectiveness is due to the concrete arching between the lateral reinforcing, both spiral and tied reinforcing, as shown in Figure 2-15.

In spirals, the confining pressure is developed in through hoop tension in the reinforcing bar. For ties, the confining pressure decreases as the distance from the bent corners of the tie increases. Near the midpoint between the bent corners of the tie, the lateral confining pressure is more dependent on the flexural rigidity of the reinforcing bar than the tension developed in the reinforcing bar (Saatcioglu and Ravzi 1992). Research has shown that ties are about half as

effective as spirals due to bowing action in the lateral reinforcing between longitudinal bars (See Figure 2-17). Equation 2-18, the area of the confined core for tied reinforcing, is reduced by half to account for the reduced effectiveness from bending of the confining reinforcing.

$$A_{core} = \frac{\pi D^2}{4} - A_{Duct}$$

Equation 2-17: A_{core} for Spiral

Where:

A_{core} = area of the confined core

D = diameter of the spiral

A_{Duct} = area of the duct

$$A_{core} = \frac{1}{2} L^2 - A_{Duct}$$

Equation 2-18: A_{core} for Ties

Where:

A_{core} = area of the confined core

L = side length of the tie

A_{Duct} = area of the duct

$$\left(1 - \frac{s}{D}\right)^2$$

Equation 2-19: Efficiency Factor

Where:

s = tie spacing or spiral pitch

D = tie side length or spiral diameter

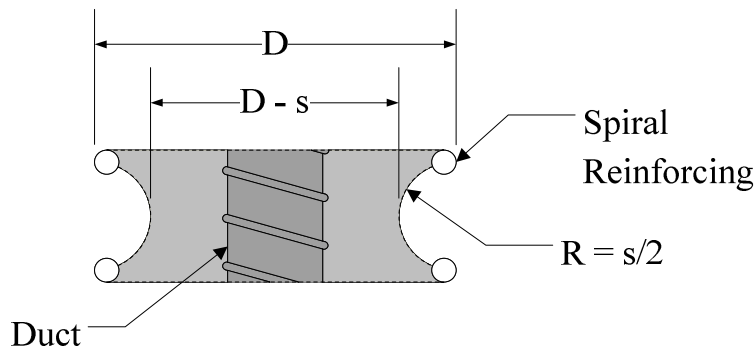


Figure 2-15: Well Confined Core with Spiral Reinforcing

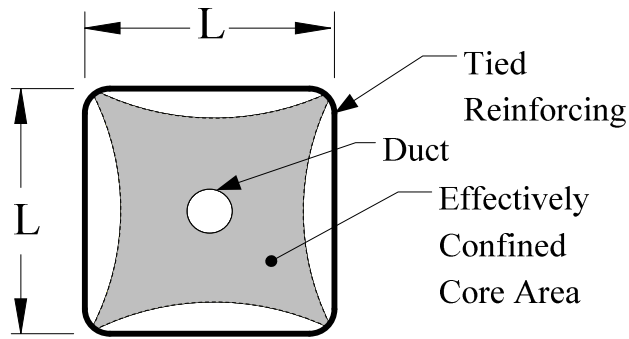


Figure 2-16: Well Confined Core with Tied Reinforcing

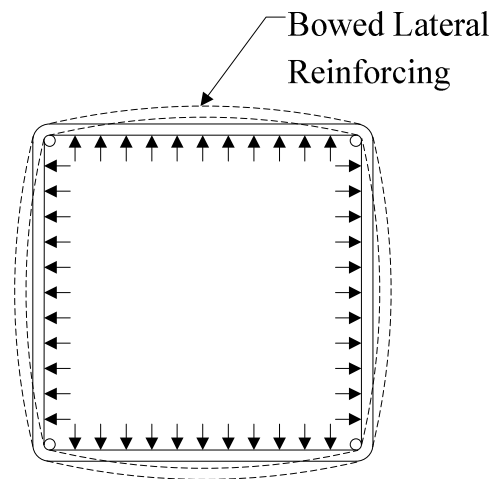


Figure 2-17: Bowing Action in Ties from Lateral Pressure

2.2.8 Bonetti (2005)

In addition to the development of an equation to estimate the ultimate bearing strength of unreinforced concrete based on a modified Mohr criterion, Bonetti also developed two equations to estimate the bearing strength of reinforced concrete. Both equations are based on his original bearing strength equation shown in Equation 2-4.

His first attempt at developing an equation to estimate the ultimate bearing strength of reinforced concrete was based on fitting a curve to data points from tests. The curve was passed on the of the ultimate bearing strength of reinforced concrete over the ultimate bearing strength of plain concrete versus the mechanical reinforcing ratio. This equation is as follows:

$$P = k \left(\frac{A f'_c}{m \beta + \alpha} \right)$$

*Equation 2-20:
Bonetti Reinforced
Bearing Equation*

Where:

P = ultimate bearing strength

k = See Equation 2-21

A = gross area of the concrete specimen

f'_c = unconfined bearing strength of the concrete

m = ratio of f'_c to f_{lat}

α = See Equation 2-7

β = See Equation 2-5

Using data from Roberts (1990), Bonetti determined that the k -value is of the following form and is based on the mechanical reinforcing ratio, ω .

$$k = 2.82\omega^{0.24} \text{ where } k < 2.4$$

Equation 2-21: k-value

Where:

ω = mechanical reinforcing ratio (See Equation 2-22)

For reference the mechanical reinforcement ratio is given as:

$$\omega = \frac{4A_s f_y}{sDf'_c} = \frac{2f_{lat}}{f'_c}$$

*Equation 2-22:
Mechanical
Reinforcement Ratio*

Where:

A_s = area of the lateral steel reinforcing

f_y = yield strength of reinforcing steel

s = tie spacing or spiral pitch of the lateral reinforcing

D = tie side length or spiral diameter of the lateral reinforcing

f'_c = unconfined compressive strength of the concrete

f_{lat} = lateral confining pressure provided by lateral reinforcing

The second equation developed to determine the ultimate bearing strength of reinforced concrete is based on Mohr's failure criterion. For this equation, the m term is modified by adding the lateral pressure, f_{lat} , to the splitting tensile strength, f_t (See Equation 2-20). This modification takes into account the additional lateral confining pressure contributed by the confining reinforcing. Bonetti also multiplied the compressive strength by 1.25 to account for the additional compressive strength enhancement of the confining reinforcing.

$$P = \frac{1.25Af'_c}{m_r\beta + \alpha}$$

$$m_r = \frac{f'_c}{f'_t + f_{lat}}$$

*Equation 2-23:
Bonetti Reinforced
Bearing Equation*

*Equation 2-24:
Modified m*

2.3 Splitting Tensile Strength of Lightweight Concrete

ACI 318-05 suggests that the tensile strength of the normal weight concrete should be estimated as 10% of the compressive strength of the concrete or 6.7 times the square root of the compressive strength of the concrete. The values listed in Table 2-1 are based on the factors for all-lightweight and sand-lightweight concrete multiplied by 6.7.

$$F_{sp} = \frac{f_{ct}}{\sqrt{f'_c}} \quad \text{Equation 2-25: } F_{sp}$$

Where:

- F_{sp} = ratio of f_{ct} to the square root of f'_c
- f_{ct} = splitting cylinder strength
- f'_c = unconfined compressive strength of the concrete

The following table presents some values of F_{sp} given from various sources.

Table 2-1: Values of F_{sp}

Source	F_{sp}
(Slate et al. 1986)	5.0
ACI 318-05, All-lightweight Concrete	5.0
ACI 318-05, Sand-lightweight Concrete	5.7
(Nilson et al. 2004)	4.0 to 6.0

A study by Ivey and Buth on the splitting tensile strength of lightweight concrete showed that the relationship between f_{ct} and the square root of the compressive strength, f'_c , is not linear as most of the equations assume. The research shows that as the compressive strength increases the value of F_{sp} decreases (Buth and Ivey 1966). Data from two sources are presented in Figure 2-18 (Buth and Ivey 1966; Hanson 1962). Both sources of data varied the aggregate used and proportions of their concrete mixes to achieve different strength lightweight concrete. The trend of the data in Figure 2-18 shows that as the compressive strength increases, the value of F_{sp} decreases.

The following equation was developed by Gjrv and Zhang (1991) from their own data and is not based on the same relationship between the splitting tensile strength and the square root of the compressive stress (See Equation 2-26).

$$f_{ct} = 0.23 \sqrt[3]{f'_c{}^2} \text{ where } f_{ct} \text{ and } f'_c \text{ are both in MPa}$$

Equation 2-26: (Gjørsv
and Zhang 1991)

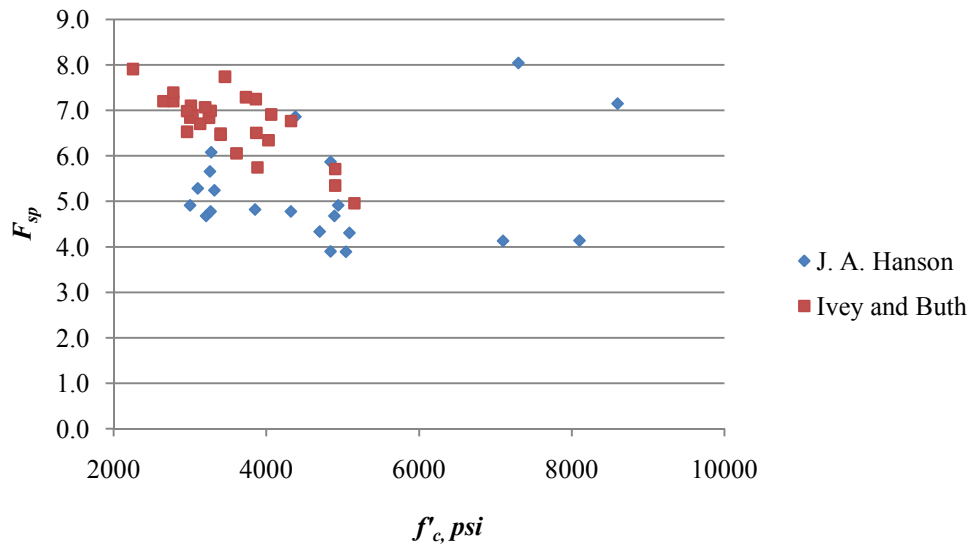


Figure 2-18: F_{sp} Data

2.4 Modulus of Elasticity of Lightweight Concrete

Below is a list of equations that have been recommended to estimate the modulus of elasticity of concrete.

$$E_c = 0.033(w_c)^{1.5} \sqrt{f'_c} \quad (ksi)$$

Equation 2-27: ACI 318-05 Modulus of Elasticity

$$E_c = (40\sqrt{f'_c} + 1,000) \left(\frac{w_c}{145} \right)^{1.5} \quad (ksi)$$

Equation 2-28: (Slate et al. 1986)

$$E_c = 0.0275(w_c)^{1.5} \sqrt{f'_{co}} \quad (ksi)$$

Equation 2-29: (Ahmad and Shah 1982)

$$E_c = 34.92\sqrt{f'_{co}} \quad (ksi) * \quad \text{Where } f'_{co} \text{ is in psi}$$

Equation 2-30: (Khaloo and Kim 1999)

$$E_c = 9.24\sqrt[3]{(f'_c)^2} \quad (psi) * \quad \text{Where } f'_c \text{ is in psi}$$

Equation 2-31: (Gjørøv and Zhang 1991)

*Equations have been converted from SI units to English units

Equation 2-27 is from ACI 318-05 and has been shown to be unconservative because it overestimates the actual modulus of elasticity (Carrasquillo et al. 1981; Slate et al. 1986). The second modulus of elasticity equation (Equation 2-28) was proposed to be a better estimation (Slate et al. 1986). Equation 2-30 is based on research done to determine the effects of curing on the modulus of elasticity of lightweight concrete (Khaloo and Kim 1999).

All equations are based on a best fit line to the data. Also, all equations except for Equation 2-30 and Equation 2-31 are based on the unconfined compressive strength of the concrete and the unit weight. Equation 2-30 and Equation 2-31 are only based on the unconfined compressive strength of the concrete.

Research has shown that the curing conditions and modulus of elasticity of the aggregate have a great deal of influence on the modulus of elasticity of lightweight concrete (Haque et al. 2004; Khaloo and Kim 1999).

2.5 Summary

Chapter 2.0 has presented the previous research that relates to the bearing strength of both confined and unconfined normal weight concrete. The research has been crucial to developing equations to design a local zone in post-tensioned concrete. The parameters that affect the local zone of post-tensioned concrete have been researched and incorporated into equations used to estimate the strength of the local zone.

There has been little research in the unreinforced and reinforced bearing strength of lightweight concrete. There has been some research into the unreinforced bearings strength of lightweight concrete and the result has been a modification factor to modify the ACI 318-05 bearing strength equation for lightweight concrete. Little research has been done to advance the knowledge of estimating the strength of the local zone of lightweight concrete. The current equation presented in the NCHRP report 356 has been shown to work for normal weight concrete, but more investigations are needed to determine if it can be applied to local zones in lightweight concrete.

With the increase of lightweight concrete being used in structural and post-tensioned applications, more research is needed to determine how the currently understood parameters that affect the bearing strength of lightweight concrete.

Chapter 3.0 Testing Program

Chapter 3.0 presents the testing program and concrete properties used in this research. Described in this chapter are the dimensional and reinforcing of all of the specimens tested in this investigation. Chapter 3.0 also presents the compressive strength, splitting tensile strength, and the modulus of elasticity of the concrete used in this investigation

3.1 Concrete Prism Properties

The specimens used were based on dimensions of specimens that were used in a previous investigation at Virginia Tech by Bonetti (Bonetti 2005). This was done for purpose of comparison of results, with the only difference being the type of concrete. Bonetti's specimens were cast of normal weight concrete and the specimens that were used in this research were cast of lightweight concrete.

The specimens had a cross section of 8 in. x 8 in. and were 16 in. in height with 1 in. of cover over the reinforcing. The local zone reinforcing was located in the top 8 in. of the specimen to imitate the typical configuration of a local zone specimen presented in Figure 1-1. Since the main area of interest within the specimens was the top 8 in., the bottom 8 in. contained nominal tied reinforcing to prevent failure in the bottom portion of the prism before the top portion. See Figure 3-1 for an example of a typical specimen. Two specimens were cast without any reinforcing to all as a benchmark to compare strength gain for the reinforced prisms.

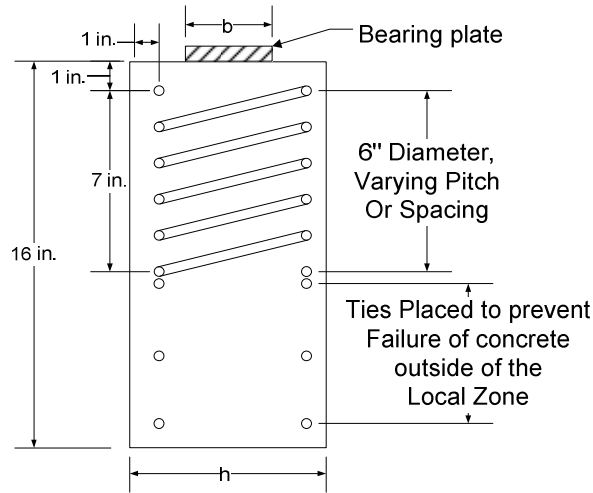


Figure 3-1: Example of Specimen (Profile view)

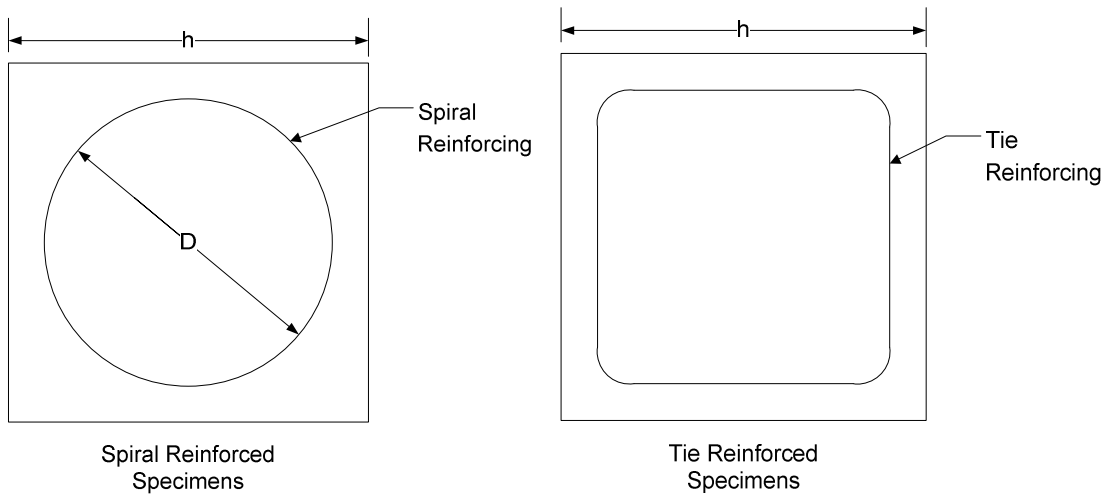


Figure 3-2: Example of Specimens (Plan View)

Gang forms were constructed out of $\frac{3}{4}$ in. plyform, which is plywood impregnated with form oil. The specimens were cast upside down (Figure 3-3). After three weeks, strips of Homasote Board, which is a compressed wood fiber board, were attached to the formwork surrounding the top of each block (See Figure 3-4). This allowed for a thin layer of low viscosity epoxy to be applied to the bottom of each block to allow for a level surface for the specimen to rest on during testing. For purposes of tracking compressive strength gain, tensile strength gain, and modulus of elasticity, 4 in. x 8 in. cylinders were cast and cured with the specimens.



Figure 3-3: Reinforcing cages in the formwork



Figure 3-4: Homasote Board attached to formwork to contain epoxy layer

Table 3-1 presents the details of all of the prism specimens, both reinforced and unreinforced.

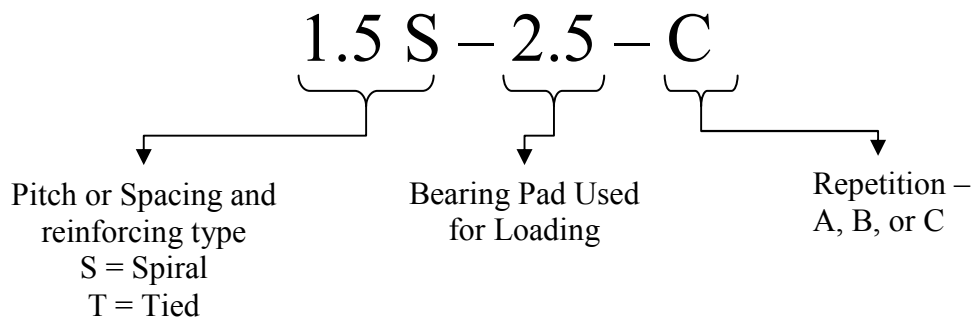
Figure 3-5 presents the naming convention used to name the reinforced prism specimens.

Table 3-1: Details of Prism Specimens

Block	Specimen Name**	Confining Reinforcing	Spacing	Pitch	D or L	h, Block*	b, Plate*	A/A _b
1	2.5T-4-A	Ties	2.5		6	8	4	4
2	2.5T-4-B	Ties	2.5		6	8	4	4
3	2T-4-A	Ties	2		6	8	4	4
4	2T-4-B	Ties	2		6	8	4	4
5	2T-4-C	Ties	2		6	8	4	4
6	1.5T-4-A	Ties	1.5		6	8	4	4
7	1.5T-4-B	Ties	1.5		6	8	4	4
8	1.5T-4-C	Ties	1.5		6	8	4	4
9	2.5T-2.5-A	Ties	2.5		6	8	2.5	10.24
10	2.5T-2.5-B	Ties	2.5		6	8	2.5	10.24
11	2T-2.5-A	Ties	2		6	8	2.5	10.24
12	2T-2.5-B	Ties	2		6	8	2.5	10.24
13	2T-2.5-C	Ties	2		6	8	2.5	10.24
14	1.5T-2.5-A	Ties	1.5		6	8	2.5	10.24
15	1.5T-2.5-B	Ties	1.5		6	8	2.5	10.24
16	1.5T-2.5-C	Ties	1.5		6	8	2.5	10.24
17	2.5S-4-A	Spiral		2.5	6	8	4	4
18	2.5S-4-B	Spiral		2.5	6	8	4	4
19	2S-4-A	Spiral		2	6	8	4	4
20	2S-4-B	Spiral		2	6	8	4	4
21	2S-4-C	Spiral		2	6	8	4	4
22	1.5S-4-A	Spiral		1.5	6	8	4	4
23	1.5S-4-B	Spiral		1.5	6	8	4	4
24	2.5S-2.5-A	Spiral		2.5	6	8	2.5	10.24
25	2.5S-2.5-B	Spiral		2.5	6	8	2.5	10.24
26	2S-2.5-A	Spiral		2	6	8	2.5	10.24
27	2S-2.5-B	Spiral		2	6	8	2.5	10.24
28	1.5S-2.5-A	Spiral		1.5	6	8	2.5	10.24
29	1.5S-2.5-B	Spiral		1.5	6	8	2.5	10.24
30	1.5S-2.5-C	Spiral		1.5	6	8	2.5	10.24
31	Unreinforced	None				8	4	4
32	Unreinforced	None				8	4	4

* Values h and b shown in Figure 3-1

** See Figure 3-5 for explanation of specimen name



3.2 Testing Procedures for Concrete Prisms

All prism specimens were tested in a 300 kip SATEC testing machine using a MTS 407 controller. The specimens were aligned with the upper load head to ensure even loading. All specimens were loaded through a 1 in. steel plate with a 1/8 in. rubber bearing pad between the plate and the concrete. The bearing pad was cut to the cross sectional dimensions of the plate being used. The plate was loaded completely over its top surface to ensure that the full area of the bearing plate and pad in contact with the concrete was transferring load to the specimens (See Figure 3-6).

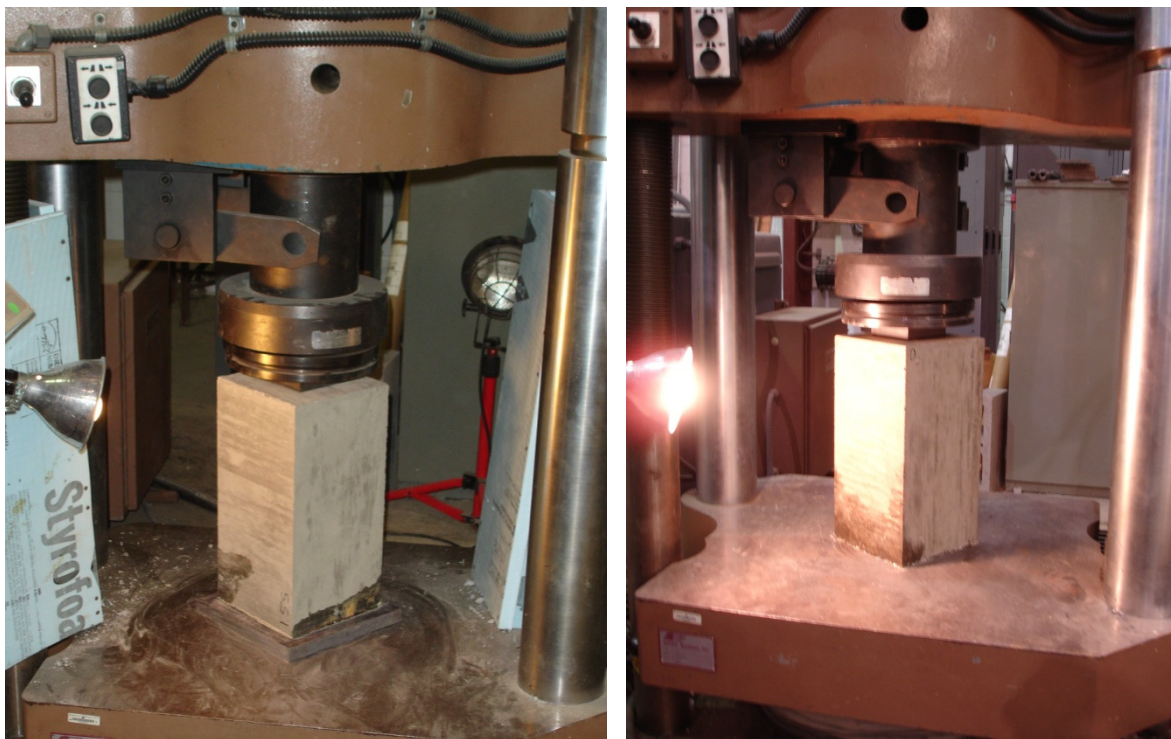


Figure 3-6: Test setup of Concrete Prisms

In previous investigations (Hawkins 1968b; Niyogi 1973) bearing pads were not used in the testing. The bearing pad was used to prevent stress concentrations in the top of the specimen from an uneven bearing surface.

The load was increased incrementally applied by force control. The load was applied without cycling as with the AASHTO testing procedure discussed in Section 1.0. Cracking on all four faces of the specimen was monitored to determine the first cracking load for each face. Each test

elapsed approximately 15 to 20 minutes. Once cracking was achieved, the load was increased until the specimen failed. The ultimate load was monitored with a computer, running StrainSmart software, attached to the MTS 407 controller.

The two unreinforced concrete prisms were tested in the same way as the reinforced concrete prisms with the only difference being that the cracking was not tracked due to safety concerns.

3.3 Concrete Cylinders

This section discusses how concrete cylinders were tested to determine the compressive strength, Splitting cylinder strength, modulus of elasticity, and the tests carried to determine the effect of the A/A_b ratio on lightweight concrete. All cylinders were made per ASTM C 138.

3.3.1 Compressive Strength Tests

4 in. x 8 in. cylinders were tested in a 400 kip Forney testing machine. The specimens were tested with neoprene caps on both the top and the bottom.

3.3.2 Splitting Cylinder Strength Tests

Specimens were tested in a device made specifically for splitting cylinder tests. The device allowed for the application of a vertical distributed force to be applied to a cylinder along its length. The load was applied through two strips of soft wood to reduce the possibility of stress concentrations between the loading plate and the concrete. The device with a cylinder is shown in Figure 3-7.

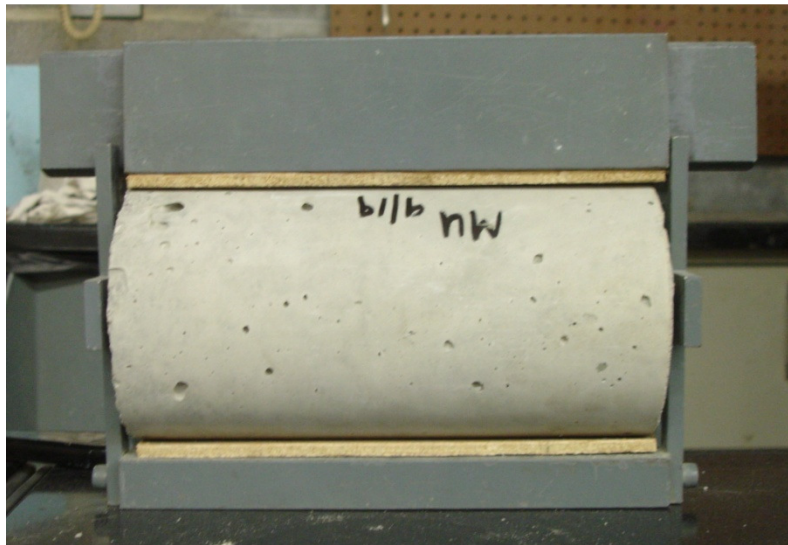


Figure 3-7: Split Cylinder Device

3.3.3 Modulus of Elasticity Tests

Starting on the seventh day 4 in. x 8 in. cylinders were axially loaded and the strains were measured using the device shown in Figure 3-8. The modulus of elasticity was determined using

a best fit line through stress strain plots. The cylinders were loaded up to 40% of f'_c that was measured on the same day as the strains. Strains were taken approximately every 4000 lbs.



Figure 3-8: External Strain Gage for a 4 in. x 8 in. cylinder

The modulus of elasticity was determined by passing a best fit line through the data.

3.3.4 A/A_b tests

4 in. x 8 in. cylinders were used to determine the effects of A/A_b ratio on the concrete. Round plates of with diameters of 2 1/6 in., 2 7/16 in. and 3 3/16 in. were used to test the cylinders.

The cylinders were placed in a 400 kip Forney testing machine on a neoprene cap that is normally used for compressive testing. The cylinders were flipped upside down from the orientation in which they were cast so that the rough top surface was down and the smooth bottom surface was up. The neoprene cap reduced the likelihood of having stress concentrations between the bottom platen and the concrete cylinder. The bearing plates were placed directly on the smooth surface of the concrete formed by the cylinder mold (See Figure 3-9). No rubber pad was used because the surface of the concrete was smooth.



Figure 3-9: Cylinder Test Setup

3.4 Concrete Properties

For the purposes of this investigation, a sand-lightweight concrete supplied by the local batch plant was used. The concrete mix was used on a previous research project at Virginia Tech and the data recorded for this research compared to the previous research (Dymond 2007). The mix proportions are given in Table 3-2. The aggregate used in this research was an expanded slate and was produced by the Stalite Company out of North Carolina (www.stalite.com).

When the concrete arrived at the lab, the unit weight of the concrete was approximately 122 pcf and this was determined using ASTM C 138. The concrete was moist cured for 7 days in its formwork. The formwork and cylinder molds were removed on day 30.

The compressive and tensile strength gain data for the current research is given in Table 3-3 and Table 3-4, respectively. The modulus of elasticity data for the current research is given in Table 3-6. The concrete properties from the previous research, Dymond (2007), are given in Table 3-5. Graphically, the compressive strength gain, tensile strength gain, and modulus of elasticity versus time are given in Figure 3-10, Figure 3-11, and Figure 3-12 respectively.

From Figure 3-10 and Figure 3-11 it is apparent that Dymond's concrete had a higher strength gain than the concrete in the current research. This is probably due to the concrete curing conditions. Dymond removed his forms after 7 days and moist cured for the first 14 days. In the current research, the moist cure only last 7 days but the forms were not removed until the 28th day. All remaining cylinders after the prism tests were complete were used for the A/Ab testing discussed in Section 3.3.4.

Table 3-2: Design Lightweight Concrete Mix Proportions

Component	Mix Design (per yd ³)
Portland Cement	520 lb.
Fly Ash	130 lb.
Natural Sand	1216 lb.
¾" Stalite Lightweight Stone	976 lb.
Water	31.2 gal.
Air Entrainment	0 oz.
Retarder	13 oz.
Super Plasticizer	20 oz.
W/C ratio	0.4
Target % Air	3-5%
Target Slump	5-7 in.

Table 3-3: Compressive Strength Gain Data

Age, days	Cylinder 1, kips	Cylinder 2, kips	Average Load, kips	f'_c , psi
2	30	28.5	29.25	2328
7	50.5	5.25	51.25	4098
14	58.5	60	59.25	4715
21	62.5	68	65.25	5192
28	74.9	74.9	74.9	5960
40	90	87.5	88.75	7063
51	95	87.5	91.25	7261

Table 3-4: Tensile Strength Gain Data

Age, days	Cylinder 1, kips	Cylinder 2, kips	Average Load, kips	f_{ct} , psi
7	14.4	14.7	14.55	289
14	23.2	21.4	22.3	444
21	27.5	25	26.25	522
28	30	30	30	597
40	30	25	27.5	547
51	35	35	35	696

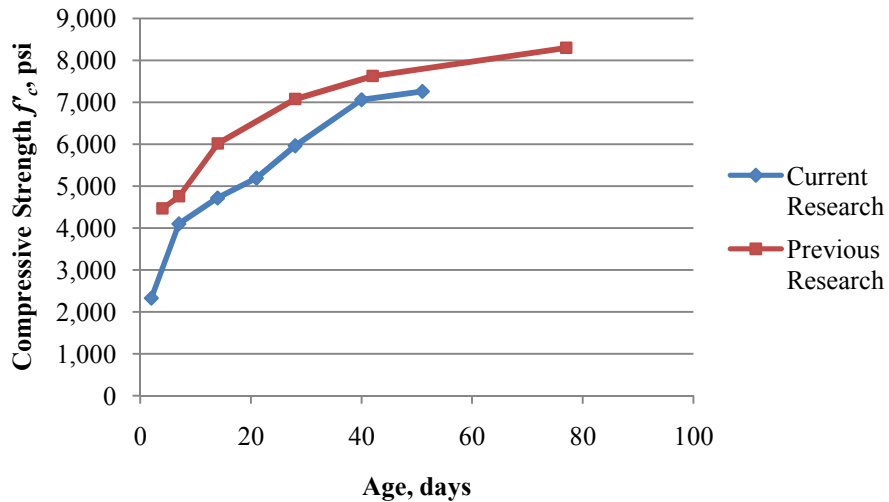


Figure 3-10: Compressive Strength Gain Chart

According to Figure 3-10, the compressive strength of the concrete from this research did not gain strength as fast as the concrete from Dymond’s research. This is expected because Dymond moist cured his concrete for 14 days unlike the concrete used in this research that was moist cured for 7 days.

Table 3-5: Concrete Properties from Dymond 2007

Day	f'_c , psi	f_{ct} , psi	Experimental Modulus, ksi
4	4,470	--	--
7	4,760	534	2,793
14	6,020	587	3,035
28	7,080	673	2,847
42	7,360	683	2,864
77	8,300	701	3,125

Table 3-6: Experimental Modulus of Elasticity Data

Day	f'_c , psi	Experimental Modulus, ksi
7	4,100	2,940
14	4,720	2,820
21	5,190	3,150
28	5,960	3,570
40	7,060	2,870
51	7,260	2,720

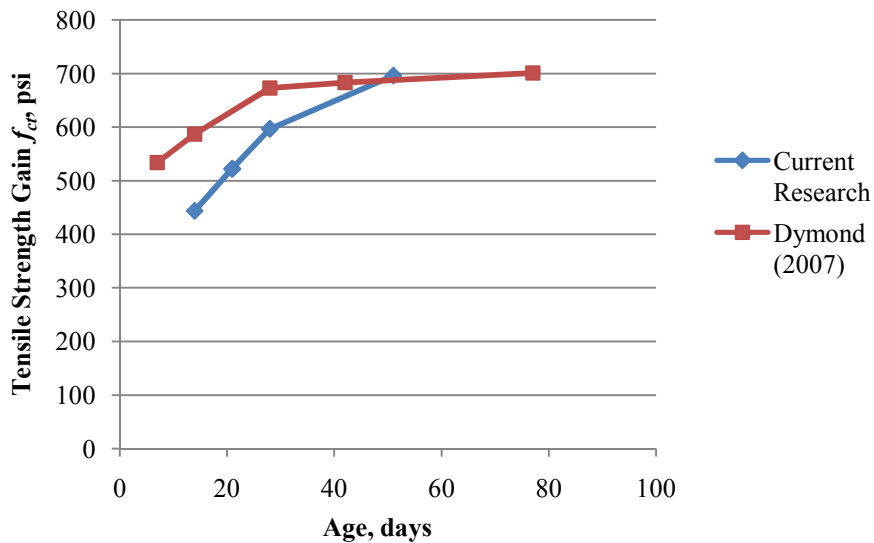


Figure 3-11: Tensile Strength Gain Chart

Similar to the compressive strength, the tensile strength of the concrete used in this research is consistently lower than the concrete used in Dymond’s research. However, on day 51, the splitting tensile strength of the concrete measured in this research was comparable to the splitting tensile strength of the concrete from Dymond’s research. Further discussion of the splitting tensile strength data is in Section 4.3.

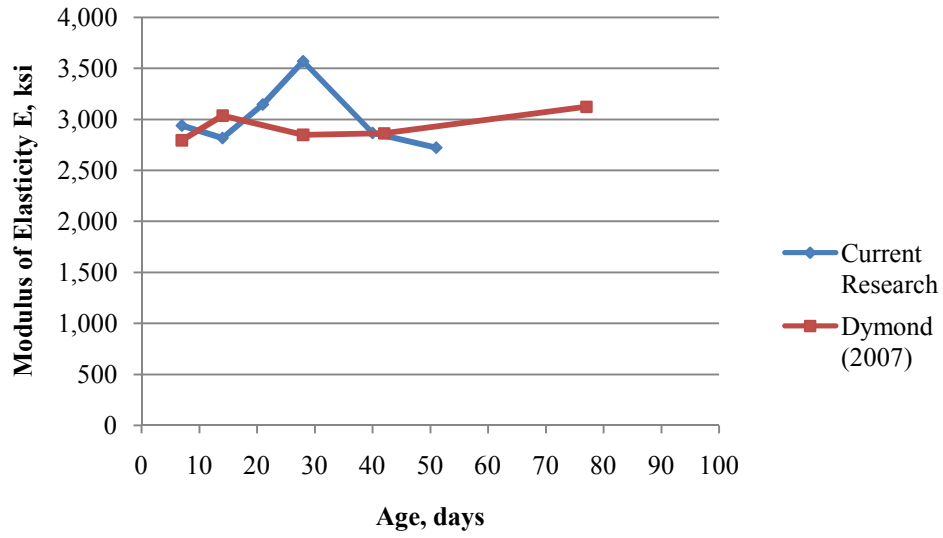


Figure 3-12: Modulus of Elasticity Data

Discussion of the modulus of elasticity data is given in Section 4.4.

Chapter 4.0 Results and Data Analysis

Chapter 4.0 presents the results and the discussion of the data collected in this investigation as data collected in other investigations.

For the analysis of the affect of the A/A_b ratio on the unreinforced bearing strength of lightweight concrete, test data from this research was compared to equations discussed in 2.1 of the literature review. These equations are Hawkin's equation (Equation 2-2), Niyogi's equation (Equation 2-3), Bonetti's equation (Equation 2-4), and Banta's modified ACI equation (Equation 2-11). Two λ factors to be used for Banta's equation are 0.70 and 0.85. Data sets from previous research that include low strength and high strength lightweight concrete were compared to the modified ACI equation (Equation 2-11) and Bonetti's equation (Equation 2-4).

To analyze the accuracy of the NCHRP equation for use with lightweight concrete, three data sets will be compared to the NCHRP equation. The three data sets are the data collected in this research, the Heilmann data, and data collected in slab anchor testing (Axson 2007a; Axson 2007b; Axson 2007c; Axson 2007d). The three data sets were also compared to two equations developed by Bonetti to determine the ultimate strength of reinforced concrete (Bonetti 2005).

4.1 Unreinforced Bearing Strength

The purpose of these tests was to determine the effect of the A/A_b ratio on the unreinforced bearing strength of lightweight concrete. Data collected from cylinder testing and from the two unreinforced 8 in. x 8 in. x 16 in. prisms in this research are compared to equations discussed in Section 2.1. Data presented in previous research is also included in the analysis.

4.1.1 Results and Observations

At the time of testing the cylinders, day 51, the compressive strength, f'_c , of the concrete was 7261 psi and the splitting tensile strength was 696 psi. The compressive strength and splitting cylinder strength of the concrete in the prisms at the time of testing was 7063 psi and approximately 650 psi, respectively.

Table 4-1 presents the results of the testing conducted in this research.

Table 4-1: Unreinforced Bearing Strength Data

Plate Size, in.	Plate Area, in. ²	Load, kips	f_b , ksi	f_b/f'_c	A/A_b
Circular plate on 4 in. x 8 in. Cylinders					
2 1/16	3.34	35000	10.48	1.44	3.76
2 1/16	3.34	35000	10.48	1.44	3.76
2 7/16	4.67	42500	9.11	1.25	2.69
2 7/16	4.67	40000	8.57	1.18	2.69
3 3/16	7.98	59000	7.39	1.02	1.57
3 3/16	7.98	52500	6.58	0.91	1.57
Square Plate on 8 in. x 8 in. x 16 in. Prisms					
4	16	123000	7.69	1.06	4
4	16	124000	7.75	1.07	4

Cylinders that were loaded through larger bearing plates failed as the concrete that surrounded the bearing plate split from the bulk of the cylinder (See Figure 4-1 and Figure 4-2). Cylinders that were loaded through smaller bearing plates exhibited a punching failure (See Figure 4-3). The fractured cylinder has a shape of a cone below the bearing pad and evidence of this is shown in Figure 4-4, which is a detailed view of Figure 4-1 and Figure 4-2.

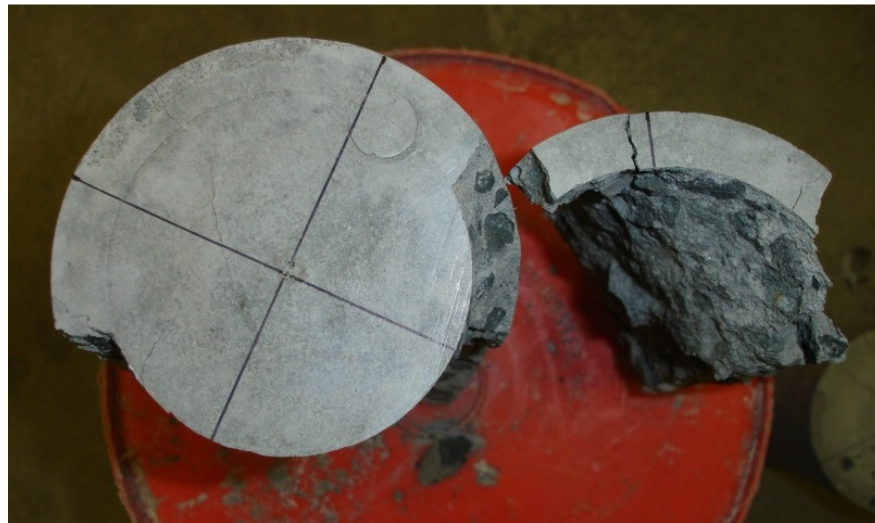


Figure 4-1: Plan View of Failed of Concrete Cylinders



Figure 4-2: Profile View of Concrete Cylinder

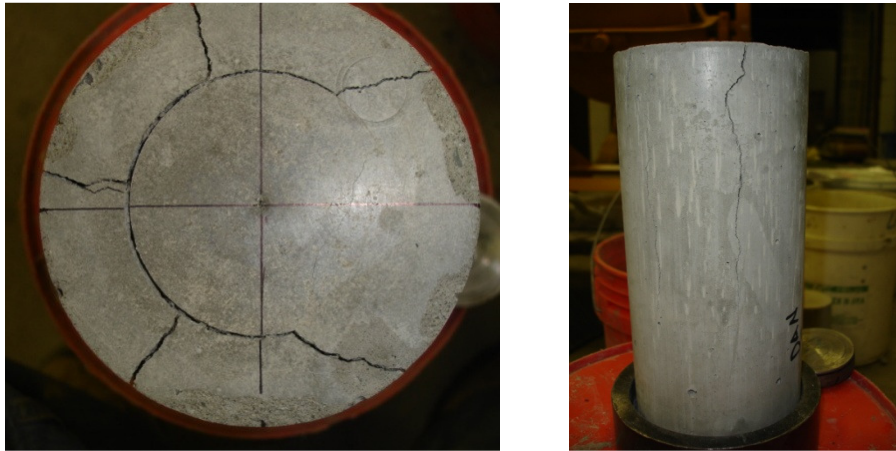


Figure 4-3: Plan and Profile View of Punching

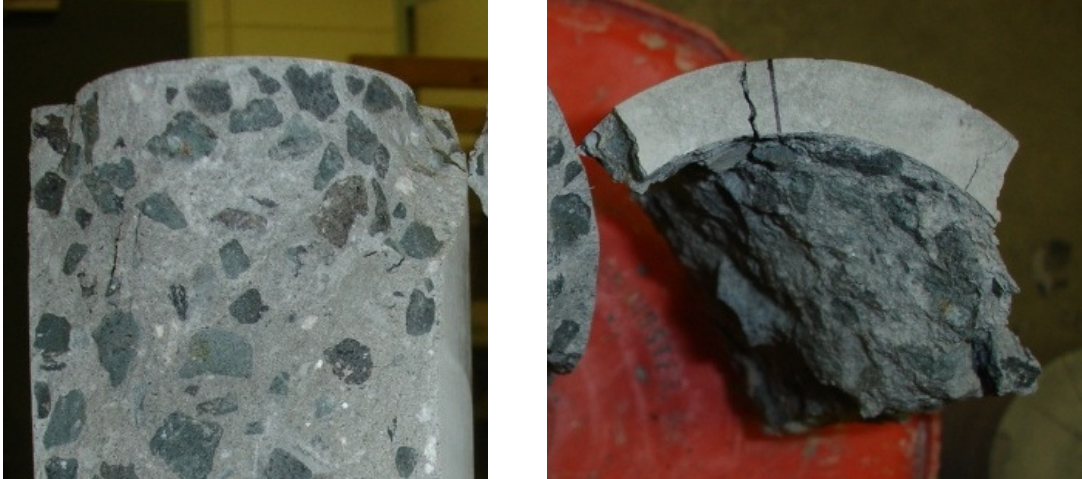


Figure 4-4: Close up of Cone of Concrete formed beneath Bearing Plate

The cracking and failure of the unreinforced prisms was not closely observed during loading due to safety concerns over the possibility of a very brittle and explosive failure. However, neither prism failed in an explosive manner. Both prisms failed as the bearing plate punched into the concrete and a crushing of the concrete beneath the bearing plate. As the bearing pad punched into the concrete, the prism split into multiple pieces (See Figure 4-5). Similarly to the cylinders, a cone of concrete in the prisms formed beneath the bearing plate as shown in Figure 4-6. The condition of the cone of concrete was very poor. The cone of concrete was heavily fractured and crumbled very easily.

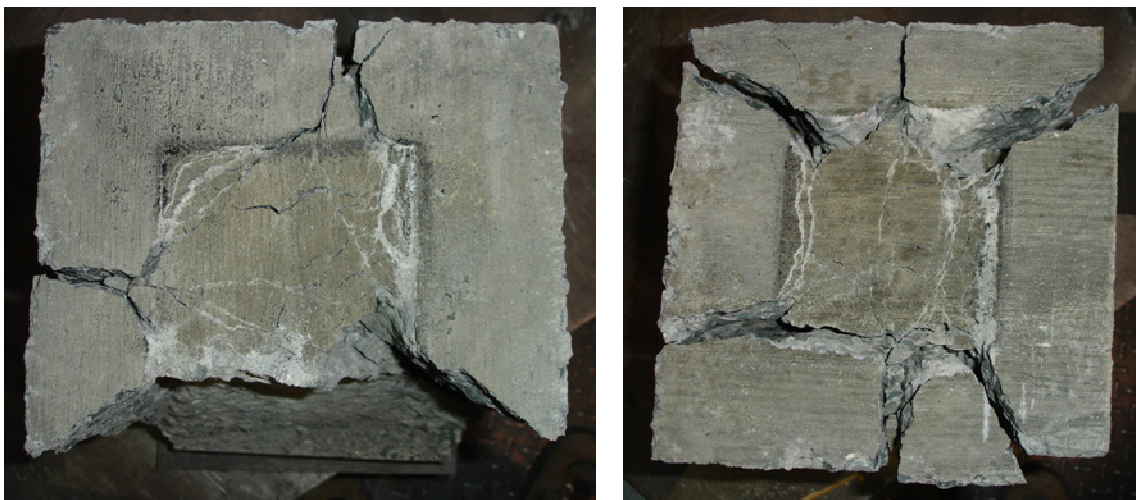


Figure 4-5: Picture of the Top of Unreinforced Prisms

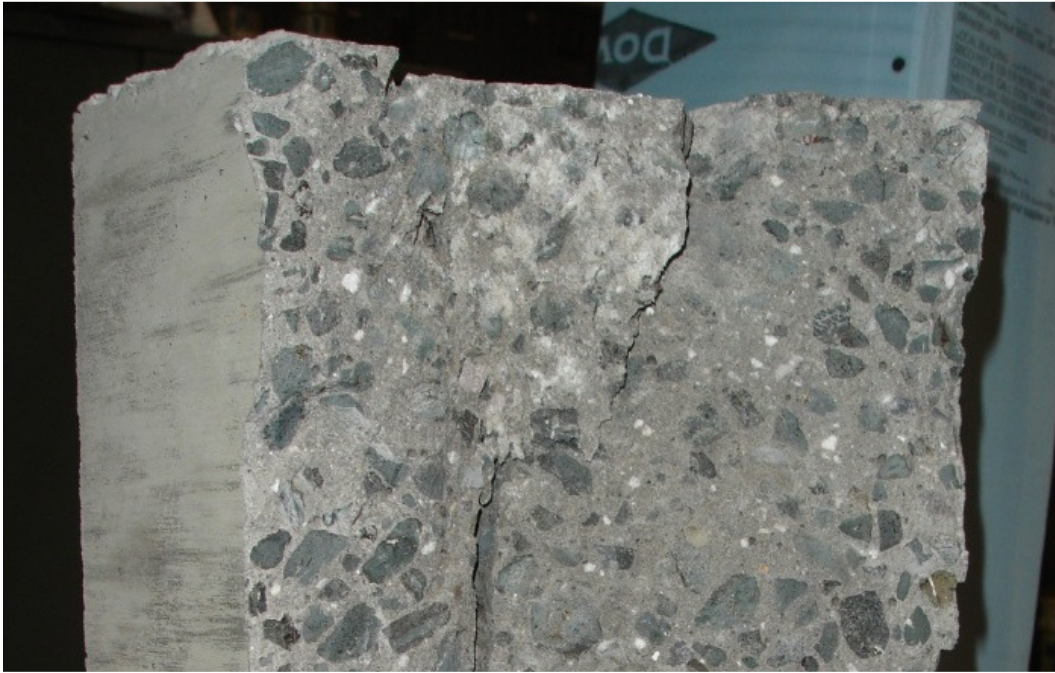


Figure 4-6: Cone of Concrete

4.1.2 Analysis of Unreinforced Bearing Strength Data

The tabulation of the experimental f_b/f'_c versus the bearing strength equations, given in Section 2.1, is given in Table 4-2. A graphical representation of the tabulated data is given in Figure 4-7.

Table 4-2: Comparison of Experimental Data vs. Bearing Strength Equations

A/A _b	f_b/f'_c					
	Current Research	Hawkins (k = 50), Equation 2-2	Niyogi, Equation 2-3	Bonetti, Equation 2-4	ACI, $\lambda = 0.85$, Equation 2-11	ACI, $\lambda = 0.70$, Equation 2-11
Circular plate on 4 in. x 8 in. Cylinders						
3.76	1.44	2.78	1.86	1.13	1.40	1.15
3.76	1.44	2.78	1.86	1.13	1.40	1.15
2.69	1.25	2.21	1.61	0.94	1.19	0.98
2.69	1.18	2.21	1.61	0.94	1.19	0.98
1.57	1.02	1.48	1.28	0.80	0.91	0.75
1.57	0.91	1.48	1.28	0.80	0.91	0.75
Square Plate on 8 in. x 8 in. x 16 in. Prisms						
4	1.06	2.90	1.91	1.00	1.45	1.19
4	1.07	2.90	1.91	1.00	1.45	1.19

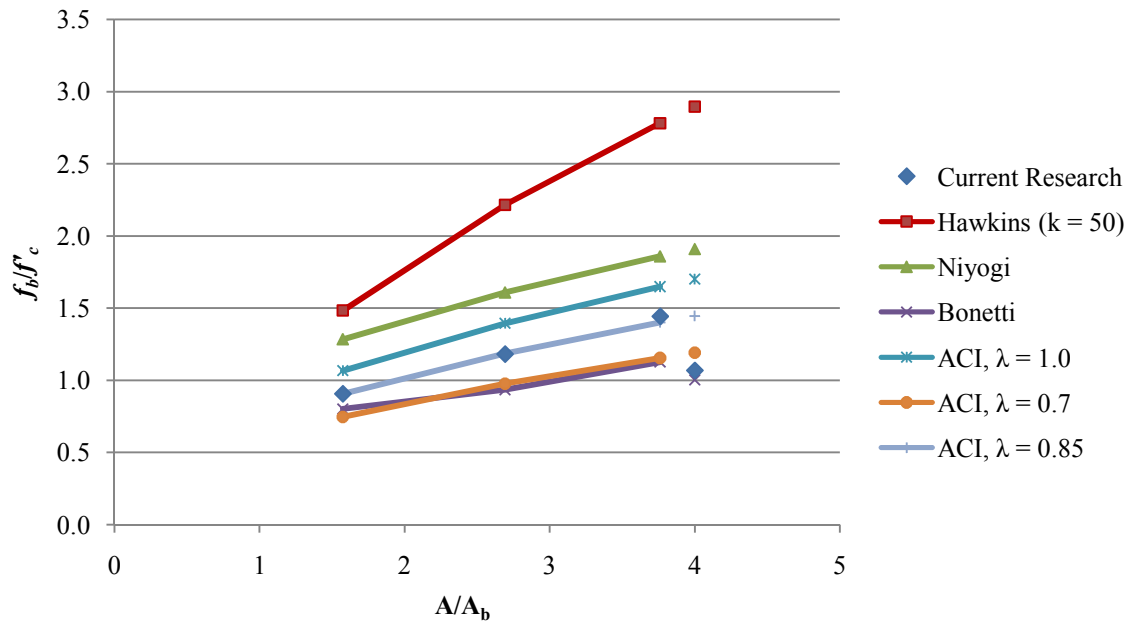


Figure 4-7: Graphical Representation of the Experimental Data vs. of Bearing Strength Equations

In Figure 4-7 the plotted lines represent the estimate for the strength of the cylinders and the individual points plotted at an A/A_b ratio of 4 represent the unreinforced prism specimens. The only equation that is affected by the relationship between the properties is Bonetti's equation,

through the m term. The m term is the ratio of the compressive strength to the tensile strength of the concrete.

The equation developed by Hawkins, with $k = 50$, overestimates the test data and the general trend of the experimental data of the cylinders by a considerable amount. As the A/A_b ratio increases, the calculated values diverge from the experimental values. Niyogi's bearing strength equation and the ACI 318-05 equation, with $\lambda = 1.0$, both overestimate the bearing strength of the lightweight concrete. However, both bearing strength equations have the same general trend as the experimental data.

Once multiplied by a λ -factor of 0.7, the ACI 318-05 equation becomes conservative for the compressive strength of the cylinders. The λ -factor of 0.85 is fairly close to a best fit estimation of the compressive strength of the cylinders. However, a λ -factor of 0.85 gives an unconservative estimate of the strength of the unreinforced prisms. The bearing strength equation developed by Bonetti greatly underestimates the strength of the cylinders but gives a fairly accurate estimate of the bearing strength of the unreinforced prisms.

The Hawkins, Niyogi, and ACI 318-05 with $\lambda = 1.0$ equations are more unconservative for the two unreinforced prism specimens than for the cylinders. The ACI 318-05 equation with $\lambda = 0.7$ and the Bonetti equation both estimate the bearing strength well. The ACI 318-05 equation is slightly unconservative and Bonetti's equation is slightly conservative.

When comparing the bearing strength ratio, f_b/f'_c , of the cylinders and the prisms, it should be noted that the bearing strength ratio of the prisms is lower than expected for the same A/A_b ratio. The bearing strength ratio values of the cylinders indicate that for a A/A_b ratio of 4, the bearing strength ratio of the prisms should be in the just above 1.5. However, the actual bearing strength ratio from testing of the prisms is 1.06 and 1.07. Findings reported by Niyogi showed that as the size of specimens of similar shape increases, the bearing strength ratio decreases (Niyogi 1974). All of the specimens had about the same aspect ratio, but the prisms were about 10 times more massive by volume.

Figure 4-8 presents the experimental data gathered in this research compared to the experimental data gathered in previous research along with the ACI 318-05 bearing strength equation and the bearing strength equation developed by Bonetti. Bonetti recommends that $\lambda = 0.7$ for lightweight concrete and ACI 318-05 recommends that $\lambda = 0.85$ for a sand-lightweight concrete. The ACI 318-05 equation with both $\lambda = 0.7$ and 0.85 are presented in Figure 4-8 along with data from several sources (Bonetti 2005; Heilmann 1983; Roberts-Wollmann et al. 2006).

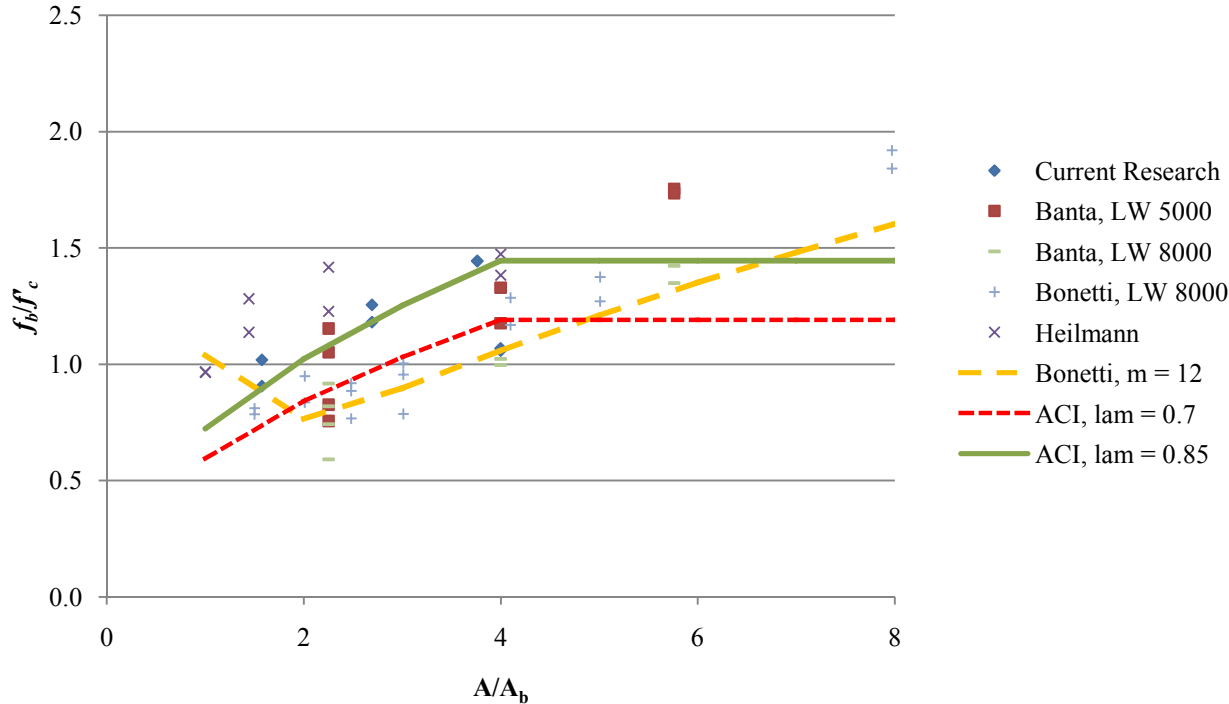


Figure 4-8: Comparison of Experimental Data and Previous Data vs. Bearing Strength Prediction Equations

4.2 Reinforced Bearing Strength

4.2.1 Results and Observations

Table 4-3 includes all of the data recorded from the testing of the reinforced prisms. The load at which the first cracking appeared was recorded for each side of the prism. In some cases a face did not crack until failure of the prism; this is represented with a dashed line in Table 4-3.

Table 4-3: First Cracking and Ultimate Load Data

Block	First Cracking Load, kips				Ult. Load, kips	Age, days
	Side A	Side B	Side C	Side D		
2.5T-4-A	120	120	145	145	181.3	41
2.5T-4-B	142.5	140	155	140	189.7	41
2T-4-A	155	155	155	155	191	40
2T-4-B	165	165	145	130	180.8	41
2T-4-C	145	110	115	120	196.5	42
1.5T-4-A	110	140	158	120	211	42
1.5T-4-B	90	151	156	151	210.2	42
1.5T-4-C	95	165	-----	155	192.4	42
2.5T-2.5-A	97.3	97.3	115	97.3	123.8	41
2.5T-2.5-B	95	90	75	95	124.2	41
2T-2.5-A	106	95	85	75	126.8	42
2T-2.5-B	100	110	100	106	136.5	42
2T-2.5-C	50	90	95	95	131.2	42
1.5T-2.5-A	80	90	95	105	122.7	42
1.5T-2.5-B	95	95	95	95	130.6	44
1.5T-2.5-C	105	105	95	90	126	44
2.5S-4-A	-----	120	115	135	165	46
2.5S-4-B	125	-----	-----	-----	184.9	49
2S-4-A	95	135	-----	-----	175.9	47
2S-4-B	140	155	155	-----	204	47
2S-4-C	165	125	145	60	182	46
1.5S-4-A	155	30	155	170	226.8	50
1.5S-4-B	145	145	140	165	210	51
2.5S-2.5-A	90	85	110	90	136.7	44
2.5S-2.5-B	110	100	105	-----	127.7	46
2S-2.5-A	30	-----	90	-----	103.6	46
2S-2.5-B	117	105	105	110	132	47
1.5S-2.5-A	80	120	135	120	144.5	50
1.5S-2.5-B	100	105	-----	-----	120	50
1.5S-2.5-C	115	110	110	110	151.6	51

The first cracks to form on the side faces of the prism formed in two manners. In the first case, the crack extended down from the top face and in the second, the crack did not extend up to the top face. In each case the crack began near the center of the face and the length of the crack varied. Figure 4-9 and Figure 4-10 show typical crack patterns for both spiral and tied blocks.



Figure 4-9: Failed Prisms with Tied Reinforcing



Figure 4-10: Failed Prisms with Spiral Reinforced

Depending on the size of the bearing plate used, the top surface experienced different types of crack patterns. Prisms loaded through the 2.5 in. bearing pad had a very pronounced punching of the bearing pad into the top of the prism to a depth around 1/8 in. As the loading increased, the bearing pad expanded due to poisson's effect and at failure the bearing plate cut through the rubber bearing pad. Prisms loaded through the 4 in. bearing pad left a circular depression on the top surface of the concrete. The circular depression is very similar to pictures presented in the Hawkins report on flexible bearing plates (Hawkins 1968a). Similarly to the 2.5 in. bearing pad, the 4 in. bearing pad expanded but the bearing plate did not cut through the bearing pad at failure.

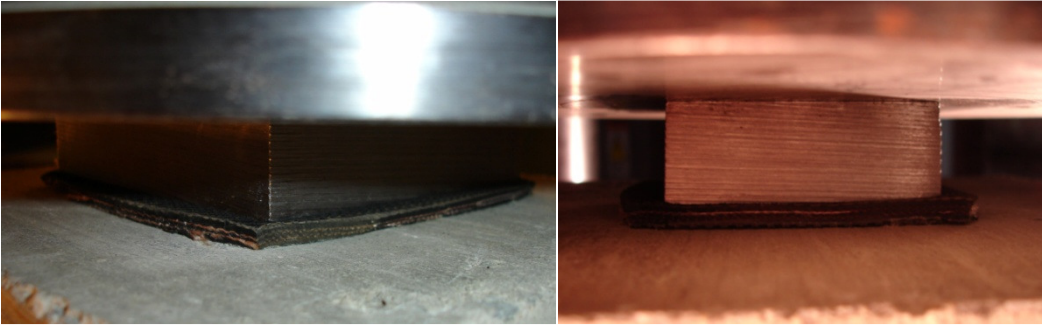


Figure 4-11: Bearing Pad Expansion under 4 inch and 2.5 inch bearing pad

In each case of failure of the top surface, cracks extended from the corners of the bearing pad in the direction of the corners of the prism. Representative pictures of the top surface after failure loaded through a 4 in. and 2.5 in. bearing pad are given in Figure 4-12 and Figure 4-13 respectively.

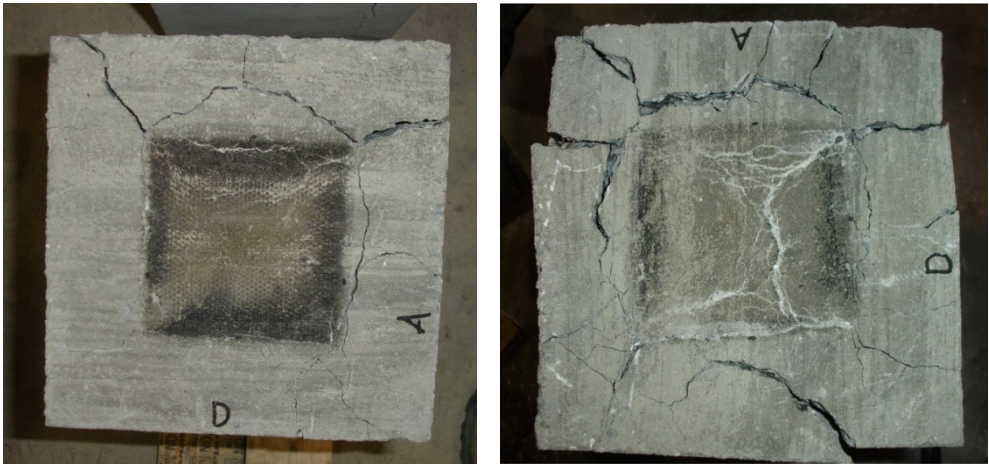


Figure 4-12: Top Surface after failure: 4 in. bearing pad

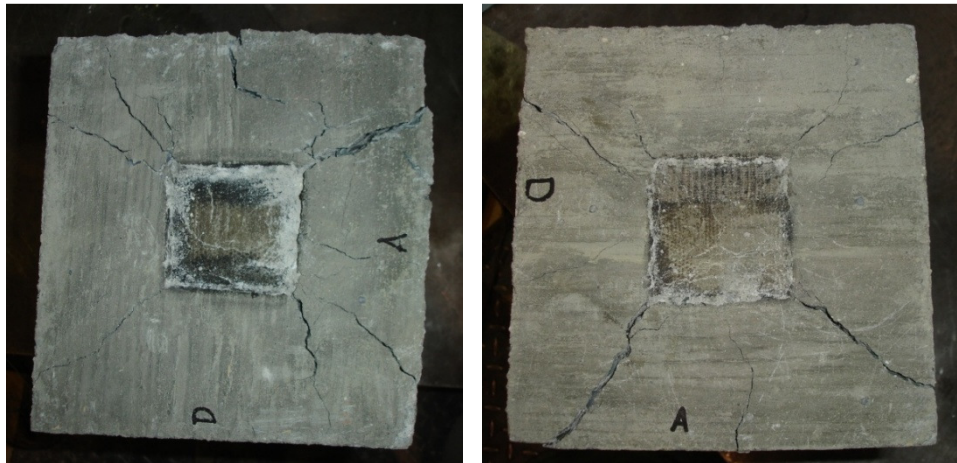


Figure 4-13: Top Surface after failure: 2.5 in. bearing pad

In all cases, the concrete and aggregate directly beneath the bearing pad was crushed. Figure 4-14 shows three pictures that give a good representation of the condition of the concrete beneath the bearing plate after failure.



Figure 4-14: Detail of Concrete Beneath the Bearing Plate

4.2.2 Analysis of Reinforced Bearing Strength Data

In this section the ultimate strengths of the reinforced prisms are compared to the NCHRP 356 report (Equation 1-1) and the equations developed by Bonetti (Equation 2-20 and Equation 2-23). Modifications of the NCHRP equation are examined to determine the best form of the equation to estimate the ultimate bearing strength of the local zone. Data from the research performed for this thesis along with data from Heilmann and Slab Anchor tests, performed for VSL Corporation, are compared to the recommended equation (Axson 2007a; Axson 2007b; Axson 2007c; Axson 2007d).

Three modifications are applied to the NCHRP equation in order to determine the most effective way to predict the ultimate bearing strength of the local zone for lightweight concrete. The NCHRP equation is broken down into two basic parts, the bearing strength of unconfined concrete enhanced by the A/A_b ratio and the strength enhancement provided by the lateral steel confinement.

From Section 4.1, it is apparent that an increase in the A/A_b ratio increases the ultimate bearing strength of lightweight concrete at a lower rate than for normal weight concrete. One modification to account for the reduced strength is to apply a λ -factor to the first part of the NCHRP equation. From unreinforced tests on lightweight concrete, research suggests that a λ -factor of 0.7 to predict the contribution to the ultimate strength of the concrete by the confinement added by the concrete (Roberts-Wollmann et al. 2006). However, for sand-lightweight concrete ACI 318-05 suggests the λ factor should be 0.85.

Two modifications are considered for the second half of the equation. The first modification is to the k-factor, which is 4.1 for the basic NCHRP equation. Martinez et al. reported that this value should be 1.5 for lightweight concrete and is based on confined lightweight concrete column tests. Another modification considered for the second half of the equation will be the use of the area of the bearing plate, A_b , in place of the effective core area. The effective core area, A_{eff} , is defined as the area of the core multiplied by the efficiency factor (Equation 2-19). This is referred to as the Area Modification.

4.2.2.1 Analysis of Test Results

As can be seen in Figure 4-15, in the raw data in Table 4-4, and in the statistical analysis provided in Table 4-5, the NCHRP equation's prediction for the ultimate strength of the local zone is unconservative for lightweight concrete. Also included in Figure 4-15 is the data from Heilmann (1983), whose research used a sand-lightweight concrete with a unit weight of 93.0 pcf.

Table 4-4: Comparison of the Experimental Loads vs. the NCHRP predicted load

Block	Experimental Load, kips	NCHRP Predicted Load, kips	Experimental/Analytical
2.5T-4-A	181.3	202.9	0.89
2.5T-4-B	189.7	202.9	0.94
2T-4-A	191	216.9	0.88
2T-4-B	180.8	216.9	0.83
2T-4-C	196.5	216.9	0.91
1.5T-4-A	211	241.7	0.87
1.5T-4-B	210.2	241.7	0.87
1.5T-4-C	192.4	241.7	0.80
2.5T-2.5-A	123.8	135.1	0.91
2.5T-2.5-B	124.2	135.1	0.92
2T-2.5-A	126.8	149.1	0.85
2T-2.5-B	136.5	149.1	0.92
2T-2.5-C	131.2	149.1	0.88
1.5T-2.5-A	122.7	173.9	0.71
1.5T-2.5-B	130.6	173.9	0.75
1.5T-2.5-C	126	173.9	0.73
2.5S-4-A	165	215.5	0.77
2.5S-4-B	184.9	215.5	0.86
2S-4-A	175.9	237.5	0.74
2S-4-B	204	237.5	0.86
2S-4-C	182	237.5	0.77
1.5S-4-A	226.8	276.5	0.82
1.5S-4-B	210	276.5	0.76
2.5S-2.5-A	136.7	147.7	0.93
2.5S-2.5-B	127.7	147.7	0.86
2S-2.5-A	103.6	169.7	0.61
2S-2.5-B	132	169.7	0.79
1.5S-2.5-A	144.5	208.6	0.69
1.5S-2.5-B	120	208.6	0.58
1.5S-2.5-C	151.6	208.6	0.73

Table 4-5: Summary of data in Table 4-4

	Ties	Spiral	Overall
Mean	0.853	0.767	0.813
Standard Deviation	0.072	0.097	0.094

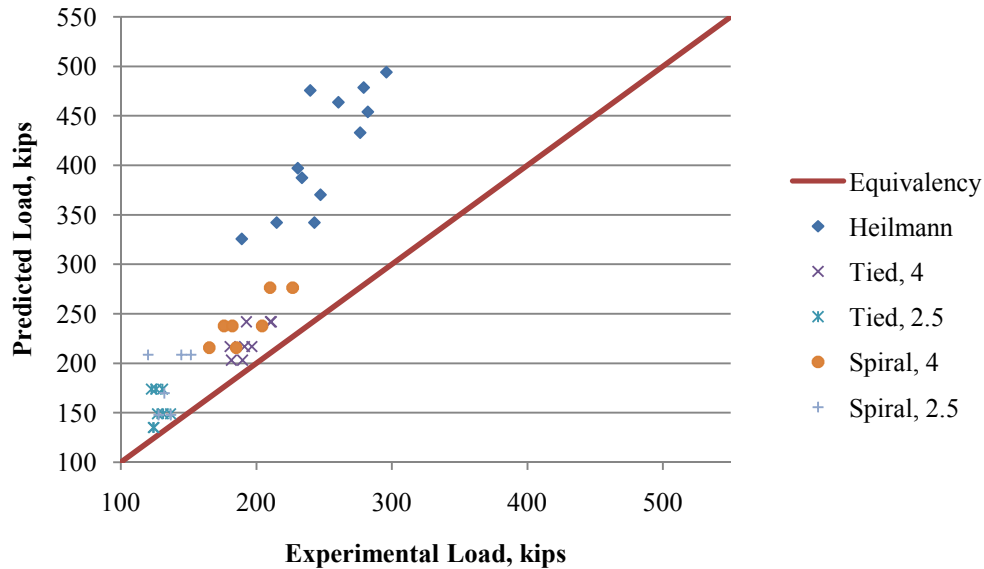


Figure 4-15: NCHRP Equation with no modification (Equation 2-15)

Previous research has shown that lateral reinforcing has a smaller effect on the ultimate load of the local zone for lightweight concrete. For both the tied and spiral reinforced prisms loaded through the 4 in. bearing pad, there is an increase in failure load of the block as the spacing or pitch of the lateral reinforcing decreases. However, for the tied and spiral reinforced prism loaded through the 2.5 in. bearing pad there is little to no increase in ultimate load for the same decrease in the spacing or pitch (See Figure 4-16). The lateral confining pressures were calculated according to the equations in Section 2.2.6.

Figure 4-17 presents the experimental and NCHRP estimate for each spacing or pitch versus the lateral confining pressure with the plotted linear trend line of the prisms loaded through a 4 in. bearing pad. The figure shows that the NCHRP equation predicts that the confining reinforcing enhances the strength at a higher rate of strength increase for decreasing pitch than the experimental results show.

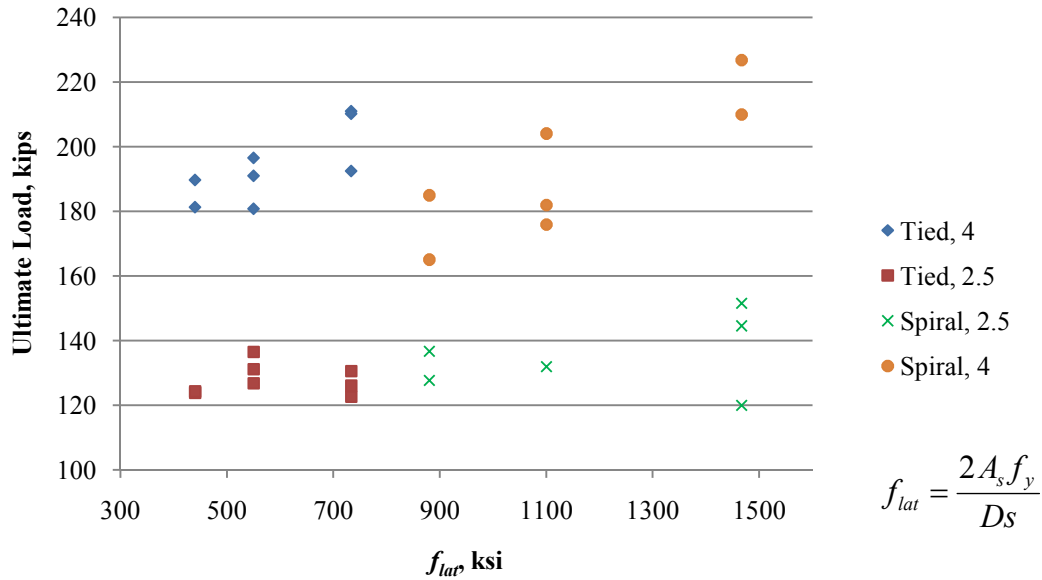


Figure 4-16: Ultimate load vs. Lateral Confining Pressure

Setting the k-factor to 2.5 and the λ -factor to 0.9, the NCHRP equation better estimates both the ultimate load and the strength gain provided by the confining reinforcing, f_{lat} (See Figure 4-18). The calculation of f_{lat} is given in Equation 2-15 and Equation 2-16 and the general form of the equation is shown in Figure 4-16. Using the new factors, the NCHRP equation slightly overestimates the strength of the spiral reinforced blocks while slightly underestimating the strength of the tied reinforced blocks. The concrete used in this research is considered to be a sand-lightweight concrete and the recommended λ -factor by ACI 318-05 is 0.85. Using 0.85 offers a more conservative prediction.

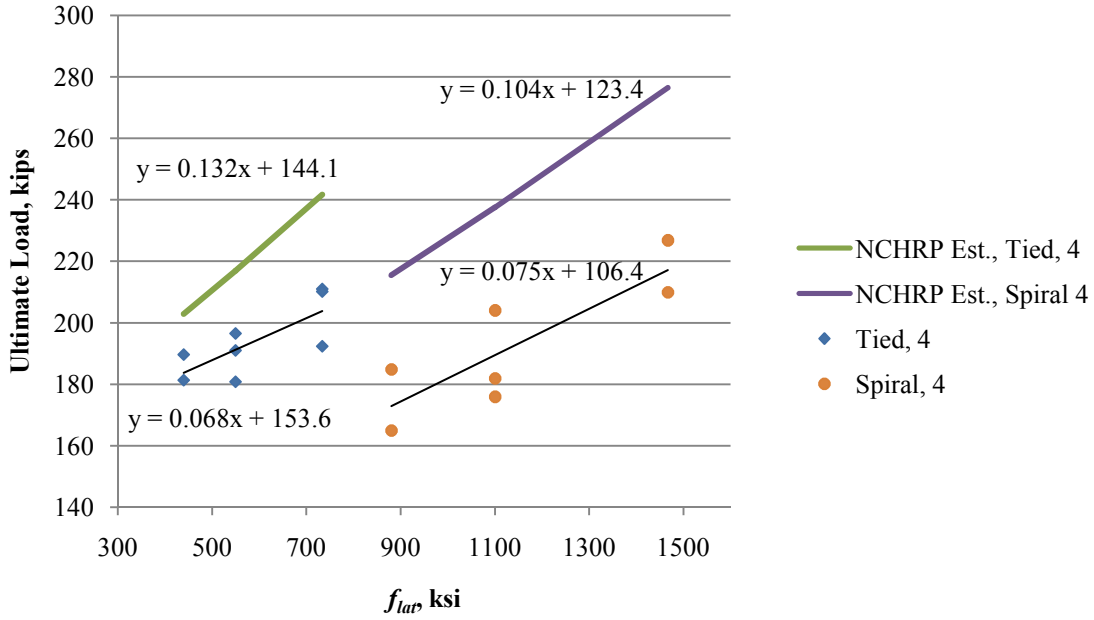


Figure 4-17: Experimental and NCHRP Ultimate Load vs. Lateral Confining Pressure for 4 in. Bearing Pads ($k = 4.1$ and $\lambda = 1.0$)

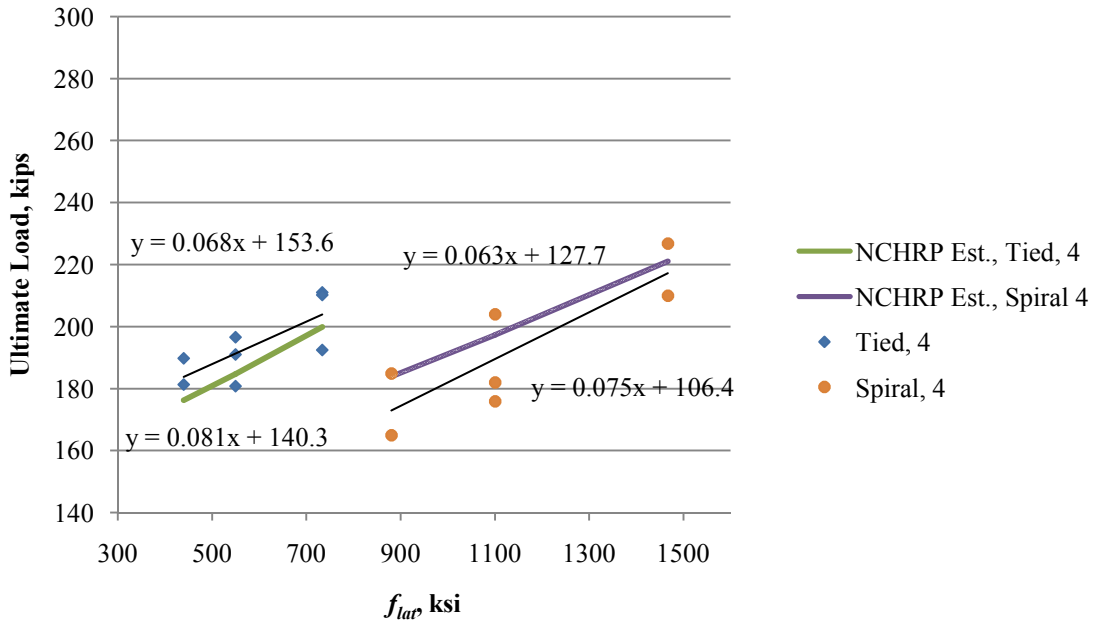


Figure 4-18: Experimental and Modified NCHRP Ultimate Load vs. Lateral Confining Pressure ($k = 2.5$ and $\lambda = 0.9$), 4 in. bearing pad

The k-factor and λ -factor for the 2.5 in. bearing pads are 0.5 and 1.0 respectively, reinforcing the observation that there is little increase in strength as the pitch or spacing of the reinforcing decreases.

Figure 4-19 and Figure 4-20 show the experimental ultimate load versus the NCHRP predicted ultimate load. Figure 4-19 presents the data using the A_{eff} for all of the NCHRP predicted values and Figure 4-20 presents the data where the minimum of the A_{eff} or A_b is used. A_b controls for all of the prisms loaded through a 2.5 in. bearing pad and for the prisms with tied reinforcing spaced at 2.5 in.

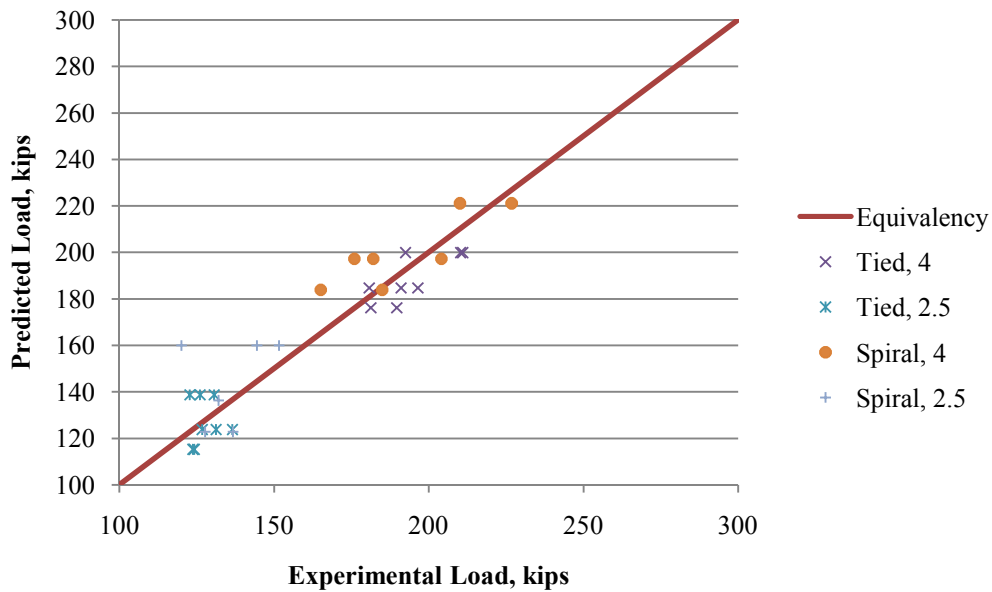


Figure 4-19: Experimental vs. Predicted load for $k = 2.5$ and $\lambda = 0.90$ (Current Research)

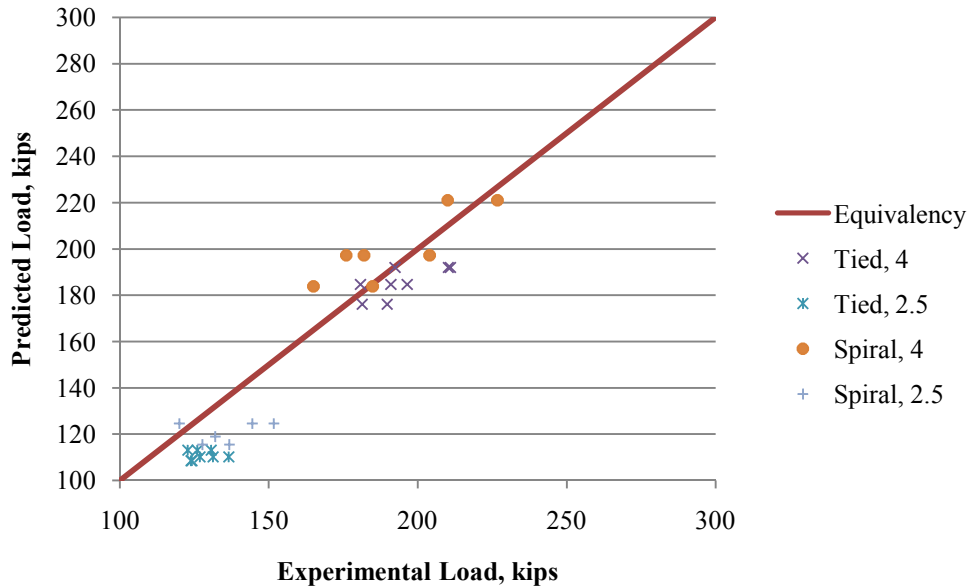


Figure 4-20: Experimental vs. Predicted load for $k = 2.5$ and $\lambda = 0.90$, Area Modification (Current Research)

The area modification provides more conservative results overall, but with a slightly higher standard deviation (See Table 4-6). Table 4-6 includes the data from specimens loaded through 2.5 and 4 in. bearing plates.

Table 4-6: Comparison of Experimental/Analytical Mean and Standard Deviation for Area Modification (Current Research) ($k = 2.5$ and $\lambda = 0.90$)

	Effective Core Area, A_{eff}		
	Ties	Spiral	Overall
Mean	1.02	0.958	0.992
Standard Deviation	0.066	0.098	0.083

	Minimum of A_p and the Effective Core Area		
	Ties	Spiral	Overall
Mean	1.0993	1.0358	1.0709
Standard Deviation	0.0693	0.1106	0.0941

The data gathered in the research performed for this thesis was also compared to the two equations proposed by Bonetti (Equation 2-20 and Equation 2-23). Figure 4-21 compares the experimental data versus the equation Bonetti developed through curve fitting (Equation 2-20 and Table 4-7). Figure 4-22 compares the experimental data versus the equation Bonetti developed using a modified m parameter, m_r (Equation 2-23 and Table 4-8).

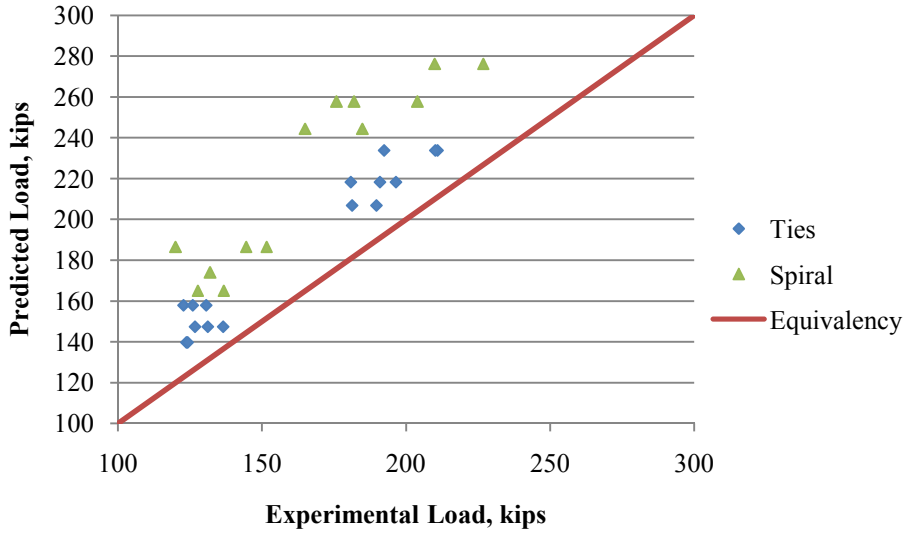


Figure 4-21: Comparison of Experimental Data versus Equation 2-20 (Current research)

Table 4-7: Comparison of Experimental/Analytical Mean and Standard Deviation for Equation 2-20 (Current Research)

	Ties	Spiral	Overall
Mean	0.8675	0.7350	0.8162
Standard Deviation	0.0439	0.0590	0.0767

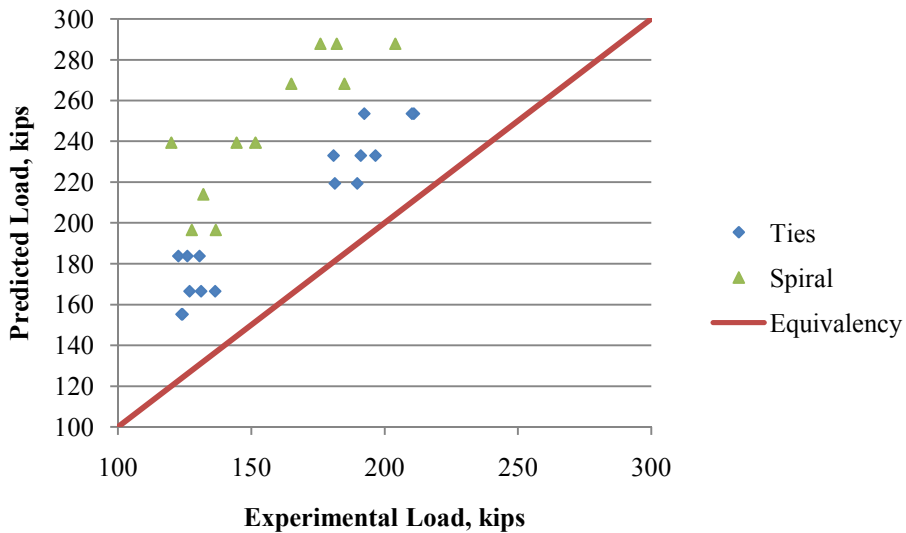


Figure 4-22: Comparison of Experimental Data versus Equation 2-23 (Current research)

Table 4-8: Comparison of Experimental/Analytical Mean and Standard Deviation for Equation 2-23 (Current Research)

	Ties	Spiral	Overall
Mean	0.787	0.642	0.722
Standard Deviation	0.092	0.058	0.092

Both equations proposed by Bonetti yield unconservative results for the data collected in this research. From the results, it is apparent that the better performing of Bonetti’s two reinforced bearing strength equations that is the one based on a curve fitting (Equation 2-20). The conclusion is based on a better mean and lower standard deviation.

4.2.2.2 Analysis of Heilmann Data

Figure 4-23 presents the experimental data from Heilmann (1983) in a similar chart as Figure 4-17. As before, it is necessary to modify both the k-factor and the λ -factor to allow the NCHRP equation to correctly estimate the strength of the local zone. The k-factor and the λ -factor that best predict the results of the Heilmann data are 1.5 and 0.75 respectively when the area modification is not applied to the NCHRP equation (See Figure 4-24). For Figure 4-23 and Figure 4-24, the NCHRP estimated values cannot be represented as a line, as in Figure 4-17 and Figure 4-18, because for each test, Heilmann recorded different yield strengths of his reinforcing and compressive strength for his concrete for each test specimen.

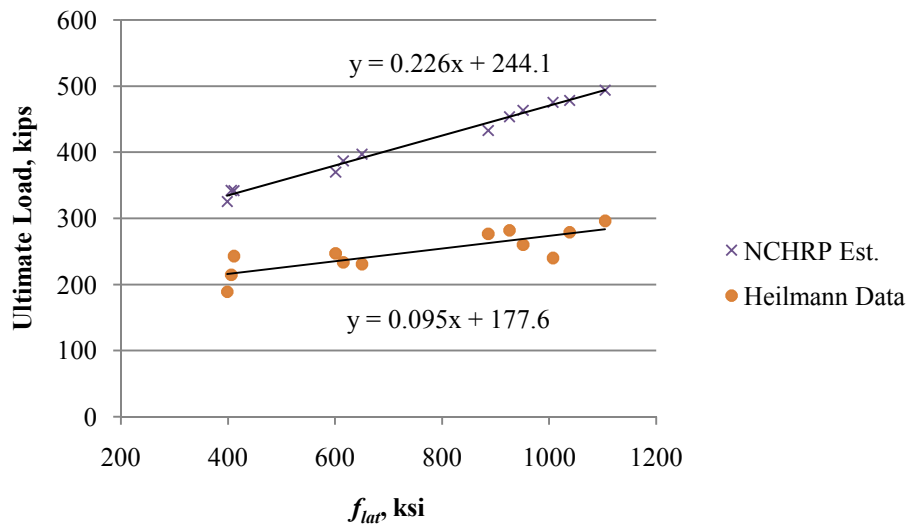


Figure 4-23: Heilmann and NCHRP Ultimate Load vs. Lateral Confining Pressure ($k = 4.1$ and $\lambda = 1.0$)

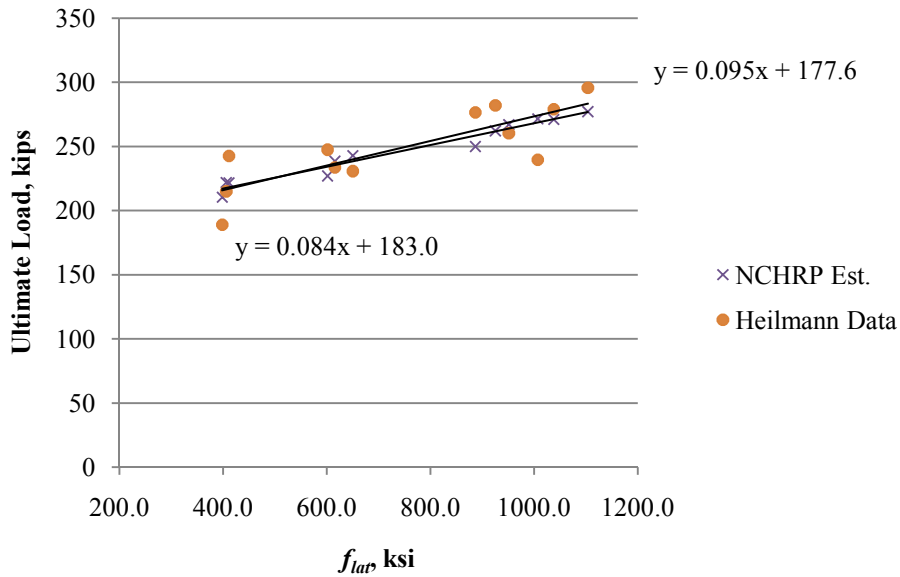


Figure 4-24: Heilmann and Modified NCHRP Ultimate Load vs. Lateral Confining Pressure ($k = 1.5$ and $\lambda = 0.75$)

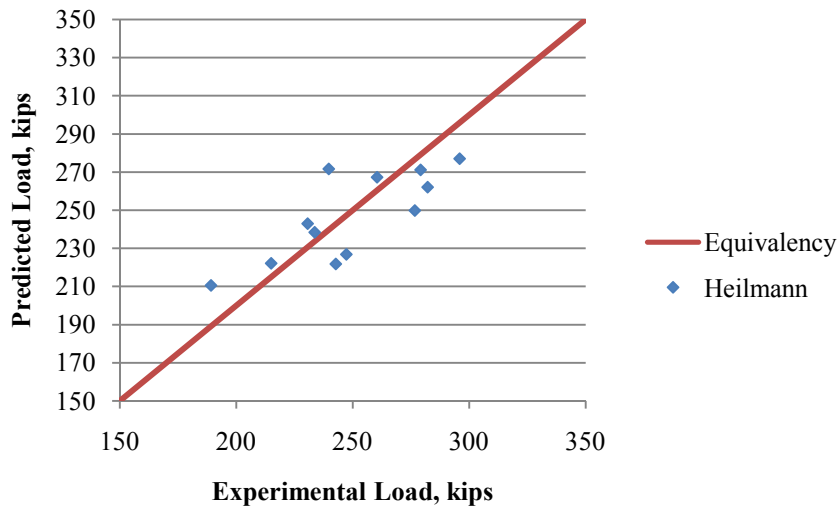


Figure 4-25: Experimental vs. Predicted load for $k = 1.5$, $\lambda = 0.75$, and Area Modification (Heilmann Data)

After applying the area modification, the best k -factor used is 2.5 while the λ -factor should be 0.75. The bearing area for Heilmann’s data is 34.9 in² and the A_{eff} is 53.7 in² and each is kept constant through his tests. Therefore, the bearing area controls in the area modification.

Comparing Figure 4-26 and Figure 4-24 it is apparent that using the minimum of A_b and the A_{eff} a better approximation of the rate of increase in ultimate load as the confining pressure increases.

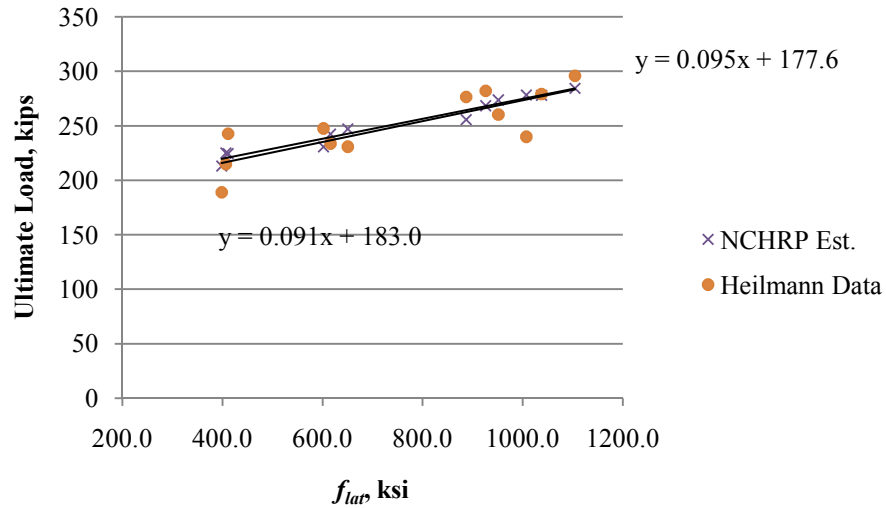


Figure 4-26: Heilmann and Modified NCHRP Ultimate Load vs. Lateral Confining $k = 2.5$, $\lambda = 0.75$, and Area Modification

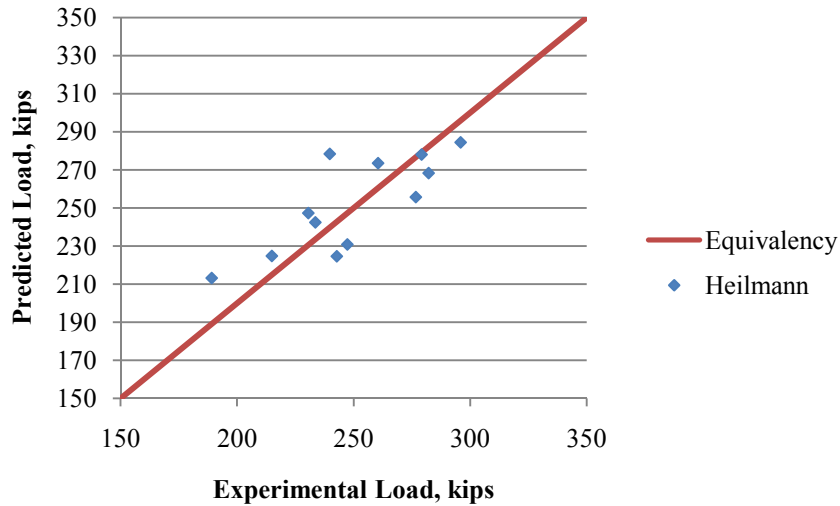


Figure 4-27: Experimental vs. Predicted load for $k = 2.5$, $\lambda = 0.75$, and Area Modification (Heilmann Data)

Table 4-9: Comparison of Experimental/Analytical Mean and Standard Deviation for Area Modification (Heilmann Data)

Effective Core Area

	Overall
Mean	1.01
Standard Deviation	0.09

Area Modification

	Overall
Mean	1.04
Standard Deviation	0.08

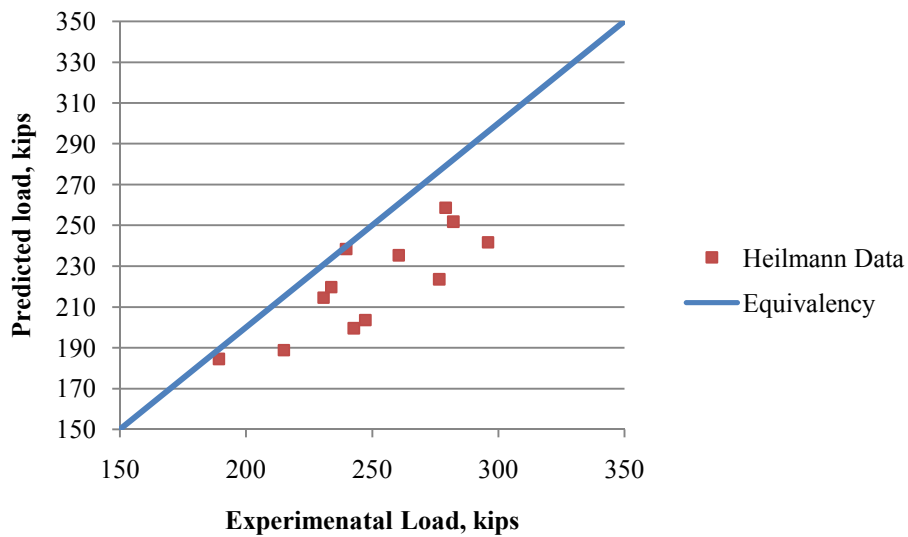


Figure 4-28: Comparison of Experimental Data vs. Equation 2-20 (Heilmann Data)

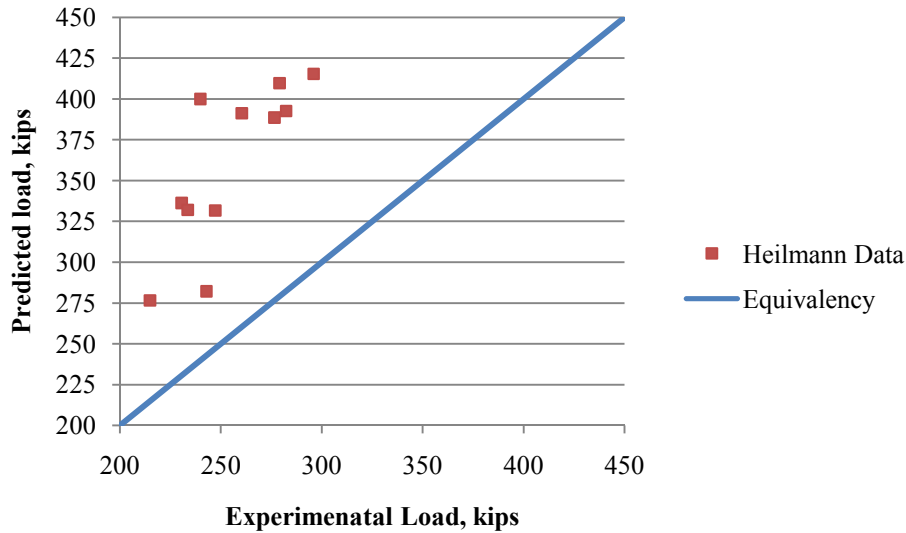


Figure 4-29: Comparison of Experimental Data vs. Equation 2-23 (Heilmann Data)

Figure 4-28 and Figure 4-29 present the comparison of the predicted load and experimental load for the two equations developed by Bonetti to predict the ultimate load of reinforced concrete. The mean and standard deviation of the data from each equation is given in Table 4-10. It is evident that Equation 2-20 better approximates the ultimate load of the Heilmann Data.

Table 4-10: Comparison of Experimental/Analytical Mean and Standard Deviation Bonetti’s Reinforced Bearing Strength Equations

	Equation 2-20	Equation 2-23
Mean	1.125	0.712
Standard Deviation	0.081	0.064

4.2.2.3 Analysis of Slab Anchor Testing

In the fall of 2006, AASHTO special anchorage device testing was done on slab anchors embedded in lightweight concrete (Axson 2007a; Axson 2007b; Axson 2007c; Axson 2007d). The concrete was a sand-lightweight concrete with a compressive strength of 5770 psi. Tensile strength data and modulus of elasticity data was not gathered for these tests. Both VSL and DSI slab anchors were designed to contain four 0.6 in. diameter strands but were tested in both a three-strand and four-strand condition. The ultimate loads recorded for the 12 tests are given in Table 4-11.

The overall specimen size is based on the size of the anchor. The DSI anchor was larger than the VSL anchor and therefore the specimen size for the DSI anchors was larger than the VSL anchor. From the details of the specimens are given in Figure 4-30 and Figure 4-31.

Table 4-11: Ultimate Loads from Slab Anchor Testing, kips

Anchor Type	
VSL	DSI
315	280
298	275
271	286
279	285
299	289
298	275

Similar Section 4.2.2.1, the k-factor was varied between 1.5 and 2.5 while the λ -factor was varied between 0.85 and 0.70. The area modification did not make a difference in the calculations since the effective core area was always less than the area of the bearing plate.

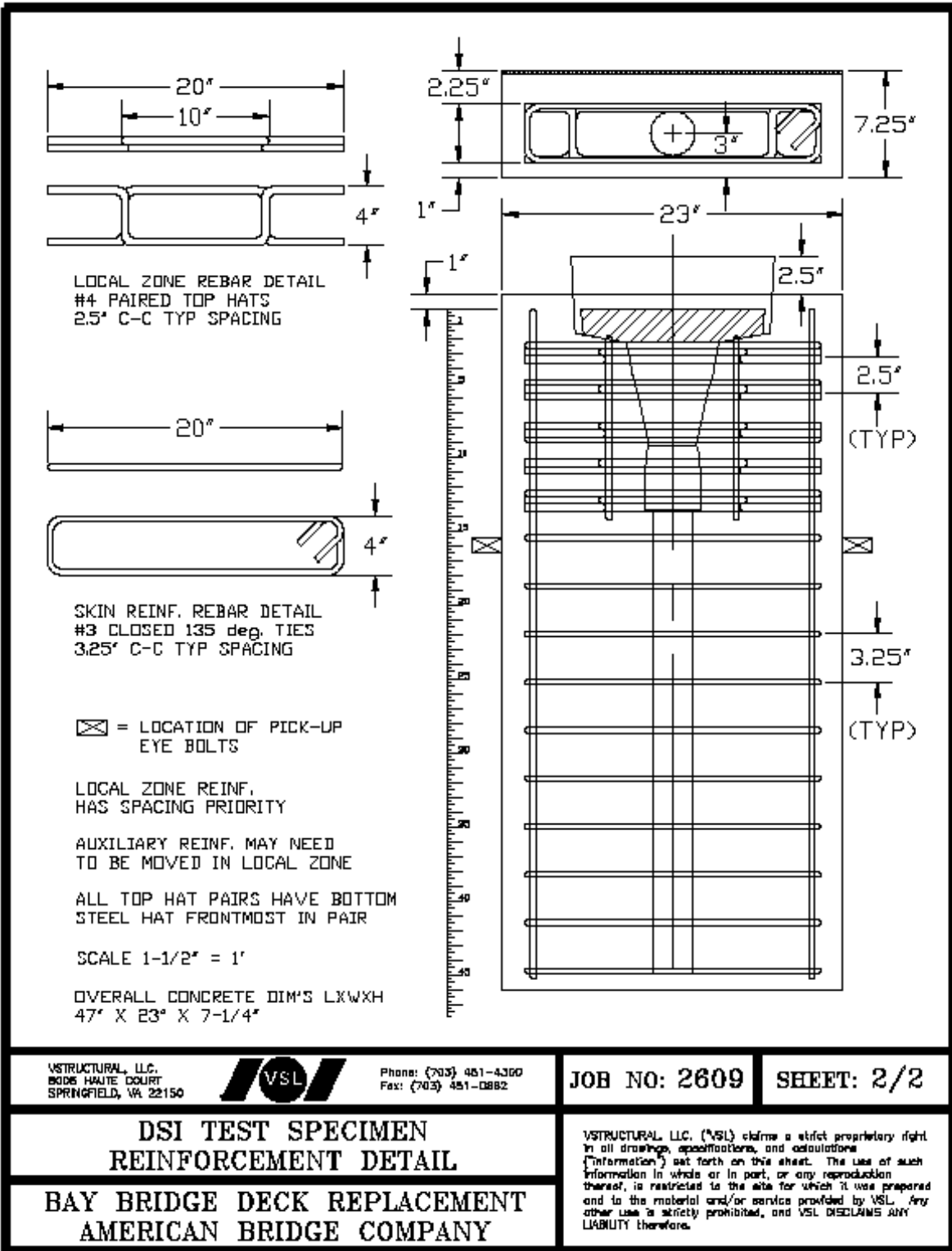
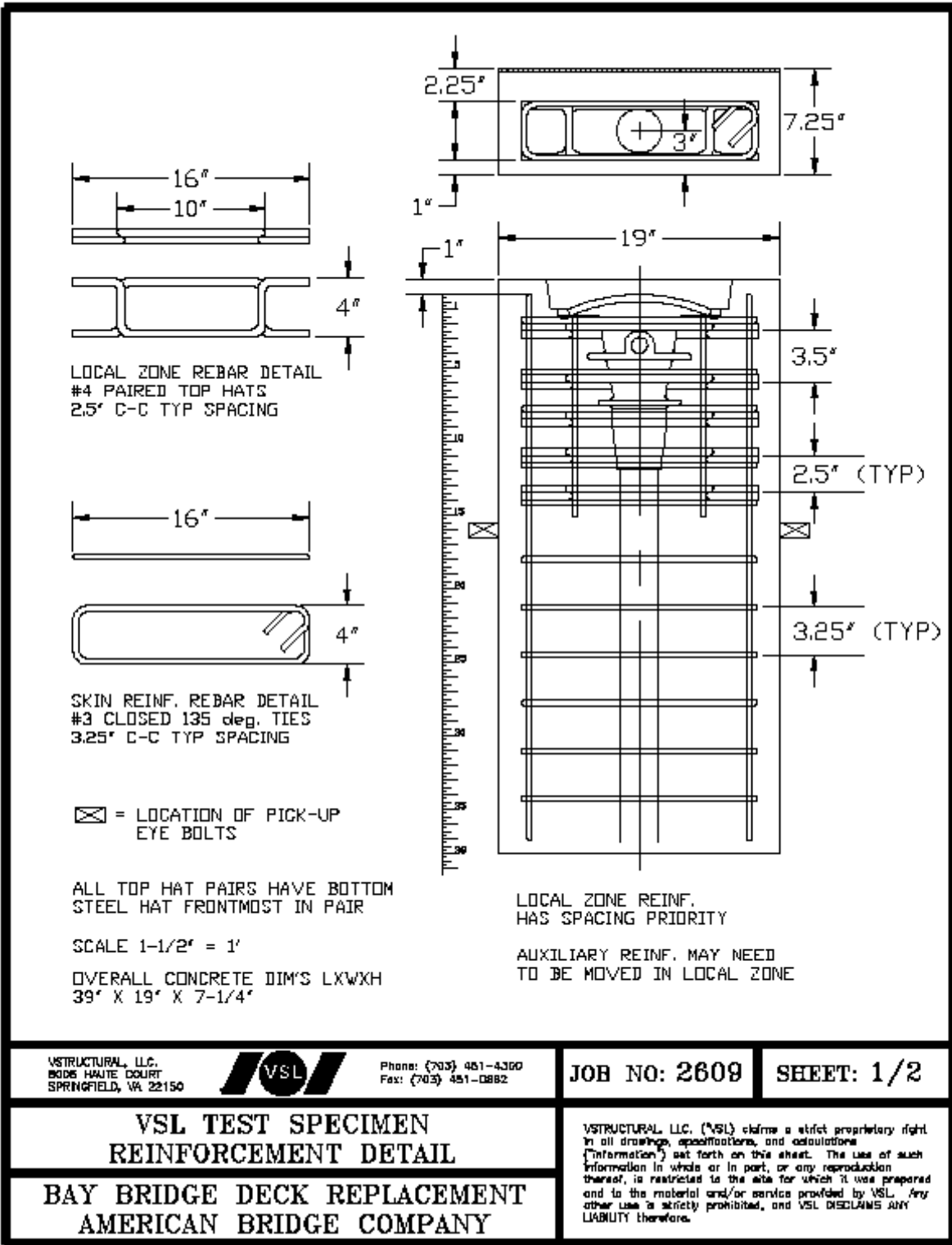


Figure 4-30: DSI Test Specimen Detail



VSTRUCTURAL, LLC.
 8016 HAUTE COURT
 SPRINGFIELD, VA 22150



Phone: (703) 451-4300
 Fax: (703) 451-0882

JOB NO: 2609

SHEET: 1/2

**VSL TEST SPECIMEN
 REINFORCEMENT DETAIL**

**BAY BRIDGE DECK REPLACEMENT
 AMERICAN BRIDGE COMPANY**

VSTRUCTURAL, LLC. (VSL) claims a strict proprietary right in all drawings, specifications, and calculations ("Information") set forth on this sheet. The use of such information in whole or in part, or any reproduction thereof, is restricted to the sole for which it was prepared and to the material and/or service provided by VSL. Any other use is strictly prohibited, and VSL DISCLAIMS ANY LIABILITY therefor.

Figure 4-31: VSL Test Specimen Detail

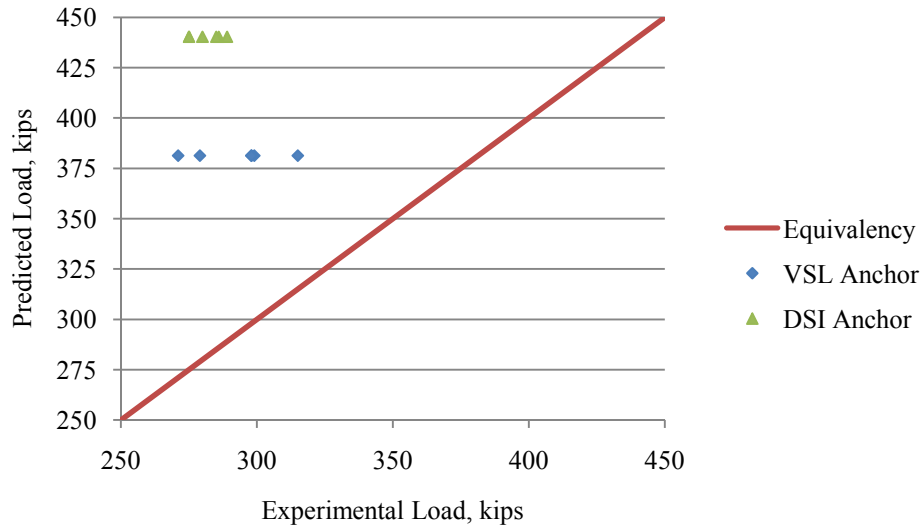


Figure 4-32: Experimental versus Predicted NCHRP Load for $k = 4.1$ and $\lambda = 1.0$

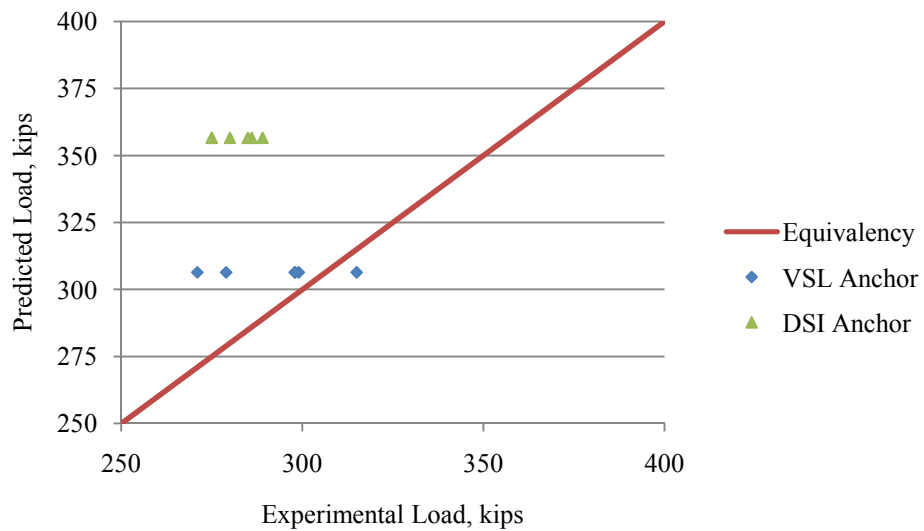


Figure 4-33: Experimental versus Predicted NCHRP Load for $k = 2.5$ and $\lambda = 0.85$

The k -factor and λ -factor of 2.5 and 0.85 respectively give unconservative results, differing from results of the current research and Heilmann data. This discrepancy could possibly stem from the fact that these specimens underwent the AASHTO testing program discussed in the introduction and the loading cycles degraded the ultimate strength of the specimens.

Another weakness of in the design of the slab anchors test is the large length to width ratio of the cross section of the specimen. The tied reinforcing is prone to bending along the long side of the cross section (Refer to Figure 2-17).

The estimation of the ultimate strength of the DSI anchor was much more unconservative than for the VSL anchors. This could be due to the shape of the anchor itself (See Figure 4-34 and Figure 4-35). The shape of the anchor would inherently transmit some of the force from the anchor into the concrete to cause tensile stresses in the concrete. The DSI system did not have any type of embedded anchor system, just an external bearing plate, unlike the VSL anchor system which has a multi-plane embedded bearing plate.

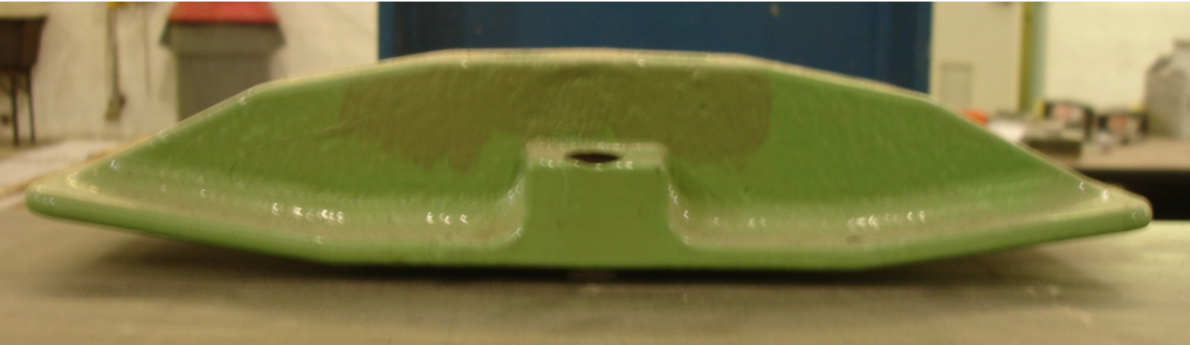


Figure 4-34: Profile View of DSI Anchor

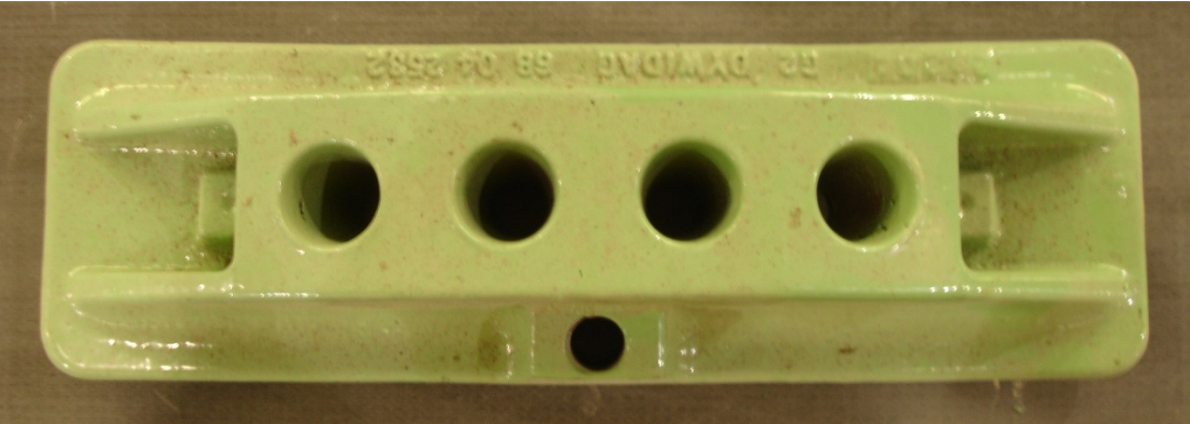


Figure 4-35: Plan View of DSI Anchor

Of the two equations developed by Bonetti to predict the ultimate load of the confined concrete, only one was used to predict the ultimate load of the slab anchor specimens. Equation 2-23 was not used because it requires the knowledge of the tensile strength of the concrete to calculate m_r . Equation 2-20 also requires that the tensile strength of the concrete be known to calculate m ,

however for the purpose of analysis m will be assumed to be 12 as suggested in Section 2.1.6 by Roberts-Wollmann et al (2005).

Bonetti's equation estimates that the ultimate load for the VSL anchor specimens as 372 kips and for the DSI anchor specimens as 428 kips. Estimates for both specimen types give a very unconservative results when compared to the experimental data presented in Table 4-11.

4.2.3 Analysis of First Cracking Data

During testing, the load at which the first cracking occurred was recorded for each face. In some cases cracking occurred at failure or did not occur at all. Table 4-3 on page 57 presents the load at which the first crack appeared on each face of each prism. The mean and standard deviation of the ratio of the first cracking stress to the ultimate bearing stress is presented in Table 4-12.

Table 4-12: First Cracking Stress / Ultimate Bearing Stress Summary

Bearing Pad Size	Mean	Standard Deviation
4	0.601	16.6%
2.5	0.667	11.7%

In a few cases, one face would crack at a much lower load than the other three faces. These cases are with prisms 1.5T-4-B, 1.5T-4-C, 2.0T-2.5-C, and 1.5S-4-A. If these low loads are ignored, the variability of the data greatly decreases (See Table 4-13).

Table 4-13: First Cracking Stress / Ultimate Bearing Stress Summary with low values removed

Bearing Pad Size	Mean	Standard Deviation
4	0.678	8.4%
2.5	0.690	8.0%

A conservative estimate would be that the first crack appears at approximately 70% of the ultimate bearing load. Figure 4-36 shows that as the A/A_b ratio increased, the cracking occurred at a lower load. Adding reinforcing by decreasing the pitch or spacing of the confining reinforcing does not seem to have an effect on the first cracking load.

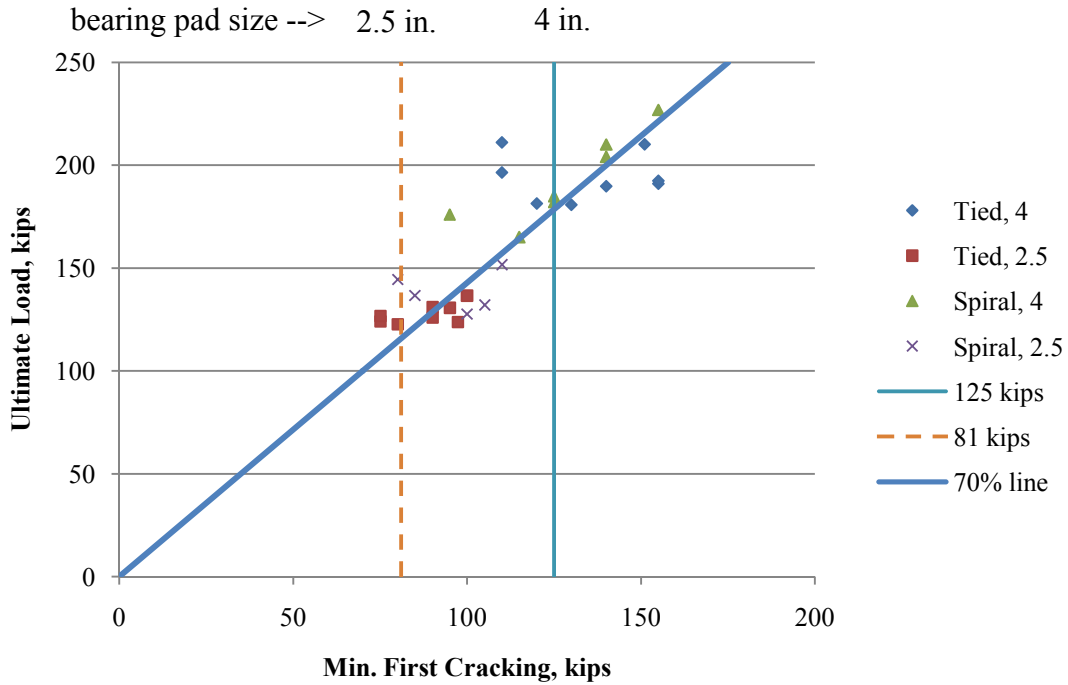


Figure 4-36: Ultimate Load vs. Min. First Cracking load: separated by reinforcing type and bearing pad size

An assumption made for the failure of unreinforced prisms is that at first cracking, the unreinforced concrete prisms fails. With this assumption and the fact that Bonetti’s unreinforced bearing strength equation predicted the failure of the unreinforced prisms with very good accuracy, we can surmise that the first cracking load should be the same as the unreinforced bearing strength prediction by Bonetti’s equation (Equation 2-4). Bonetti’s equation estimates that the unreinforced bearing strength of a prism loaded through a 4 in. and 2.5 inch bearing pad are 125 kips and 81 kips respectively. These lines are plotted on Figure 4-36. The first cracking estimate for the 4 in. bearing pad is near the average of the data but there is a large amount of variability. The first cracking estimate for the 2.5 in. bearing pad estimates the first cracking at a lower load than the average but there is less variability in the 2.5 in. bearing pad data.

4.3 Splitting Tensile Strength of Lightweight Concrete

ACI distinguishes between two different types of lightweight concrete, sand-lightweight and all-lightweight concrete. These two types of lightweight concrete have been discussed in Section 0. Only one source was found to have all-lightweight concrete in the course of the data collection and therefore the main focus of this section is sand-lightweight concrete.

The average F_{sp} value, the ratio of f_{ct} to the square root of f'_c , for sand-lightweight concrete is 7.81 with an 11% standard deviation of the data collected in this research and the data gathered from other sources. The range of f'_c values gathered are from 2250 psi to 8300 psi. ACI only allows a maximum F_{sp} value of 6.7, which is still a good best fit estimate of the data used in this analysis. Using the ACI recommended F_{sp} value of 5.7 for sand-lightweight concrete the mean of the experimental tensile strength divided by the predicted tensile strength is 1.26 and the standard deviation is 14%. The F_{sp} value of 5.7 is found by multiplying 6.7 by the λ -factor of 0.85 for sand-lightweight concrete. Using a F_{sp} of 5.7 gives a lower bound the splitting tensile strength of the lightweight concrete.

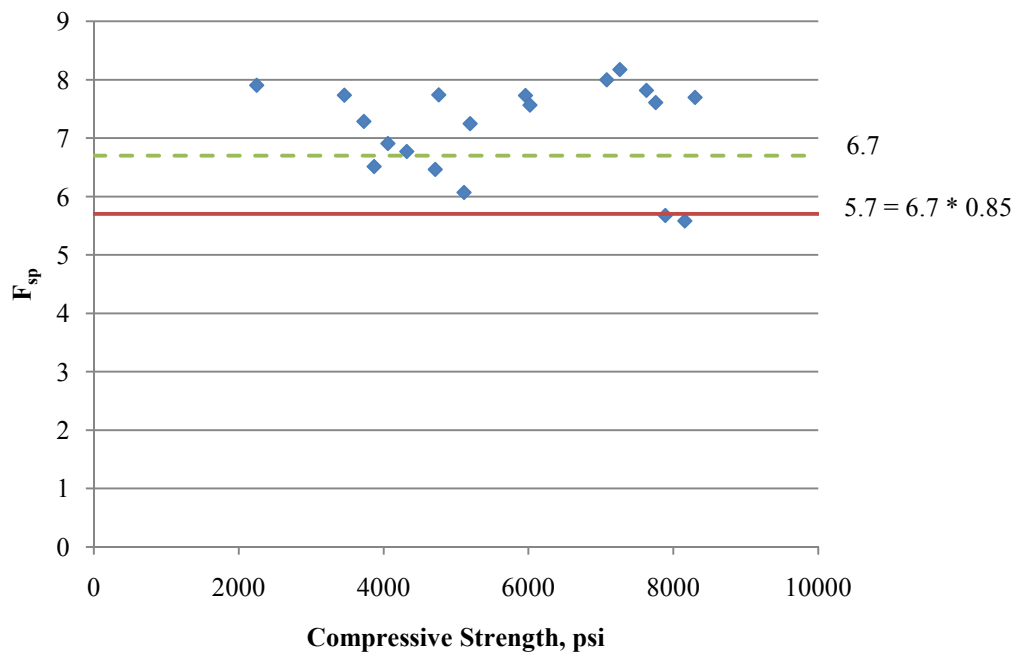


Figure 4-37: F_{sp} for Sand-Lightweight Concrete

The data values in Figure 4-37 are taken from this research, Bonetti (2005), Roberts-Wollmann et al. (2006) (unit weights from 118 to 121 pcf), and Ivey and Buth (1966) (unit weights from 92.5 to 108 pcf).

Taking 10% of f'_c is a common estimate of the splitting tensile strength of normal weight concrete. Using the same data as above and plotting the percentage f_{ct} of f'_c it is evident that the relationship is not linear (See Figure 4-38). The data shows that for sand-lightweight concretes with a compressive strength below 4000 psi, using 10% of f'_c to estimate f_{ct} would be adequate. However, above 4000 psi it would be necessary to reduce the value of 10% to around 6%.

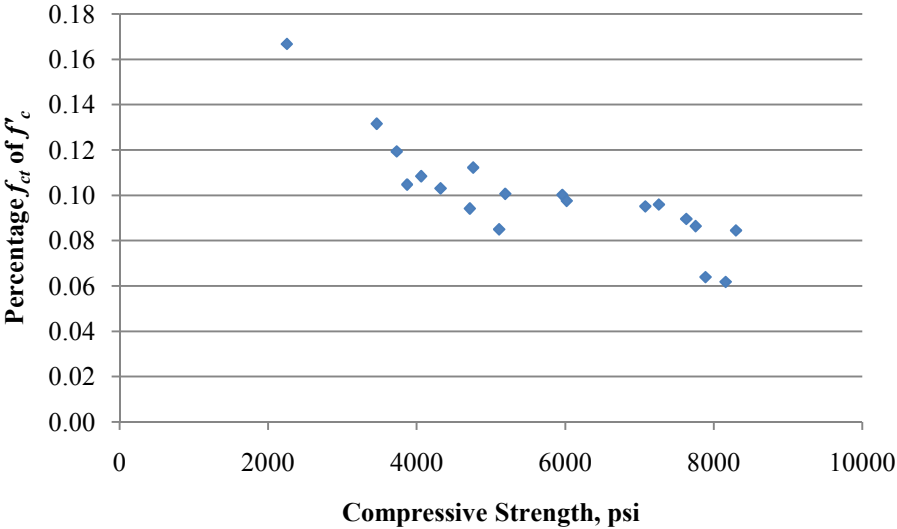


Figure 4-38: Percentage f_{ct} of f'_c versus f'_c of Sand-Lightweight Data

4.4 Modulus of Elasticity of Lightweight Concrete

The modulus of elasticity was tracked along with the compressive and tensile strength gain. The data collected in this research along with the modulus of elasticity data presented in Dymond (2007) is compared to the equations discussed in Section 2.4. Table 4-7 presents the estimated modulus of elasticity along with the data collected in this research (See Figure 4-39 and Figure 4-40).

Table 4-14: Modulus of Elasticity versus Equation Estimates

Day	f'_c , psi	Modulus of Elasticity, ksi					
		Current Research	ACI 318-05 Equation	Slate, Nilson, and Martinez	Ahmad, Shah 1982	Khaloo, Kim 1999	Gjorv, Zhang 1991
7	4098	2940	2862	2763	2385	2236	1601
14	4715	2818	3070	2907	2558	2398	1758
21	5192	3146	3221	3012	2685	2517	1875
28	5960	3571	3451	3172	2876	2696	2055
40	7063	2866	3757	3384	3131	2935	2302
51	7261	2723	3809	3420	3175	2976	2344

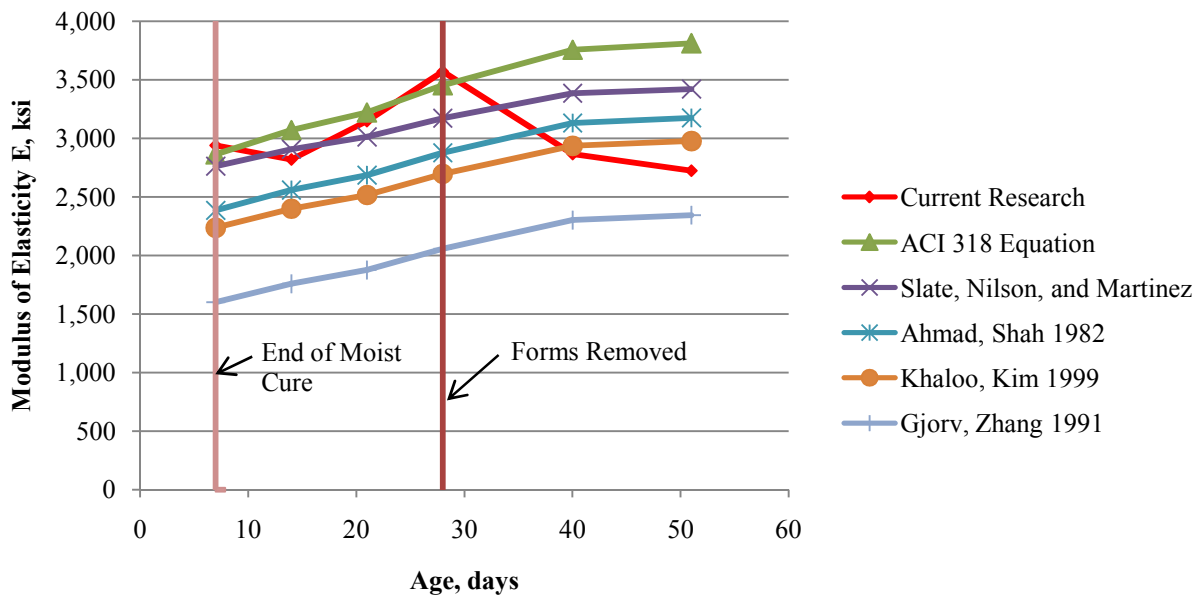


Figure 4-39: Current Research vs. Modulus of Elasticity Estimates

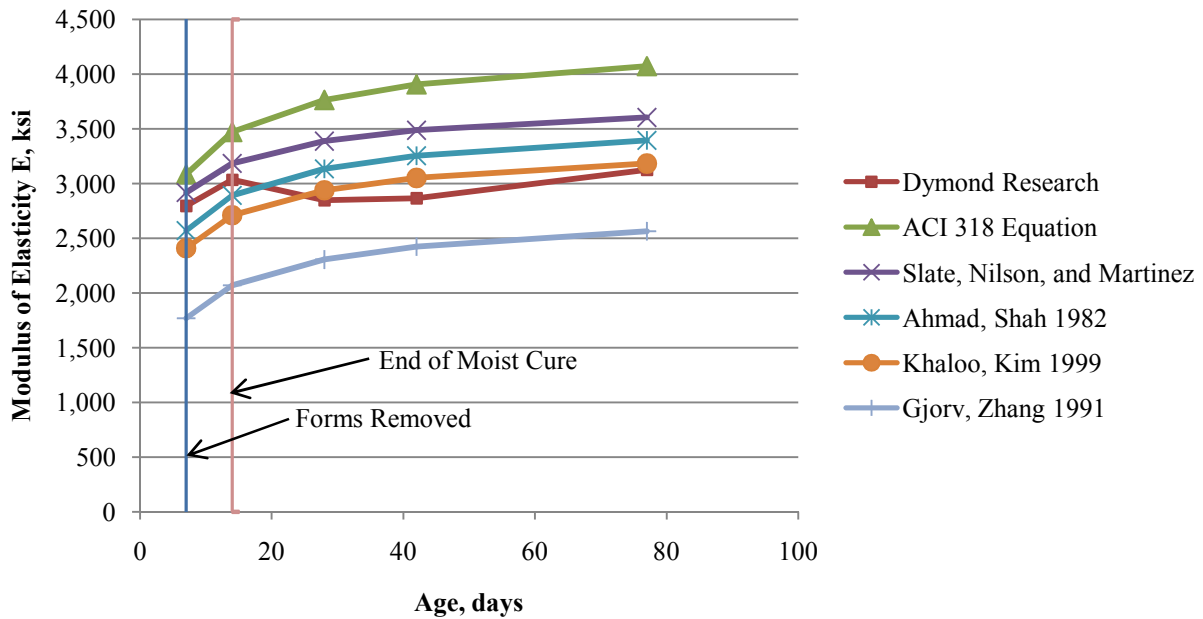


Figure 4-40: Dymond (2007) Data vs. Modulus of Elasticity Estimates

From Figure 4-39 and Figure 4-40, it is apparent that the curing condition plays a role in the estimation of the modulus of elasticity. For the data collected in this research, the equation proposed by ACI 318-05 and Slate, Nilson, and Martinez seem to estimate the modulus of elasticity well until after the forms are stripped. Two equations began to predict the modulus of elasticity of Dymond’s data up to the point that the forms were stripped. After the forms were stripped, the equation proposed by Kahloo and Kim better predicts the modulus of elasticity.

It is apparent from the data from this research and the data from Dymond’s research that ending the moist cure and removing the forms will change the trend of the modulus of elasticity over time. It seems that in each case, after the moist cure is ended or the removal of the forms occurs, the modulus of elasticity is reduced.

Chapter 5.0 Conclusions and Recommendations

5.1 Conclusions

In order to modify the NCHRP equation to predict the ultimate load of the local zone in lightweight concrete, testing was carried out to determine how two key parameters affected the strength of the local zone. The two key parameters are the A/A_b ratio and the lateral confining reinforcing. 30 reinforced prism specimens, 2 unreinforced prism specimens, and 6 unreinforced 4 in. x 8 in. cylinders were tested to analyze the affects of the two key parameters.

The first parameter tested was the A/A_b ratio and its affects were tested by varying the size of bearing plate used to load the test specimens. Two types of specimens were tested to determine the affect of the A/A_b ratio, unreinforced 4 in. x 8 in. cylinders and 8 in. x 8 in. x 16 in. prisms.

The second parameter that was tested was the affect of lateral confining reinforcing on the ultimate bearing strength of the local zone. Both spiral and tied confining reinforcing with varying pitches and spacing were used. This helped determine the effectiveness of each type of confining reinforcing and how much the ultimate load was increased for an increased amount of lateral reinforcing.

The data gathered for this research to modify the NCHRP Equation to predict the ultimate load of the local zone for lightweight concrete support the following conclusions:

- The current NCHRP equation is not conservative or accurate when used with lightweight concrete. The current NCHRP equation for normal weight concrete overestimates the strength by about 80% (See Figure 4-15).
- The λ -factor and k-factor are dependent on the properties of the concrete used.
- Using the area modification and a k-factor of 2.5 with the appropriate λ -factor will yield conservative predictions of the ultimate load of the local zone.
- Using the ACI recommended λ -factors of 0.7 for all-lightweight concrete and 0.85 for sand-lightweight concrete will give a conservative result when used with the plain bearing strength equation (Equation 2-9) as well as the NCHRP equation to predict the ultimate load of the local zone.

- Extensive research is still required into the effectiveness of the NCHRP equation to estimate the ultimate load of the local zone in lightweight concrete.

Current NCHRP equation to estimate the strength of the local zone in post-tensioned concrete:

$$F_{ult} = 0.80f'_c\sqrt{A/A_b}(A_b) + 4.1f_{lat}A_{eff}$$

Proposed NCHRP modifications for all-lightweight and sand-lightweight concrete:

$$F_{ult} = \lambda 0.80f'_c\sqrt{A/A_b}(A_b) + 2.5f_{lat}A_{eff}$$

Where:

$\lambda = 0.70$ for all-lightweight concrete
 0.85 for sand-lightweight concrete

The investigation into the prediction of the modulus of elasticity of lightweight concrete has shown that more research is needed to understand all of the parameter that affect the modulus of elasticity of lightweight concrete. A conservative prediction of the splitting tensile strength of lightweight concrete can be found using an F_{sp} value of 5.7.

5.2 Recommendations

The following recommendations are given for future research into the design of post-tensioned local anchorage zones in lightweight concrete. The following parameters should be investigated

- An investigation into how the strength of the lightweight concrete affects the behavior and strength of the confined local zone
- An investigation into how the size of the specimen or concrete cross section affects the behavior and of the confined local zone
- An investigation into the behavior and strength when using both ties and spirals to confine the local zone.
- An investigation into the presence or absence of a duct affects the behavior and strength of the local zone.
- An investigation into the affect of the unit weight on the behavior and strength of the local zone

References

- [1] Stalite Company. www.stalite.com.
- [2] America Association of State Highway Transportation Officials. (2007). "*AASHTO LRFD Bridge Design Specifications*." 4th. Washington, DC
- [3] American Concrete Institute. (2005). "*Building Code Requirements for Structural Concrete and Commentary (ACI 318-05)*." Farmington Hills, Mich.
- [4] Ahmad, S. H., and Shah, S. P. (1982). "Stress-Strain Curves of Concrete Confined by Spiral Reinforcement." *ACI Journal Proceedings*, Vol. 79, No. 6, 484-490.
- [5] Axson, D. "*Load Transfer Tests with Anchorage SA6-4 for 3-0.6 in. dia. Strands in 6000 psi Lightweight Concrete In Accordance with AASHTO LRFD Bridge Design Specifications 2004 Aggressive Environment*." Report #456 R1. VSL Corporation. Springfield, VA. April 12, 2007.
- [6] Axson, D. "*Load Transfer Tests with Anchorage SA6-4 for 4-0.6 in. dia. Strands in 6000 psi Lightweight Concrete In Accordance with AASHTO LRFD Bridge Design Specifications 2004 Aggressive Environment Criteria*." Report #457 R1. VSL Corporation. Springfield, VA. April 12, 2007.
- [7] Axson, D. "*Load Transfer Tests with DSI Anchorage FA4-0.6" for 3-0.6 in. dia. Strands in 6000 psi Lightweight Concrete In Accordance with AASHTO LRFD Bridge Design Specifications 2004 Aggressive Environment Criteria*." Report #454 R1. VSL Corporation. Springfield, VA. April 12, 2007.
- [8] Axson, D. "*Load Transfer Tests with DSI Anchorage FA4-0.6" for 4-0.6 in. dia. Strands in 6000 psi Lightweight Concrete In Accordance with AASHTO LRFD Bridge Design Specifications 2004 Aggressive Environment Criteria*." Report #455 R1. VSL Corporation. Springfield, VA. April 12, 2007.
- [9] Basset, R., and Uzumeri, S. M. (1986). "Effect of Confinement on the Behavior of High-Strength Lightweight Concrete Columns." *Canadian Journal of Civil Engineering*, Vol. 13, No. 6, 741-751.
- [10] Billig, K.(1948). "*A Proposal for a Draft Code of Practice for Prestressed Concrete*." Cement and Concrete Association, London.
- [11] Bonetti, R. A. (2005). "Ultimate Strength of the Local Zone in Load Transfer Tests," Virginia Tech, February 2005.

- [12] Breen, J. E., Burdet, O., Roberts, C. L., Sanders, D., and Wollmann, G. P.(1994). "*Anchorage Zone Reinforcement for Post-Tensioned Concrete Girders.*" NCHRP Report 356, Transportation Research Board, Washington D.C.
- [13] Buth, E., and Ivey, D. (1966). "Splitting Tensile Strength of Structural Lightweight Concrete." *Journal of Materials*, Vol. 1, No. 4, 859-871.
- [14] Carrasquillo, R. L., Nilson, A. H., and Slate, F. O. (1981). "Properties of High-Strength concrete Subject to Short-Term Loads." *ACI Journal Proceedings*, Vol. 78, No. 3, 171-178.
- [15] Cowan, H. J. (1953). "The Strength of Plain, Reinforced and Pre-stressed Concrete under the Action of Combined stresses, with Particular Reference to Combined Bending and Torsion of Rectangular Sections." *Magazine of Concrete Research*, Vol. 5, No. 14, 75-86.
- [16] Dymond, B. (2007). "Shear Strength of a PCBT-53 Girder Fabricated with Lightweight, Self-Consolidating Concrete," Virginia Tech, December 2007.
- [17] Gjrrv, O. E., and Zhang, M. (1991). "Mechanical Properties of High-Strength Lightweight Concrete." *ACI Materials Journal*, Vol. 88, No. 3, 240-247.
- [18] Guyon, Y. (1953). *Prestressed Concrete*, John Wiley and Sons, Inc., New York.
- [19] Hanson, J. A. (1962). "Tensile Strength and Diagonal Tension Resistance of Structural Lightweight Concrete." *Journal of the American Concrete Institute*, Vol. 58, No. 1, 1-40.
- [20] Haque, M. N., Al-Khaiat, H., and Kayali, O. (2004). "Strength and Durability of Lightweight Concrete." *Cement and Concrete Composites*, Vol. 26, No., 307-314.
- [21] Hawkins, N. M. (1968a). "The Bearing Strength of Concrete Loaded Through Flexible Plates." *Magazine of Concrete Research*, Vol. 20, No. 63, 95-102.
- [22] Hawkins, N. M. (1968b). "The Bearing Strength of Concrete Loaded through Rigid Plates." *Magazine of Concrete Research*, Vol. 20, No. 62, 31-40.
- [23] Heilmann, H. G. (1983). "Versuche zur Teilflächenbelastung von Leichtbeton für Tragende Konstruktionen." *Deutscher Ausschuss für Stahlbeton*, Heft 344, (In German).
- [24] Khaloo, A. R., and Bozorgzadeh, A. (2001). "Influence of Confining Hoop Flexural Stiffness on Behavior of High Strength Lightweight Concrete Columns." *ACI Structural Journal*, Vol. 98, No. 5, 657-664.
- [25] Khaloo, A. R., and Kim, N. (1999). "Effect of Curing condition on Strength and Elastic Modulus of Lightweight High-Strength Concrete." *ACI Materials Journal*, Vol. 96, No. 4, 485-490.

- [26] Komendant, A. E. (1952). *Prestressed Concrete Structures*, McGraw-Hill.
- [27] Martinez, S., Nilson, A. H., and Slate, F. O. (1984). "Spirally Reinforced High-Strength Concrete Columns." *ACI Journal Proceedings*, Vol. 81, No. 5, 431-442.
- [28] Meyerhof, G. G. (1953). "The Bearing Capacity of Concrete and Rock." *Magazine of Concrete Research*, Vol. 4, No. 12, 107-106.
- [29] Nilson, A. H., Darwin, D., and Dolan, C. W. (2004). *Design of Concrete Structures*, McGraw-Hill, New York.
- [30] Niyogi, S. K. (1973). "Bearing Strength of Concrete - Geometric Variations." *ASCE Journal of the Structural Division*, Vol. 99, No. ST7, 1471-1490.
- [31] Niyogi, S. K. (1974). "Concrete Bearing Strength - Support, Mix, Size Effect." *ASCE Journal of the Structural Division*, Vol. 100, No. ST8, 1685-1702.
- [32] Niyogi, S. K. (1975). "Bearing Strength of Reinforced Concrete Blocks." *ASCE Journal of the Structural Division*, Vol. 101, No. ST5, 1125-1137.
- [33] Richart, F. E., Brandtzaeg, A., and Brown, R. L.(1928). "*A Study of the Failure of Concrete Under Combined Compressive Stresses.*" University of Illinois Engineering Experiment Station, University of Illinois.
- [34] Richart, F. E., Brandtzaeg, A., and Brown, R. L.(1929). "*The Failure of Plain and Spirally Reinforced Concrete in Compression.*" University of Illinois Engineering Experiment Station, University of Illinois.
- [35] Roberts-Wollmann, C. L., Banta, T., Bonetti, R. A., and Charney, F. (2006). "Bearing Strength of Lightweight Concrete." *ACI Materials Journal*, Vol. 103, No. 6, 459-466.
- [36] Roberts, C. L. (1990). "Behavior and Design of the Local Anchorage Zone of Post-tensioned Concrete Members," University of Texas at Austin, May 1990.
- [37] Saatcioglu, M., and Ravzi, S. R. (1992). "Strength and Ductility of Confined Concrete." *Journal of Structural Engineering*, Vol. 118, No. 6, 1590-1607.
- [38] Shah, S. P., Naaman, A. E., and Moreno, J. (1983). "Effect of Confinement on the Ductility of Lightweight Concrete." *International Journal of Cement Composites and Lightweight Concrete*, Vol. 5, No. 1, 15-25.
- [39] Slate, F. O., Nilson, A. H., and Martinez, S. (1986). "Mechanical Properties of High-Strength Lightweight Concrete." *ACI Journal Proceedings*, Vol. 83, No. 4, 606-613.

- [40] Zieliński, J., and Rowe, R. E.(1960). "*An Investigation of the Stress Distribution in the Anchorage Zones of Post-Tensioned Concrete Members.*" Cement and Concrete Association, London, England.